DEVELOPMENT OF MAGNETIC ALLOYS BY THE DIRECT REDUCTION OF OXIDES

By

SHARDA NAND PRASAD

ME
1986
M1
PRA
Thesis
669.95
P886d
DEV

DEPARTMENT OF METALLURGICAL ENGINEERING

INDIAN INSTITUTE OF TECHNOLOGY KANPUR

APRIL, 1986

DEVELOPMENT OF MAGNETIC ALLOYS BY THE DIRECT REDUCTION OF OXIDES

A Thesis Submitted
in Partial Fulfilment of the Requirements
for the Degree of
MASTER OF TECHNOLOGY

By
SHARDA NAND PRASAD

to the

DEPARTMENT OF METALLURGICAL ENGINEERING
INDIAN INSTITUTE OF TECHNOLOGY KANPUR
APRIL, 1986

23 SEP 1987
CENTRAL LIBRARY
I I T, Kanpur.
Acc. No. A 98011

ME - 1986 - M - PRA - DEV

CERTIFICATE

Certified that the thesis entitled, 'DEVELOPMENT OF MAGNETIC ALLOYS BY THE DIRECT REDUCTION OF OXIDES', has been carried out by Mr. Sharda Nand Prasad under my supervision and it has not been submitted elsewhere for the award of a degree.

April 1986.

K.N. Rai
Professor
Metallurgical Engineering Deptt.
Indian Institute of Technology,
Kanpur-208016.

ACKNOWLEDGEMENTS

I wish to express my sincere thanks to Professor K.N. Rai for his valuable suggestions, guidance and encouragement of every stage of this work without which this work could not have been completed.

I am also grateful to Dr. Bahadur for his help during the magnetic measurements, an essential part of the work. I must thank to Mr. A. Agnihotri for his kind co-operation throughout the magnetic measurements.

I wish to offer a lot of thanks to Mr. B. Sharma for materialisation of the different schemes into actual experimental apparatus. I am also thankful to Mr. S.R. Chaurasia and Mr. S.P. Rai for their kind help throughout the work.

Lot of thanks are due to my friends S.K. Rai, K.P. Rai and A. Pal for their constant help in various ways and for their entertaining company.

I must thank Mr. B.K. Jain for his excellent drafting work.

I would fail in my duties if I do not thank Saini for speedy and excellent typing and Mr. Ayodhya Prasad for his timely help in getting the thesis cyclostyled.

April, 1936 SHARDA NAND PRASAD

CONTENTS

Page No.

LIST OF TABLES

LIST OF FIGURES

ABSTRACT

The present investigation involves the study of process variables on the development of magnetic properties in Alnico alloys. These process variables are fabrication method of alloys, temperature of annealing, time of annealing, time and temperature of magnetic ageing, and addition of alloying elements (Cr, Co and Cu).

Alloys chosen for study contain 70-57% Fe, 20-28% Ni, 5% Al and 5-10% Cr in Fe-Ni-Al-Cr system and 63-52% Fe, 20-12% Ni, 10% Al, 5-20% Co and 2-6% Cu in Fe-Ni-Al-Co-Cu system. All alloys were annealed at 1000°C for 3 hrs. and then tempered at 650°C for $3\frac{1}{2}$ hrs. in H_2 atmosphere.

The microstructural features of Alnico alloys were studied by optical microscope. The phase analysis was carried out by using X-ray diffraction technique.

Microhardness and Resistivity both were found to increase linearly with increased amount of alloying elements.

Addition of Co and Cu was aimed at increasing M_s, M_r and ^iHc values. Chromium increases ^iHc, but lowers M_s and M_r values, H_2 annealing appears to improve M_s, M_r and ^iHc values.

Magnetic ageing of alloys in the field of 1200 Gauss for 1/2 hr. at 650°C showed promising improvement in M_s , M_r and ^{i}Hc values and induced loop squareness.

CHAPTER - I

INTRODUCTION AND LITERATURE REVIEW

ABSTRACT:

This chapter reviews the subject matters related to structure, properties, the general methods of fabrication , characterization and applications of Alnico magnet alloys.

1.1 Introduction:

The increased requirement for sophistication of industrial devices and development of modern instruments necessitated the development of various kinds of magnetic materials. The relation among magnetic properties composition, crystal structure and the method of fabrication, has immense important. As a consequence this has stimulated much scientific and technological development work aimed at influencing the magnetic properties in order to develop materials with most advantageous combination for applications in telecommunication and electrical engineering.

The discoveries in this field are Alnico alloys as permanent magnet by Mishima in 1931,

ferromagnetic resonance by Griffith in 1946, anti-ferromagnetism by Neel in 1948, theory of single domain particles by Wolliams and Bozorth in 1949, magnetic ferrite by Snock in 1949 and so on.

A permanent magnet is a storage device. The requirement of every saving as well as miniaturisation of devices employing magnets has generated in recent years a renewed interest in the development of new, high energy product magnetic materials. Wide spread interest in Alnico alloys which had anisotropy constant (K_1) in the range of ($.3 \times 10^6 - 1.9 \times 10^6$) ergs/cm^3 which is much larger than that of steels. Properties of some important permanent magnets are in Table (1.1).

A high quality permanent magnet material must have the following properties: (i) high saturation magnetization (M_r), (ii) high curie temperature (T_c), (iii) Uni-axial anisotropy (iv) larger value of magneto crystalline anisotropy constant (K_1), (v) high coercive force (H_c), (vi) a large fulness factor and (vii) low permanent permeability.

Besides these requirements, the material must have high corrossion resistant, thermal stability and should be cheap.

The main contribution towards the saturation magnetization (M_s) of alnico magnet alloys is made by

TABLE : 1.1

Properties of some Permanent Magnet Materials

Materials	Composition (weight %)	Remanence B_r (Gauss)	Coercivity H_c Orsted	Maximum energy product $(BH)_{max}$ M.G.Oe
36 Co Steel	36 Co, 3.75 w, 5.75 Cr, 0.8 C	9600	228	.93
Alnico 1	12 Al, 23 Ni, 5 Co, 60 Fe	6600	540	1.4
Alnico 2	10 Al, 18 Ni, 13 Co, 6 Cu, 63 Fe	7000	650	1.7
Alnico 3	12 Al, 26 Ni, 3 Cu, 59 Fe	6400	560	1.4
Alnico 4	12 Al, 28 Ni, 5 Co, 55 Fe	5500	730	1.4
Alnico 5*	8 Al, 15 Ni, 24 Co, 3 Cu, 50 Fe	12000	720	5.0
Alnico 5 DG*	8 Al, 15 Ni, 24 Co, 3 Cu, 50 Fe	13100	700	6.5
Alnico 6*	8 Al, 17 Ni, 23 Co, 3 Cu, 45 Fe, 4 Ti	7500	975	2.8
Alnico 8*	8 Al, 14 Ni, 38 Co, 3 Cu, 29 Fe, 8 Ti	7100	2000	5.5
Alnico 9*	7 Al, 15 Ni, 35 Co, 4 Cu, 34 Fe, 5 Ti	10400	1600	8.5

* Anisotropic properties

parallel (i.e. ferromagnetically coupled) magnetic moment of Fe atoms in the ferromagnetic phase α (Fe_{38} Ni Al) and in weakly magnetic phase α' (Fe_6 Ni_8 Al_7). Both phases have Body-centred crystal structure (1). The alnico alloys have body-centred crystal structure with unixial anisotropy i.e. due to easy direction of magnetization is in the [100] direction as shown in Fig. (1.1).

The coercive force of alnico alloys depends on many factors. High coercive force is due to very large anisotropy fields varying with composition of alloys. The coercive force finally developed in a magnet is however, influenced by many processing perameters (2). High coercive force can be developed by making conditions favourable for pinning domain walls. This approach has been used in some alnico alloys. Yet another method to increase coercivity is by precipitating out elongated particles of the magnetic phase in a non-magnetic matrix, thereby coupling high magneto-crystalline anisotropy field as well as shape anisotropy effect to yield high value of coercivity.

1.2 Alnico Alloys:

The alloys of the Fe-Ni-Al system with or without specific alloying additions, are known as Alnico alloys. Depending upon composition, history of

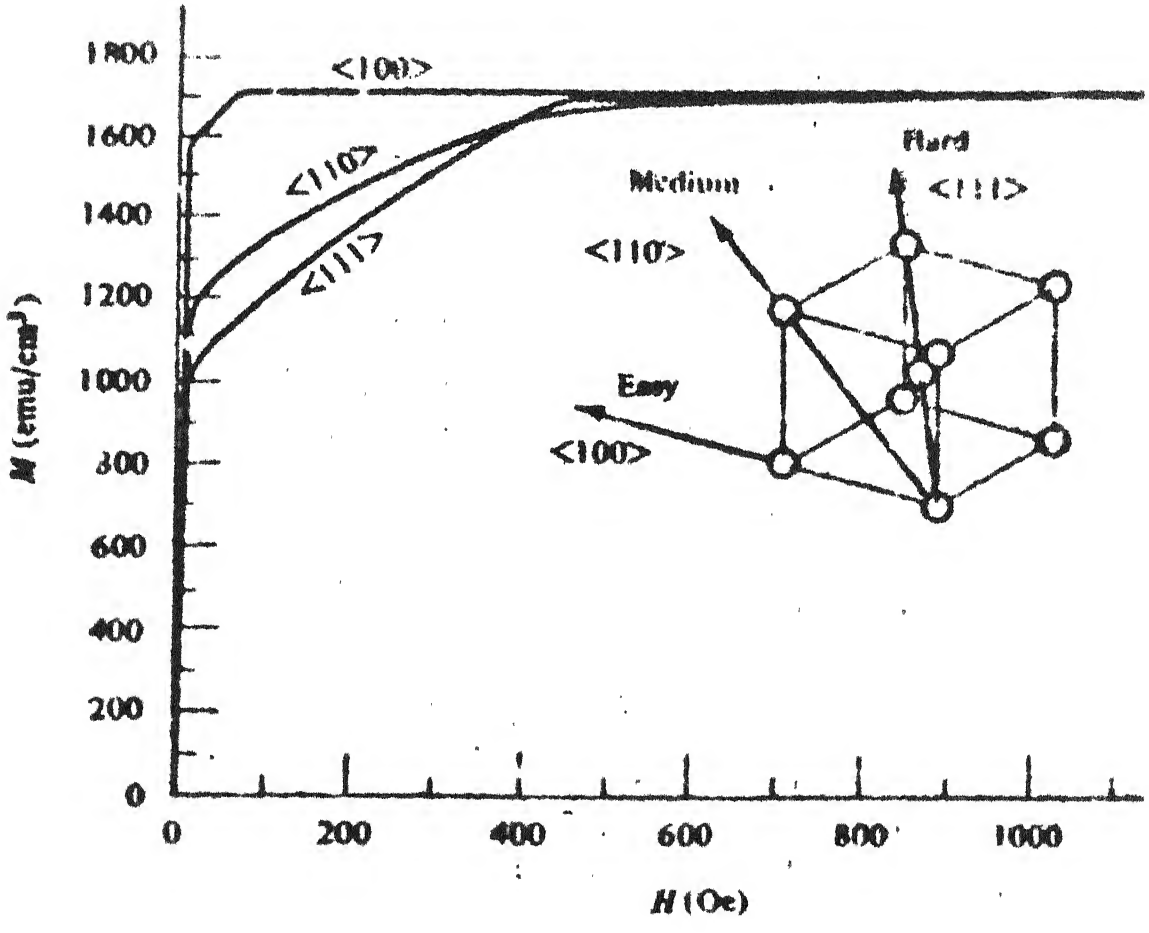

Fig. 1.1 : Magnetization curves for single crystal of iron

of fabrication and purpose of development, they may be further classified as Alnico - 1, 2, 3, 4, 5, 5 DG, 6, 7, 8 and 9 etc. (3). They have wide range of magnetic properties and are suitable for using as permanent magnets. These alloys are brittle and must be cast to shape. Details of the optimum composition and heat treatment of these isotropic alloys in which magnetic properties are independent of orientation, have been studied by Betteridge (4). The best properties were obtained for an alloy containing 60% Fe - 28% Ni - 12% Al which had been quenched at 28°C per second from the single phase state at 1100°C and tempered for 4 hours at 650°C. This treatment gave a coercivity ($^{B}H_{c}$)=515 Orsted and a maximum energy product $(BH)_{max}$ = 1.35 x 10^{6} G. Oe. The coercivity was shown to depend very critically on the Al content while the remanence depended more on the Ni content.

The magnetic properties of Alnico alloys can be improved by the addition of Co, Cu and other alloying elements. Betteridge (4) also investigated the effect of addition Cu to (Fe - Ni - Al) system alloys and found that a 3.5 weight percent Cu addition increased $(BH)_{max}$ to 1.5 x 10^{6} G.Oe after quenching from 1100°C and tempered at 550°C. The Cu addition increased the rate of precipitation of phases so that alloys required more rapid cooling.

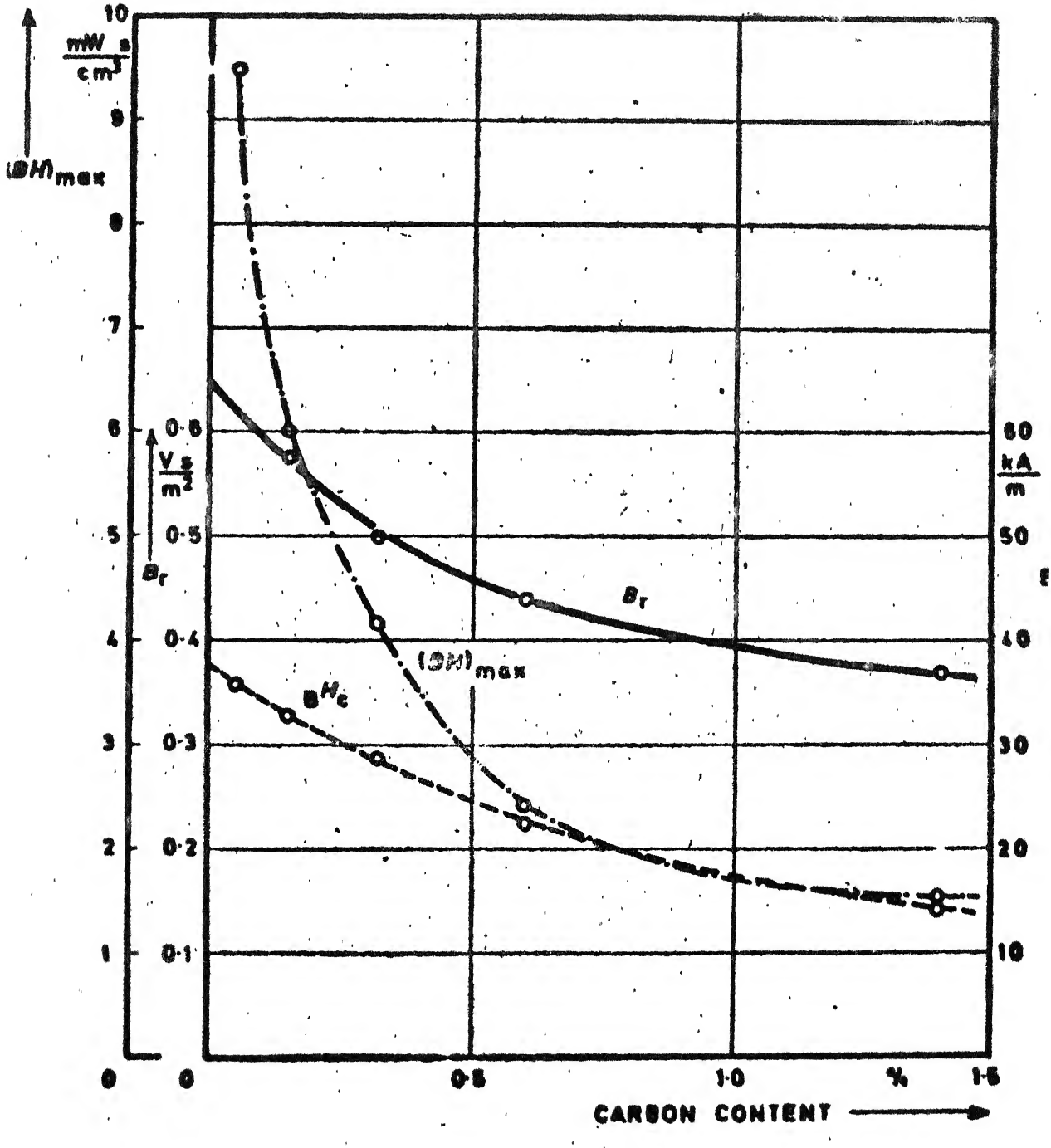

Fig. 1.2 : Effect of carbon on the magnetic properties of Fe-Ni-Al - system alloys.

The effect of elastic stress on the precipitation of phases and addition of Cu and Ti on magnetic properties of Fe - Ni - Al system alloys have been investigated by Yermolenko and Korolyov (5) who obtained improved optimum permanent magnetic properties.

The carbon content of Fe - Ni - Al system alloys is kept as low as possible, since M_r and intrinsic coercivity (^iH_c) are seriously reduced with carbon content even below .1%. However, small additions of Ti and Cr (about 0.5 %) are made to combine with carbon and counteract its deleterious effect. The effect of carbon on magnetic properties of Fe - Ni - Al system alloys is shown in Fig. (1.2), observed by Betteridge (4).

Betteridge and Zumbush (6) had found that the magnetic properties of Alnico alloys could be improved by the addition of Co as shown in Fig. (1.3). The gains were progressive as the Co content was increased to as high as 20 - 25 % , although the benefits may become uneconomic at higher Co content. A higher solution temperature of about (1250°C - 1300°C) is required. The critical cooling rate varies with composition. The ageing temperature remains in the range of 600°C - 650°C.

The composition and magnetic properties of some known Alnico magnet alloys are given in Table (1.2).

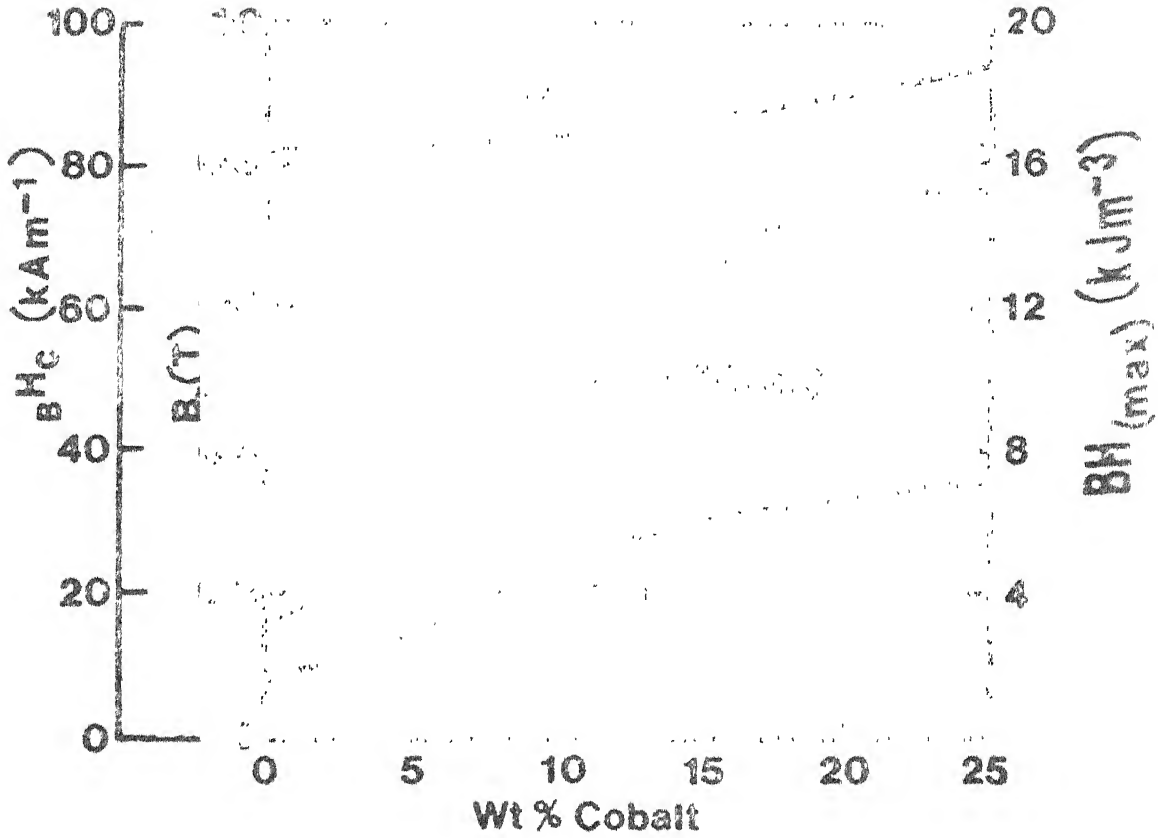

Fig. 1.3 : Dependence of [illegible], remanence and energy product on cobalt content of Fe-Ni-Al system alloy

TABLE : 1.2

Compositions and magnetic properties of isotropic Alnico magnets.

Composition (Wt %) (Balance Fe)					Remanence (B_r) Gauss	Coercive force ($_BH_c$) Orsted	$(BH)_{max}$ G.Oe x 10^3
Ni	Co	Al	Cu	Ti			
24	0	12	2	0	5000	502	1257
21	3	11	3	1	5500	530	1383
16	12	9	4	1	6500	620	1635
18	17	8	4	4	7000	725	1760

1.3 Anisotropic Alnico Magnet Alloys:

Oliver and Shedden (7) improved the magnetic properties of alnico alloys by imposing a strong magnetic field during cooling from the solution treatment temperature. The critical temperature range over which the magnetic field must be maintained is 900°C - 600°C. The resulting magnetic properties are anisotropic, being higher in the direction of the applied field than perpendicular to it. The improvement in properties are mainly shown by increase remanence (B_r), which may become as high as .9 times the saturation flux in stead of only .6 times to isotropic alloys. This results in

a much square demagnetizing curve and a high value of $(BH)_{max}$.

The compositions and magnetic properties of anisotropic alnico magnet alloys are given in Table (1.3).

TABLE : 1.3

Compositions and magnetic properties of Anisotropic Alnico magnet alloys

Composition (Wt %) (Balance Fe)					Remanence (B_r) Gauss	Coercive force (H_c) Orsted	$(BH)_{max}$ G.Oe x 10^6
Ni	Co	Al	Cu	Ti			
12	23	7.8	2	0.5	12,000	580	5.03
14	32	7	4	4	8,000	1380	5.28

1.4 Sintered Alnico Magnet Alloys:

Planchard and Bronner (8) have produced small magnets in large quantities by powder techniques. The powder magnets have lower magnetic properties than those of cast alloys of the same basic composition, because of the presence of porosity or non-magnetic blinders. The sintered magnets can be heat treated in magnetic field to give improved anisotropic properties. The best magnetic properties are obtained when the

particle elongation occurs along the < 100 > axis lying most nearly parallel to the field direction. Typical composition and magnetic properties for the same common alnico alloys, permitting a comparison between sintered and cast materials, are given in Table (1.4).

TABLE : 1.4

Magnetic properties of cast and sintered Alnico Magnet alloys.

Alloy Composition (Wt %) (Balance Fe)				Desig-nation	B_r Gauss	$_BH_c$ Orsted	$(BH)_{max}$ x 10^6 G.Oe
Al	Ni	Co	Cu	Alnico			
10	19	12	6	Cast	7400	528	1.59
				Sintered	7000	503	1.53
10	21	12	9	Alnico			
				Cast	6800	610	1.59
				Sintered	6100	591	1.53
8	11.5	21	4	Alcomax-II			
				Cast	1270	578	4.27
				Sintered	1120	566	3.27
9	21	20	2	Hycomax			
				Cast	8500	792	2.72
				Sintered	7900	780	2.61

1.5 Columnar Grained Alnico Magnet Alloys:

Wright (9) have improved the magnetic properties of the alnico magnets by explotting the difference in properties in different crystallographic directions with

the help of producing columnar grained structure in the alloys. By careful control of thermal gradient during solidification, it is possible to grow long columnar grains with the <100> axes of the alloys lying along the direction of growth. When these alloys are heat treated in a magnetic field, the magnetic properties are better than those of field treated random grain alloys.

The compositions and magnetic properties of columnar grained alnico magnets are given in Table (1.5).

TABLE : 1.5

Compositions and magnetic properties of columnar Alnico magnet alloys

Composition (Wt %) (Balance Fe)						Remanence (B_r) Gauss	Coercive force (H_c) Orsted	$(BH)_{max}$ G. Oe $\times 10^6$
Ni	Co	Al	Cu	Nb	Ti			
13	24	7.8	2	1	4	13,000	704	7.04
14	32	7	4	1	4	10,000	1380	7.54

1.6 Phase Relation in Fe-Ni-Al System Alloys:

De Vos (10, 11) had investigated the phases present in Fe-Ni-Al system alloys using X-ray technique as shown in Fig. (1.4). One single Body-centred crystal

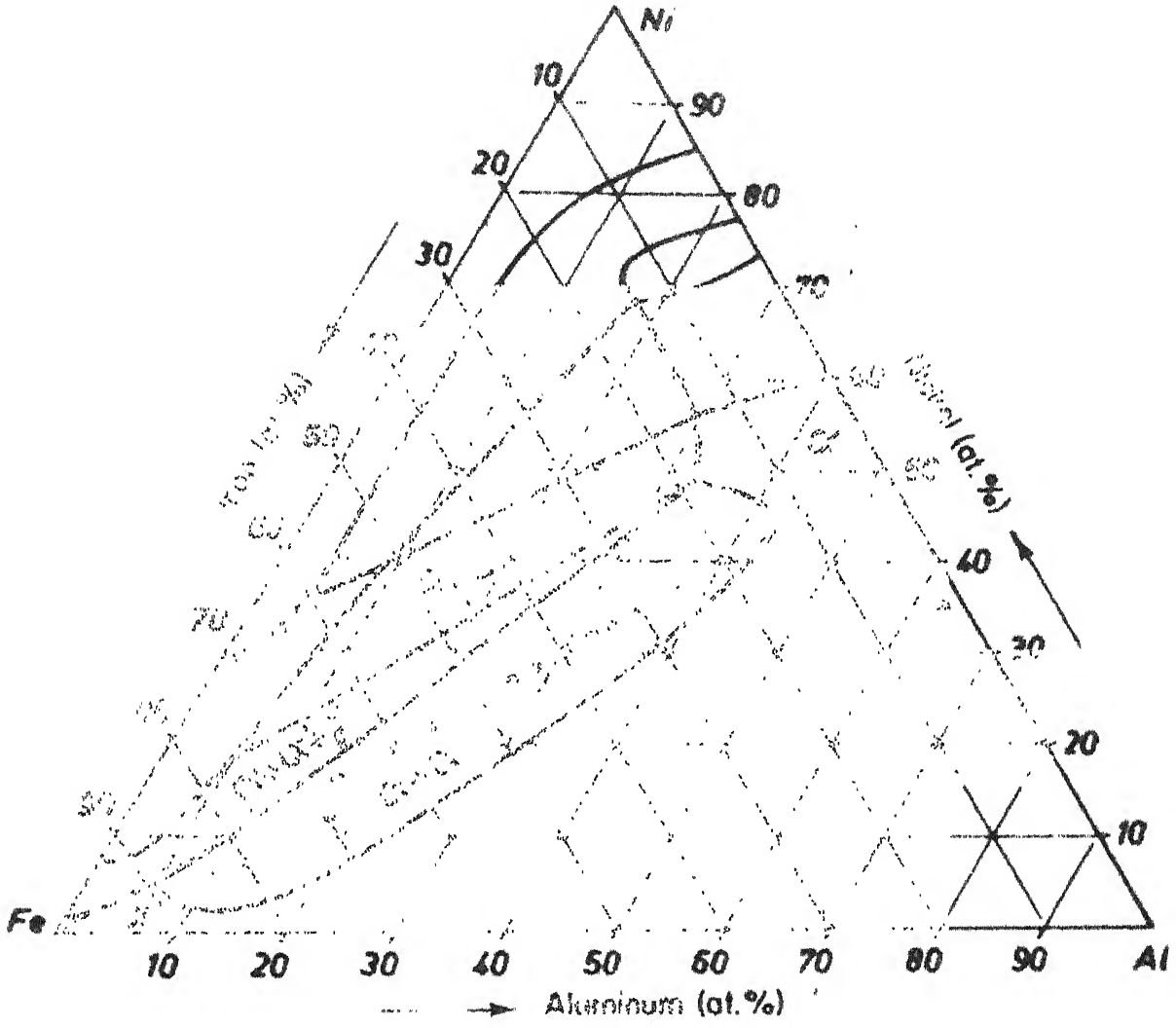

Fig. 1.4 : Phase diagram for the Fe-Ni-Al system.

structure α - phase having a super-structure of the Cs Cl type exists above 1200°C. Between 1200 - 850°C, a B.C.C.α' (Fe_{38} Ni Al) and another F.C.C.γ_1 phase exist. γ_1 phase can not be supercooled to room temperature, but spontaneously transform into a B.C.C. structure known as α phase (Fe_6 Ni_8 Al_7) during cooling. Below 850°C, the alloy consists of two B.C.C. phases. These are α' (Fe_{38} Ni Al), rich in Fe content (ferromagnetic) and α (Fe_6 Ni_8 Al_7), low in Fe content (para magnetic). After tempering for about two months at 600°C, gives rise to another F.C.C. phase (γ).

1.7 The Effect of Heat Treatment on Magnetic Properties of Alnico Magnet Alloys:

The alnico magnet alloys show high coercivity, produced by precipitation hardening method. The stress anisotropy is introduced by high cooling rate during casting in order to obtain high coercivity. The alloy can be heat treated by the following routine: (i) quenching from high temperature (1000 - 1100°C) to room temperature and a subsequent ageing to a medium temperature (550 - 750°C). With the duration of ageing, the coercivity first increases, reaches a maximum and then falls.

The effect of temperature and time of ageing is shown in Figs. (1.5 to 1.6), as reported by Kronenberg

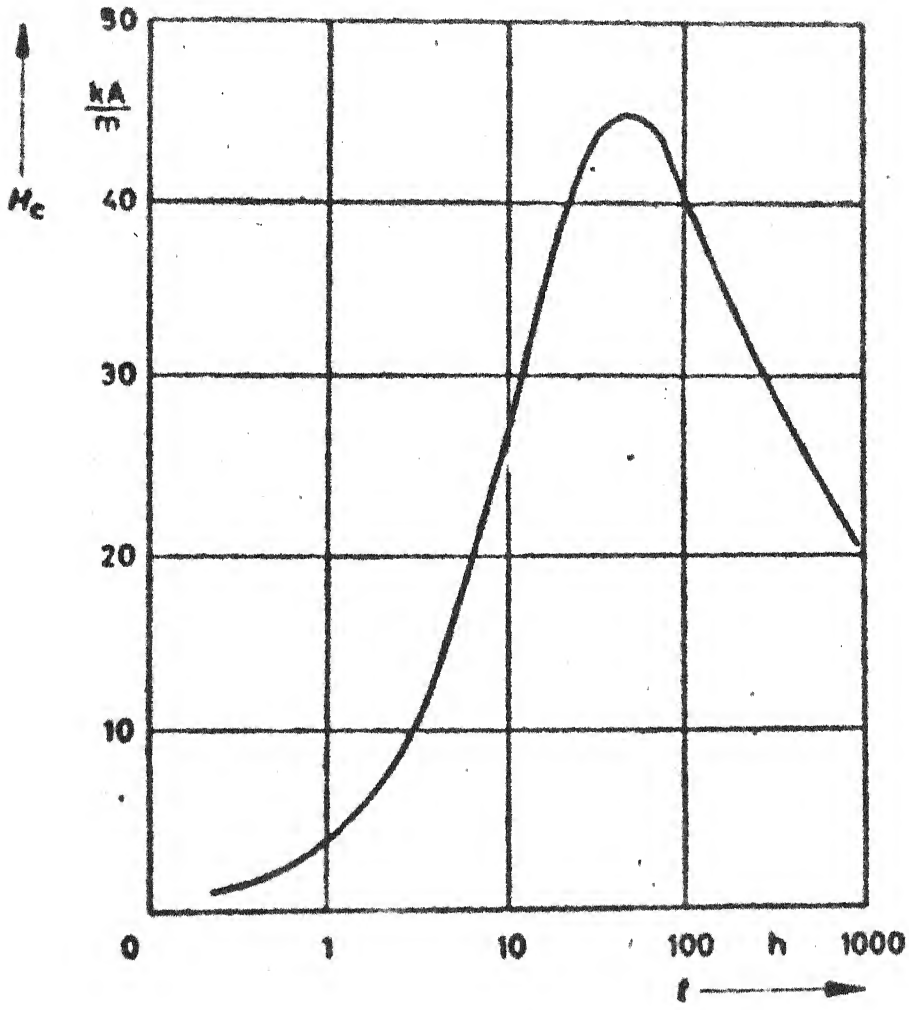

Fig. 1.5 : Dependence of coercivity on duration of temper[illegible] temperature (600°C) for Alnico 5

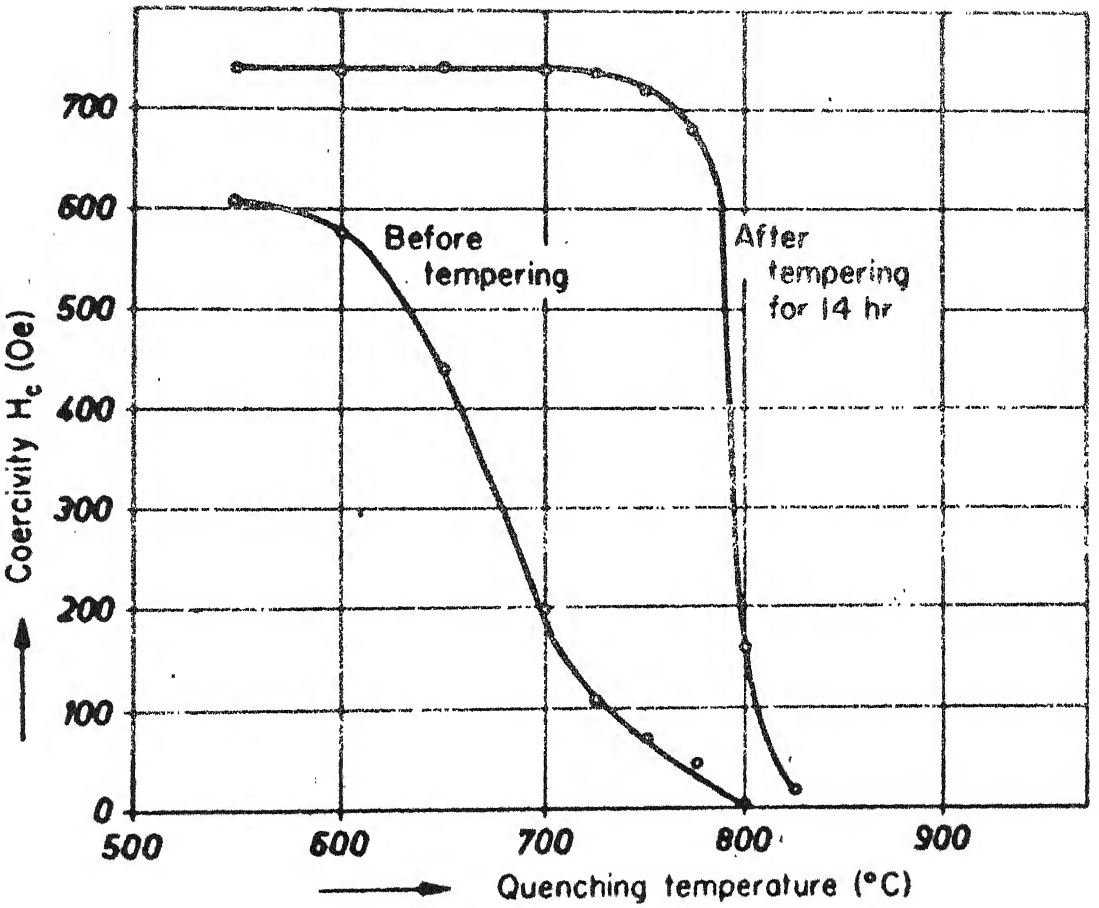

Fig. 1.6 : Variation of coercivity of Alnico 5 before and after tempering as a function of quenching temperature.

and Bohlmann (12).

During ageing a fine precipitation of the insoluble particles (non-magnetic) results. The dis-porsion of these insoluble particles promotes optimum coercivity as a result of their pinning action on do-main walls. The particles grow in size with further ageing and larger is-lands and inclusions are formed. These induce decrease in coercivity from maximum value.

1.8 Effect of Magnetic Annealing:

In order to develop the magnetic properties with commercial viability, further attempts have been made to design new treatments. There are two other techniques worth mentioning for this purpose, namely the magnetic annealing and magnetic cooling both require heating or cooling essentially in a fixed magnetic field in order to facilitate alignment of magnetic domains around the curie temperature during para to ferromagnetic transformation and induce magnetic anisotropy. The coercivity of the alloy depends on the degree of shape anisotropy and effective particle size. This is achieved by the spionodally decomposed microstructure, comprising of interconnected α phase (paramagnetic) in a α'(Fe rich) ferromagnetic matric. The application of magnetic field induces anisotropy in the bulk magnetic parameters as confirmed by Moesbaur spectroscopy (13,14).

Okade (15) has noticed the elongation of the microstructure in the direction of applied field and improvement in magnetic properties in Fe - 28% Cr - 15% Co - 1% Nb alloy.

Cremer and Pfeffier (16) also found a readily obserable induced shape anisotropy in the microstructure of an Fe - 29% Cr - 23.5% Co alloy and noticed that Mo addition enhanced the effect. The particle alignment was parallel to the <100> direction e.g. the direction of applied field.

Kaneko (17) found that particle orientation in a single crystal specimen of Fe - 30% Cr - 23% Co - 1% Si alloy, did not show preferrence for precipitation along defined crystallographic directions, although magnetic properties were marginally better for specimens, field treated in <100> direction.

The effectiveness of the magnetic annealing depends upon various parameters such as magnetic field intensity, temperature and time of annealing.

1.9 Effect of Annealing Atmosphere:

The annealing atmosphere is advisable to be carried out in inert or reducing atmosphere (18). The annealing atmosphere has profound effect on the magnetic properties of Fe - Ni - Al system alloys. It suggests (19) that the atmosphere probably affects the concentration

and distribution of impurity atoms through annealing and through this alters the orientation dependence of grain boundary mobility and thus influence the formation of nucleii. Another group of workers (20) atribute the due effect to an obsorbed otygen layer on the specimen surface, which causes decrease in magnetic properties.

However, many workers feel (19) that H_2 atmosphere annealing develops the best magnetic properties in these alloys, because H_2 being a strong reducing agent, may be instrumental in removing O_2 , C, N_2 or S from the matrix.

1.10 Effect of Cooling Rate on Magnetic Properties:

The rate of cooling affects the grain size and coercivity of alloys. Higher rate of cooling develops stress anisotropy in the solidified alloys after casting which increases the coercivity and remanence. The stress anisotropy constant (K_s) is defined as $K_s = \frac{3}{2} \lambda_{si} \times \sigma$ where λ_{si} is saturation magnetostriction (assumed to be isotropic) and σ is uni-axial stress. For stressed particles of the solidified alloys, the coercivity (H_c) is proportional to $\frac{\lambda_{si} \sqrt{n}}{M_s}$ where M_s is saturation magnetization and n is the dislocation density of the solidified alloy (21).

1.11 The Effect of Grain Size and Inclusion on Magnetic Properties:

Besides dissolved impurities, inclusion and grain size have marked effect on magnetic properties. Uniformity among grain size and distribution is also important as large and small grains scattering is supposed to cause greater magnetic loss because of difference in hysteris characteristics (22).

Pfeiffier (23) summarises the effect of grain size and inclusion on coercivity of Fe - Ni - Al system alloy by the relation

$$H_c = \frac{15}{16} \pi \frac{\gamma_w}{\mu_o M_s} \cdot \frac{1}{d_g}$$

where γ_w is wall energy, M_s is saturation magnetization, μ_o is initial permeability, H_c is coercivity of alloy with inclusion and d_g is grain diameter.

Thus the coercivity of alloy with inclusion is larger than that of pure alloy of same composition. The effect of inclusion size and distribution in Fe - Ni - Al system alloy with alloying elements such as Co, Cu and Cr etc. notes that submicron dispersion of inclusion is advisable for achieving high coercivity by heat treatment (ageing).

1.12 General Methods of Fabrication:

Generally alnice magnet alloys were fabricated by induction melting technique. The earliest method used for fabrication was by solidification of liquid alloy in permanent mold during thermite process, as result of aluminothermic reaction where during solidification rod like precipitates form parallel to the cooling direction. However, the casting approach run into insurmountable difficulties and is ruled out now.

The most commonly used technique for producing alnico magnets is through powder metallurgy route. In this process, pre-alloyed powder such as iron-aluminium or cobalt-aluminium may be taken with elemental iron and nickel powders and after mixing in the correct proportion, they are pressed to shape and sintered in vaccume or purely H_2 (24).

An alternative technique involves the milling of alloyed cast material to powder and compacting to solid form by the inclusion of 30 - 40% by volume thermosetting resin powder and then sintered to form magnets (25).

The other possible variation as the formation of alloy from the pure oxides of components through co-reduction process (26). In this case, the alloy is obtained in fine powder form and hence comminution

steps are reduced. Industrial production method follows classification and blending of powders to get a narrow size distribution of fine powders. The powders are made into compacts of required size under magnetic field so that all the fine particles orient their easy direction of magnetization along the applied field direction (26). Then the important stage is sintering of these green bodies to increase their density. It could be solid state sintering or liquid phase sintering.

In liquid phase sintering, a low melting point powders is added and sintered. The low melting point powder melts and fills the gaps and alloys with the high melting point powder particles of the compact to shift the stoichiometry of the final alloys to the right value. By this method, higher density sintered magnets can be made (27). A post sintering heat treatment is usually given to the sintered magnets to improve their magnetic properties.

Another modern technique (28) used for fabrication of Alnico magnet alloys with fully columnar grained structure. In this process, by careful control of thermal gradients during solidification, it is possible to grow long columnar grains with <100> axes lying along the direction of growth. The columnar grain growth is achieved by casting the molten alloy

into a chill face mould with the side walls pre-heated. Solidification is predominantly from the chill face, giving required orientation of the columnar grains. The addition of sulphur, tellurium and carbon helps the columnar growth.

1.13 Application of Alnico Magnets:

The development of alnico magnets alloys was followed by a great increase in the industrial applications such as in various machines and in electronic devices. Their applications are based on different functions which they can perform.

These are used to convert the mechanical energy into the electrical energy (or vice-versa) in the magnetic field. This function of magnets is used in small electric motors, dynamos, loudspeakers, microphones, speedometers, magnetos etc. The alnico magnets exert a force on a ferro-magnetically soft body. This function of magnets is used in relays, couplings, bearings, clutches, magnetic chucks, clamps and separators (extraction of iron impurities, concentration of ores).

These are also subjected to a direction force exerted by a magnetic field. This function of magnets is used in positioning mechanism, compasses, in some ammeters.

The alnico magnets exert a force on moving charge carriers. This function of magnets is used in magnetrons, travelling wave tube, some cathode rays tube, Hall plates, television devices etc.

1.14 Statement of Problem:

The development of permanent magnets, involving a contineous research for materials, having good magnetic properties, has been going on for past three decades. Many problems are to be solved concerning re-magnetization theory in the magnetically hard materials of the Alnico type. The basic composition and micro addition influence of some elements on the material's magnetic properties have been established. Nevertheless magnetic properties of the Alnico type alloys observed in practice are far from the those theoretically predicted. There is the still unsolved problem of how to reach higher coercive force and magnetic induction values-closer to the theoretical ones - and how to maximize magnetic induction with the highest coercive force existing at the same time.

Although, in India, these Alnico magnets are in use, they are imported from other country. Yet not much effort has been done to fabricate very good permanent magnets of Alnico type. The magnetic properties of these alloys depend on their composition

and processing parameters. Therefore, investigations on the thermal treatment and chemical composition optimization are carried on with the aim of ensuring the existence of conditions for obtaining the better magnetic properties in Alnico type magnet alloys.

REFERENCES

1. A.E. Berkowitz and E. Kneller, Magnetism and Metallurgy, (Academic Press), Vol. I, Page 360-361.

2. K. Hoselitz, Modern Hard Magnetic Materials, Journal of Scientific Instruments, Vol. 23, 65, 1946.

3. R.J. Parker and R.J. Studders, Permanent Magnets and their Applications, John Wiley and Sons, Inc., New York, Page 90-91.

4. W. Betteridge, Fe-Ni-Al Permanent Magnet Alloys, J. Iron Steel Inst., 139, 187-203, 1953.

5. A.S. Yermolenko and A.V. Korolyov, I.E.E.E. Trans. Magn. MAG-6, 252, 1970.

6. W. Betteridge and W. Zumbush, Arch. Eisenbuttenw, 16, 101, 1942a.

7. D.A. Oliver and J.W. Shedden, Nature (Lond) 142, 209, 1943.

8. E. Planchard and C. Bronner, Improvement to the Preparation of Sintered Fe-Ni-Al Co Alloys, I.E.E.E. Trans. MAG-6, Page-304, 1970.

9. W. Wright, Cobalt No-48, 115, 1970.

10. K.J. de Vos, J. Appl. Phys., 29, 302, 1958.

11. R.M. Bozorth, Ferro-Magnetism, Van Nostrand, New York, 1951, Page 522-525

12. K.J. Kromenberg and M.A. Bohlmann, Congterm Magnetic Stability of Alnico and Barrium Ferrite Magnets, J.Appl. Phys., 31, 825 May 1960.

13. M.E. Houghton and P.L. Rossiter, Induced Anisotropy in an Fe-Cr-Co-Al alloy, Phys., Stat. Sol. a43, 71, 1948.

14. S. Miyahara, Effect of Magnetic Annealing on Precipitation of Ferro-Magnetic Phase, Journal Physical Society of Japan, Vol. 71, 534, 1952.

15. M. Okada, XXI Conf. Magnetism and Magnetic Materials, 29, 620, 1975.

16. R. Cremer and I. Pfeiffer Physica, 80B, 164, 1975.

17. H. Kaneko, J. Appl. Phys. 34, 3581, 1963.

18. Hoselitz, Ferro-Magnetic Properties of Metals and Alloys, Oxford Press, 1952, Page-310.

19. Stefan and Arato, Metal Science, 537, Nov. 1977.

20. Morita Fukui, J. Japan Inst. of Metals, 37, 861, 1973.

21. Rado, George T., Suhl and Harry eds., Magnetism (Academic Press), New York, Vol III, 1963, Page 361.

22. B.D. Cullity, Introduction to Magnetic Materials, Addison-Wesely Publ. Co., 1972, Page 317-319.

23. Alderand and Pfeiffer, I.E.E.E. Trans Magn,, 10, 172, 1974.

24. D.K. Das, I.E.E.E. Trans. Magn. 5, 214, 1969.

25. M.G. Banz and D.L. Martin, Appl. Phys. Letters, 17, 176, 1970.

26. D.A. Oliver, Manufacturing of Ferro-Magnetic Materials, U.S. Patent - 2331, 363, Aug. 7, 1945.

27. W. Jellinghous, Fe-Ni-Al-Co-Cu Alloys with Magnetic Preferred Directions, Archiv Fur Das Eisenhuttenwesen, Vol. 16, 247, 1942-43.

28. P.A. Naastepad, Z. Angew Phys., 21, 104, 1966.

CHAPTER - II

THERMITE PROCESS

As the aluminothermic reaction has been used for preparing various Alnico magnet alloys in the present investigation, this chapter deals with the thermodynamic kinetics of the thermite process. A brief description of equipments and materials used in practice and applications of thermite process are also presented.

2.1 Thermite Process:

The preparation of metals and alloys by thermic reduction of metal oxides was discovered by a German Chemist, Hans Goldschmidt (1). He defined thermite reaction as " the reduction of metallic compound by one or several reducing agents in such way that when the mixture (metal compound and reducing agent) is ignited at one place, the reaction continues to go on spontaneously with complete oxidation of the reducing agent, a fluid slag being formed, while the reduced metal or alloy is obtained as a compact regulus.

This aluminothermic reaction is a special case of thermite reaction where aluminium is used as

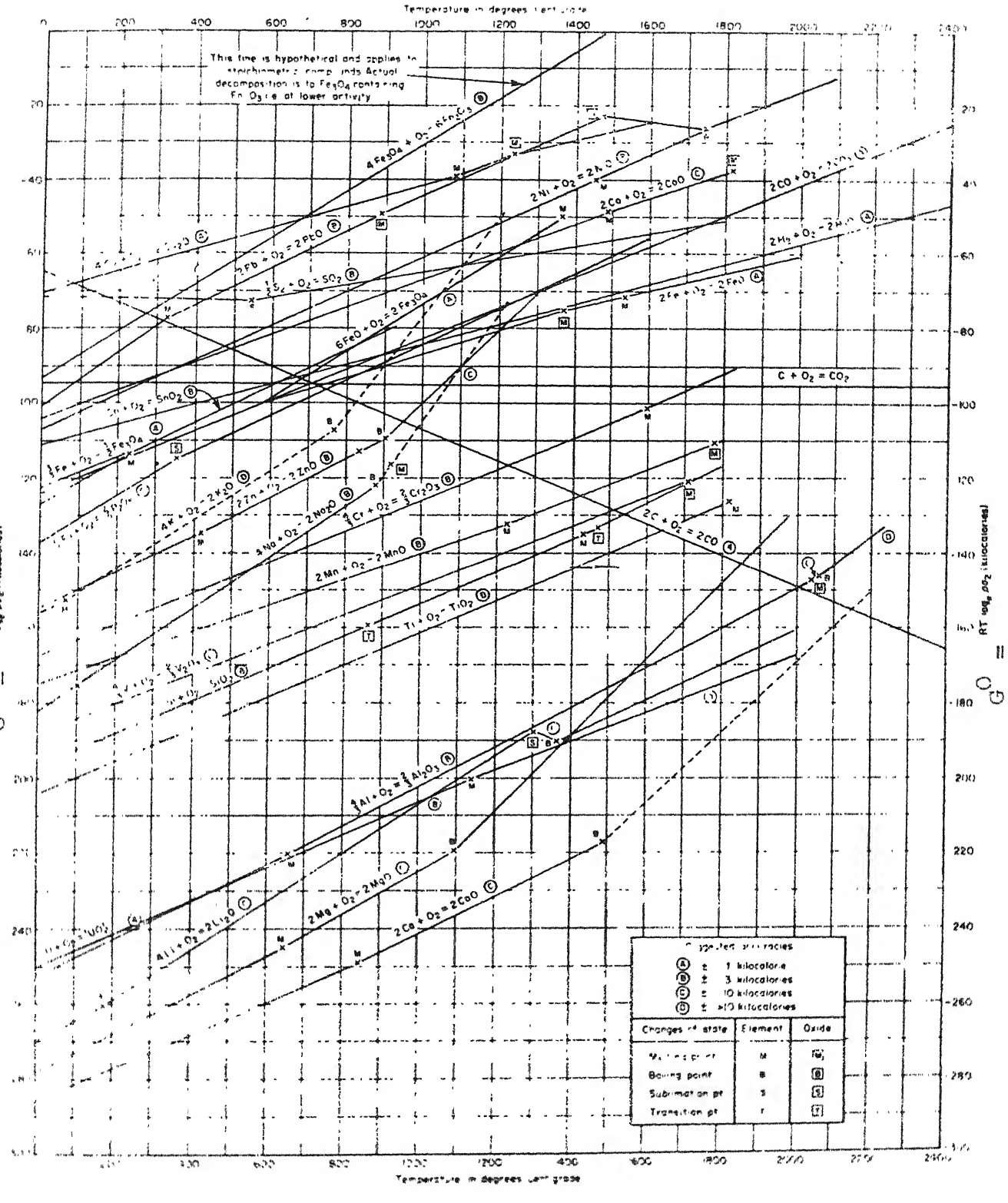

Fig. 2.1 : Free energy diagram for oxides

the reducing agent. The use of aluminium is especially attractive due to its availability in high purity at relatively moderate cost, its chemical stability even in finely powdered form and its tendency to reduce most oxides due to having high affinity for oxygen. Fig. (2.1) shows the standard values of free energy of oxide formation as a function of temperature, related to one mole of oxygen (2).

The least stable of the oxides as shown in Fig. (2.1) is that of Mo and the most stable is calcium oxide (CaO). The stability of oxides decreases with increasing temperature with the exception of carbon monoxide (Co). The data shown in Fig. (2.1) can be used to estimate the possibility of using the element as a reductant.

An element, for example Al, which forms a more stable oxide under appropriate conditions can be used to reduce all the metallic oxides shown in Fig. (2.1) expect those of Ca and Zr. The presence of iron or iron oxides can facilitate some reduction processes. Iron dissolves a reduced element, forms a compound with it and thus lowers the activity of that element and removes it from the reaction zone. The general equation for this process is

$$Me'O + Me'' \rightarrow Me''O + Me' + Heat$$

TABLE NO. 2.2

The temperature function of heat capacity ($Cp(T) = a+b.10^{-3} T + C.10^{+5} T^{-2}$), standard value of enthalpy, entropy, heat of fusion, heat of vaporization of metals

Metal	Entropy ΔS_{293}^{OK} cal/deg/mole	M.P.	B.P.	Heat of fusion (Hf) Kcal/mole	Heat of vaporization (Hv) kcal/mole	$H_T-H_{298}^{OK}$ (2300^{OK})	$Cp=a+bx10^{-3}.T+Cx10^{5}.T^{-}$ cal/deg/mole		
							a	b	c
Al	6.77	660°C	2467	2.55	70.7	17.93	4.94	2.96	-
Al(1)							7.0	-	-
Fe	6.49	1539°C	2877°C	3.70	72.00	33.24	4.18	5.92	-
Fe(1)							10.0	-	-
Ni	7.12	1453°C	2902°C	6.60	89.6	25.26	6.03	-2.49	-
Ni(1)							9.02	-	-
Cr	5.68	1898	2665	5.00	81.28	16.98	5.84	2.36	-.88
Cr(1)							9.40	-	-
Co	7.34	1492°C	2677°C	3.64	91.4	20.96	5.26	2.54	-
Co(1)							9.96	-	-
Cu	7.97	1083	2547	3.12	72.00	13.58	5.41	1.50	-
Cu(1)							7.50	-	-

TABLE NO. - 2.1

Standard free energy of formation of oxides ($\Delta G^{O} = A + BT$) Kcal/mole, Heat of fusion (H_f) Kcal/mole, Standard enthalpy change ($\Delta H^{O}_{293^{OK}}$) Kcal/mole and entropy of oxides ($\Delta S^{O}_{293^{OK}}$) cal/deg/mole

Oxide	$\Delta G^{O}_{293^{OK}}$ Kcal/mole (-)	Heat of fusion (Hf) Kcal/mole	$\Delta H^{O}_{293^{OK}}$ Kcal/mole (-)	S^{O}_{298} cal/deg/mole	ΔG^{O}=A+BT Kcal/mole (Temp. Range - 1500-2300^{OK})	
					A (-)	B (+)
Fe_3O_4	129.43	33.00	267.00	35.00	260.00	.075
Al_2O_3	252.65	26.00	400.4	12.24	425.50	.035
Cr_2O_3	164.35	-	272.7	19.46	230.45	.064
CuO	33.66	-	36.7	10.19	43.30	.023
CoO	104.35	-	57.1	12.66	65.50	.024
NiO	106.65	-	57.3	9.03	60.10	.020

where Me'O is metal oxides and Me" is reducing agent. The reaction is highly exothermic and large negative free energy changes are associated with this reaction as seen from Tables (2.1 to 2.2) and temperature developed during process is expected to be 2525°C.

2.2 Thermodynamic Kinetics:

The general equation for the thermite process is

$$Me'O + Me'' \rightarrow Me' + Me'O + Heat$$

with the equilibrium constant (K) for the reaction as

$$K = \frac{a_{Me''O} \cdot a_{Me'}}{a_{Me'O} \times a_{Me''}}$$

where $a_{Me''O}$, $a_{Me''}$, $a_{Me'O}$, $a_{Me'}$ are the activities of reactants and products. The standard isobaric isothermal potential for the reaction is defined as

$$\Delta Z^{O} = \Delta Z^{O}_{Me''O} - \Delta Z^{O}_{Me'O} \text{ and}$$

$$\ln K = \frac{-\Delta G^{O}}{RT}$$, where ΔG^{O} is the standard free energy change for the overall reaction. Generally the value of K in the thermite process is in the range of 10^{10} to 10^{25}. Thus for the above reaction to proceed from the left to right, the condition

$$\Delta Z^{O}_{Me''O} < \Delta Z^{O}_{Me'O}$$

should be satisfied.

The oxygen potential of oxides (3) is defined as

$$\pi_{O(Me'O)} = \Delta Z^{O}(Me'O) - RT \ln \frac{a_{Me'}}{a_{Me'\,O}} + \varepsilon(\Delta Z)\, Me', Me'O$$

and

$$\pi_{O(Me''O)} = \Delta Z^{O}Me''\,O - RT \ln \frac{a_{Me''}}{a_{Me''\,O}} + \varepsilon(\Delta Z)\, Me'', Me''O$$

where $\varepsilon\ (\Delta Z)\ Me, MeO$ indicates the free-energy change due to phase transformation of metals and oxides.

The effectiveness of the reaction is determined by

$$\pi_{O(Me'O)} > \pi_{O(Me''O)}$$

$$\Delta Z^{O}\ Me'O - RT \ln \frac{a_{Me'}}{a_{Me'O}} + \varepsilon\ (\Delta Z)\ Me', Me'O$$

$$> \Delta Z^{O}\ Me''O - RT \ln \frac{a_{Me''}}{a\ Me''O} + \varepsilon(\Delta Z)\ Me'', Me''O$$

The effectiveness of the reaction can be increased by raising $\pi_{O}\ (Me'O)$ which is achieved by

(1) dissolving the Me' formed in the metal solvent and lowering ($^{a}Me' < 1$).

(2) maintaining $^{a}Me'O \rightarrow 1$ during the process.

The value of $\pi_O(Me'' O)$ can be lowered by

(1) using a pure metallic reducer ($^{a}Me'' \rightarrow 1$)

(2) melting and slaging the oxide (Me'' O)

(3) lowering the activity of oxide Me'' O through the addition of flux ($^{a}Me'' O < 1$).

These factors promote greater completion of the process and recovery of reduced elements. The sucessful preparation of high purity magnetic alloys by the Al reduction depends on the use of an excess amount of Al (about 2% of the required Al).

2.3 Thermochemical Aspect :

Once the reaction is complete, a metallic phase and a lighter slag will separated out. The slag should be in molten state to prevent the oxidation of metallic phase from atmospheric oxygen. The possible thermite reaction between Al and oxides of various metals (4) is as given below:

$$Fe_3O_4 + 8Al = 9Fe + 4Al_2O_3$$

$$\Delta G^{O} \ (2800^{OK}) = - 922 + .115 \ T \ Kcal/mole$$

$$Cr_2O_3 + 2Al = Al_2O_3 + 2Cr$$

$$\Delta G^{O}(2800^{OK}) = - 145 + .021 \ T \ Kcal/mole$$

$$3NiO + 2Al = Al_2O_3 + 3Ni$$

$$\Delta G^{O}(2800^{OK}) = - 245.2 + .025 \ T \ Kcal/mole$$

$$3CoO + 2Al = 3Co + Al_2O_3$$

$$\Delta G^O(2800^{OK}) = -229.0 + .013\ T\ Kcal/more$$

$$3CuO + 2Al = 3Cu + Al_2O_3$$

$$\Delta G^O(2800^{OK}) = = 279.1 + .016\ T\ Kcal/more$$

when calcium oxide (CuO) is used as flux in the process, then following reaction will occur.

$$3Fe_3O_4 + 8Al + 2CaO = 9Fe + 2(CaO \cdot 2Al_2O_3)$$

$$\Delta G^O(2800^{OK} = -922 + .115\ T\ Kcal/more$$

$$2Cr_2O_3 + 4Al + CaO = 4Cr + CaO\ 2Al_2O_3$$

$$\Delta G^O(2800^{OK}) = -145 + .021\ T\ Kcal/more$$

$$6NiO + 4Al + CaO = 6Ni + CaO \cdot 2Al_2O_3$$

$$\Delta G^O(2800^{OK}) = -245.2 + .025\ T\ Kcal/more$$

$$6CoO + 4Al + CaO = 6Co + CaO \cdot 2Al_2O_3$$

$$\Delta G^O(2800^{OK}) = -229.0 + .013\ T\ Kcal/mole$$

$$6CuO + 4Al + CaO = 6Cu + CaO \cdot 2Al_2O_3$$

$$\Delta G^O(2800^{OK}) = -279.0 + .016\ T\ Kcal/mole.$$

2.4 Materials and Equipments:

Materials and equipments required for thermite process can be classified into three headings:

(1) Thermite charge

(2) Ignitors.

(3) Thermite crucible and casting mold.

2.4.1 Thermite Charge:

The charge for aluminothermic reduction contains the oxides of metals to be reduced, Al powder alone or in combination with Si. A fluxing agent such as calcium oxide (CaO) or salt-peter ($NaNO_3$) is used to decrease the activity of slag thereby increasing the fluidity of slag and thermal blast to either absorb or evalve heat depending upon the process.

Studies conducted on thermite reaction rate by Dubrovinetal (6) proved that the decreasing particle size of oxides results in better mixing and faster rate of reduction. This is due to larger contact area available for reaction.

Al is used in the powdered form and has to be mixed with the oxides. A small excess of Al (2% by weight of total Al) is added to make up for the evaporation losses at high temperatures. For fluxing, lime is mostly used, fluorspar (CaF_2) and salt peter ($NaNO_3$) are also used either in combination with lime or separately. Thermal ballast can be in the form of iron ore, scrap iron and sulphur (7). Sulphur is used when the neat evolved during reaction is not enough to

TABLE NO. 2.3

Ferro-alloy charges

All figures refer to weight in kg.

Alloy	Ore	Reducing Agent	Flux	Ballast	Recovery
Fe-Cr	Chrome ore (53% Cr_2O_3) 2900	Al 350	Saltpetre 30	-	87%
Fe-v	Fused V_2O_5 (75% V_2O_5) 970	Fe-Si 380	Lime 1500	Iron trimming 210	98%
Fe-Ti	Ilemite Conc. (38% TiO_2) 1030	Al 400 Fe-Si 10	Lime 100	Scrap 85	70-75%
Fe-Nb	Nb ore conc. (Nb_2O_5) 100	Al 32-34	-	Iron ore 16-17	96%
Fe-Zr	Zirconium conc. 100	Al 67	Lime 30	Iron ore 15	-
Fe-Mo	Mo ore conc. (51% Mo) 1190	Al-56 Fe-Si 362	Lime 265 Fluorspar 3	Iron ore 290 Steel scrap 210	98.7%

melt the products. Scrap iron or iron ore may added for alloying or to remove excess heat to prevent increase in temperature above the desired level. Table (2.3) summarizes the details of the manufacturing processes for some ferro-alloys.

2.4.2 Ignitors:

The thermite charge requires an ignitor to initiate the reaction. The strip of magnesium is used generally which ignites by applying heat. This method is dangerous as the operator does not get much time to move away from the crucible. Bozzelli (8) had developed a safer ignition system using potassium permanganate crystals and glycerin. The reaction between $KMnO_4$ and glycerin is an exothermic oxidation and provides enough heat to initiate the thermite reaction. A charge of about 1 kg requires 15 gms $KMnO_4$ and 5-10c.c. of glycerin. The $KMnO_4$ is placed in a depression on the surface of hot (200°C) thermite charge and glycerin is then added. The time taken for thermite reaction to initiate is about 30-60 seconds as giving ample time for experimenter to move away from the site of the reaction.

2.4.3 Thermite Crucible and Casting Mold:

A cylindrical steel vessel (15 cm dia, 15 cm height), open at the top and a hole of about 2 cm. dia.

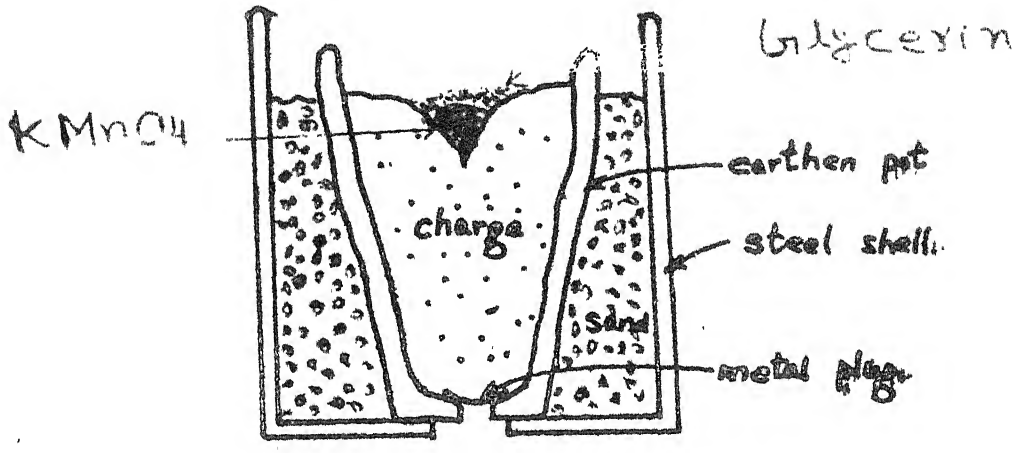

Arrangement for firing

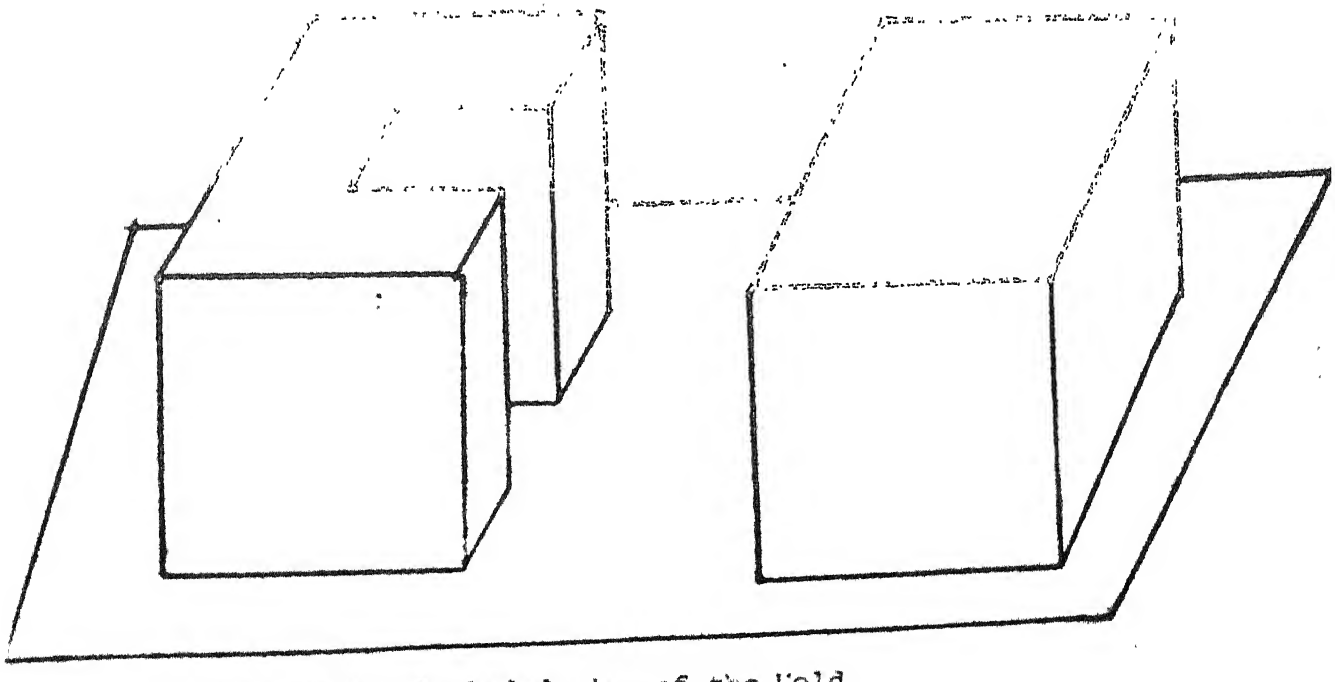

Fig. 2.2 : Exploded view of the mold

at the bottom centre is used. Holds were provided for lifting the heated vessel. An earthen pot with a hole (.5 to .8 cm dia) drilled through its base and a Al foil is placed over this hole, was used to hold the charge. This was placed inside the vessel and the intervening space was packed with sand. The two holes had been aligned to be one over the other.

Since a large number of ingots had to be made, it was thought that making a sand mold every time would be tedious. Therefore, a permanent mold of cast iron as shown in Fig. (2.2) was used. The stacking of the liquid metal, alloy and slag to the surface of the mold was avoided by coating the walls with graphite.

2.5 Applications:

Simple thermochemical concept of thermite process has received much attention in industrial applications due to the following advantages (9).

(1) The expensive step of preparation of metals or alloys is eliminated.

(2) Inert gas atmosphere, which is essential if highly reactive metals is handled, may not be required for this process.

(3) Alloying with a metal whose density is far too low compared to that of base metal might lead to segregation. However, with this process,

this problem is significantly reduced.

A few of the important applications are being discussed in the following paragraphs.

2.5.1 The Preparation of Ferro-Alloys:

The thermite process using alluminothermic reduction is used in the production of ferro-chrome, ferro-vanadium, ferro-titanium, ferro-niobium, ferro-molybdenum and other ferro-alloys (10, 11). This insures the production of carbon free products (12).

2.5.2 The Preparation of Nuclear Materials:

Aluminium - plutonium alloys which find application as fuel materials in research reactor and as spike elements in power reactors have been largely prepared by aluminothermic reduction (13). The chemical reaction involved in the process is as given below:

$$PuF_3 + Al = Pu + AlF_3$$

$$\Delta G^0_{1500^{OK}} = -15 \text{ Kcal/mole}$$

$$3PuO_2 + 4Al = 3Pu + 2Al_2O_3$$

$$\Delta G^0_{1500^{OK}} = -42 \text{ Kcal/mole}$$

Plutonium yields average 99.8 and product quality is quite high. Similarly alloys of gallium, germanium and silicon can also be prepared by aluminothermic reduction (14).

this problem is significantly reduced.

A few of the important applications are being discussed in the following paragraphs.

2.5.1 The Preparation of Ferro-Alloys:

The thermite process using alluminothermic reduction is used in the production of ferro-chrome, ferro-vanadium, ferro-titanium, ferro-niobium, ferro-molybdenum and other ferro-alloys (10, 11). This insures the production of carbon free products (12).

2.5.2 The Preparation of Nuclear Materials:

Aluminium - plutonium alloys which find application as fuel materials in research reactor and as spike elements in power reactors have been largely prepared by aluminothermic reduction (13). The chemical reaction involved in the process is as given below:

$$PuF_3 + Al = Pu + AlF_3$$

$$\Delta G^{O}_{1500^{OK}} = -15 \text{ Kcal/mole}$$

$$3PuO_2 + 4Al = 3Pu + 2Al_2O_3$$

$$\Delta G^{O}_{1500^{OK}} = -42 \text{ Kcal/mole}$$

Plutonium yields average 99.8 and product quality is quite high. Similarly alloys of gallium, germanium and silicon can also be prepared by aluminothermic reduction (14).

2.5.3 Aluminothermic Welding:

The reaction between Fe_2O_3 and Al is used to weld steel parts.

$$Fe_2O_3 + 2Al = 2Fe + Al_2O_3$$

$$H_{298}^{OK} = 204 \text{ Kcal.}$$

The heat liberated by this reaction is sufficient to obtain liquid iron and slag at temperatures from 1600°C to 1800°C. Thus welding of steel parts is easily possible (15,16).

2.5.4 Production of Refractory Metals:

There have been a number of papers pertaining to the preparation of refractory metals by aluminothermic reduction. Studies on the effect of particle size and relative amount of Al powder have been done by Pliner (17). Dubrovin et al (18) studied equilibrium distribution of Cr in the slag phase. Deryabin (19) added chromium oxide to molten aluminum and studied the effects in order to avoid the explosion hazards and lower yields of Al - Cr_2O_3 powder reaction.

To prepare high purity vanadium at least 10% Al should be present in V as this suppresses solubility of oxygen. Subsequent removed of volatile Al_2O is done by high temperature vaccum sintering. This investigation was carried out by Carlson (20). Carlson and

Schmidt investigated the use of a water cooled crucible as reaction vessel, which resulted in metal of lower N_2 content and consistently higher yields. Wang et al (21) modified this process and adopted it to commercial operation so that Al and oxygen wore removed during consolidation step by electron beam melting. Carlson (20) and Schmidt were able to Co - reduce U_2O_5 containing Nb_2O_5 , Ta_2O_5, MoO_3 or TiO_2 to binary alloys of V.

Wilhelm et al (22) prepared high purity niobium from Nb_2O_5. The charge bom is heated to 650°C. Any Al, O_2 or N_2 retained in the reduction product is removed during electron beam melting to give a product containing less than .003% of each impurity. This process is now used commercially.

Because of the low heat reaction of Al with Ta_2O_5 , Gupta and Jena (7) used sulphur as a thermal booster. The aluminum sulphide also serves as a flux for slag formation by forming an Al_2O_3 - Al_2S_3 eutectic. Wilhelm et al (23) accomplished similar results by adding an alloying element such as iron or manganese to form a lower melting eutectic with tantalum. Additional heat is supplied by $KclO_4$ as thermal booster. Iron or manganese with aluminum and oxygen can be removed by electron beam melting.

Mayar and Hubler (24) patented a process for producing niobium or tantalum in an open crucible. The unique feature is the addition of cupric oxide to the charge . Copper which is insoluble with Ta, Nb , wets the metal powder thus forming a protective coating around the individual particles. This adds in the coulesence of powders during subsequent melting or sintering. Copper is then removed by treatment with nitric acid.

Gupta and Jena (25) have been able to achieve yields of upto 70% in the aluminothermic reduction of molybdenum and tungston trioxides. Schmidt (26) has improved the process to increase the yield to 90% at the same time obtaining of 99.98% purity.

2.55 Coatings by Aluminothermic Process:

Panteleenko et al (27) used a mixture containing Al_2O_3 - 38, Al - 18, Cr_2O_3 - 48 and NH_4Cl - 2% (by weight) for chromizing steels preliminary galvanizing resulted in a 1.3 - 11 fold increase in the chromizing rate and significant increase in wear resistant of the coating. Service life of the galvanized-chromized screws was 3 - 3.7 times longer than uncoated ones. Conventional chromizing without galvanizing gave only 1.6 - 1.8 fold increase in service life.

Lyakhovich et al (23) developed a process for chromizing steel by aluminothermy. A two component (Cr and Si) saturation method was developed for steel using aluminothermic reduction of Cr_2O_3 and SiO_2 in the presence of NHucl activator in Al_2O_3 pack. Coatings rich in Cr_3Si and Fe_3Si with micro hardness of 715 - 800 kg/mm^2 was formed on Armco iron.

Lyakhovich et al (29) investigated thermochemical treatment of austenitic steel. Diffusional saturation of stainless steel with Cr, B, Cr - Si and Cr - Ti was studied using Al reducible Cr_2O_3, B_2O_3, SiO_2 and TiO_2 as saturation element source optimal cementation treatments increased the wear resistance 20 fold for boronizing, 6-7 for chromosiliconizing, 3 for chromizing and 1.2 times for chromizing with Ti - cementation. Boronizing did not protect the steel from high temperature gas corrosion, but other diffusional coatings increased the oxidation resistance ofthe steel by 1.2 - 1.5 times.

Yurasko (30) patented a flame spray method for coating metals with a metallothermic mixture containing a thermite component and one or more coating metals. During spraying the coating metal is superheated to a bonding temperature, resulting in high adherence. The powder blend used was 50% agglomerated NiO with 50% Al as powder of 5μ diameter bonded with sodium silicate.

The mixture was flame sprayed in an oxyacteylene torch on to a grit blasted steel substract. The resultant coating bond strength of 7245 psi was obtained. For 95% Ni with 5% Al held togather with a phenolic blinder the bond strength was only 5700 psi.

Taguchi (31) has patented coating compositions for molds. Metal oxides and aluminium were coated on to mold to diffuse on cast iron, steel or copper to improve corrosion resistance, heat and abrasion. Thus a coating composition was prepared from 152.2 gm Cr_2O_3, 53.96 gm Al and a phenolic resin as blinder.

REFERENCES

1. O.N. Carlson, Reduction of Oxides by Metals, Progresses in Extractive Metallurgy, Vol-I, Editor F. Hahashi.

2. J. Mackowiak, Physical Chemistry for Metallurgists, Editor George Allen and Unwin Ltd., 1965, Page 160-162.

3. S. Filipov, The Theory of Metallurgical Processes, Mir Publishers, Moscow, 1975, page 169-171.

4. Clarences, E. Sims, Electric Furnace Steel Making, Vol-II, page 132-136.

5. A.W. Espelunel, Aluminothermic Reduction, J. of Chem. Educ. 58, 400, (1975).

6. Dubrovin, Silepova and Kuznetsov, Fiz, Goreniya Vzryra, 6(I), 64-72 (1970).

7. C.K. Gupta and P.K. Jena, Production of Tantalum by Aluminothermic Reduction, Metals, 20, 25-23 (1963).

8. J. Bozzelli, B.B. Robert and J.B. Hickey, Thermite Lecturer Demonstration, J. of Chem. Educ. 56 (10) 675-676. (1979).

Acc. No. 38019

9. A. Volsky and E. Sergievskaya, Theory of Metallurgical Processes, M R. Publishers, Moscow, page 258-260.

10. G.W. Clark, D.H. Dainty, Thermite Smelting of Ferromoybdenum, U.S. Patent 4, 047942.

11. B. Paczula and Z. Kulmski, Making of Ferro-molybdenum by Alumino-silico-thermic method, Prace. Inst. Hutnic, 10 , 143-145 (1958).

12. E. Kanno and C. Yamamoto, Jab. Patent, 7678, 726.

13. J.D.T. Cappochi, E.G. Gertile and R.B. Tracanelia, Production of Al - Pu and Al - Pu - U alloys by liquid Aluminium, Met. ABM, 24, 331 - 841 (1969).

14. J.I. Keuchi, Nuclear Materials by a Thermite Process, Nipton Knzoku Gakkaishi, 40, 320-324 (1932).

15. G. Werneranel W. Brenner, New Brazzing Technology for Workshop and Site Applications, Ger. Patent 19763 - 324.

16. M.E. Ashton and A.J. Key, Aluminothermic Welding of Austenitic Managanese Steel, U.S. Patent 421, 6816.

17. Y.L. Pliner, E.A. Rubinshtein and A.S. Dubrovin, Fusion Rate of Aluminothermic Charge, Sb. Kly. Zavoda Ferrosplavov, 3 , 31-41 (1967).

18. A.S. Dubrovin, L.N. Rusakov, Y.L. Pliner and G.F. Ignatenko, Distribution of Chromium in Aluminothermic Slags, Sb. Tr. Kly. Zavoda Ferrosplavov 1, 50-55 (1965).

19. Y.A. Deryaben and S.I. Suchilnikov, Smelting of Technical Chromium Using Liquid Aluminium, Izv. Vyssh. Vcheb. Zaved. Chern. Met. 2, 57-62 (1963).

20. O.N. Carlson, F.A. Schmidt, W.E. Krupp, A progress for preparing vanadium, J. Metals, 18 320-323,(1966).

21. C.T. Wang, E.F. Baroch, Y.S. Shen, S.A. Worcester, Preparation and Properties of High Purity Vanadium, Met. Trans. 1, 1633-39 (1970).

22. H.A. Wilhelm, F.A. Schmidt, I.G. Ellis, Niobium by Aluminothermic Reduction, J. Metals, 18, 1303-09, (1966).

23. H.A. Wilhelm, R.M. Bergman, F.A. Schmidt, Tantalumby Bomb Reduction of Ta_2O_5 , J. Metals, 22, 45-49 (1970).

24. A. Mayer and W.R. Nubler, Niobium and Tantalum, Can. Patent 620,036 (1961).

25. C.K. Gupta and P.K. Jena, Aluminothermic Reduction of Tungstic Oxide, J. Lees Common Metals, 2, 269-73, (1967).

26. F.A. Schmidt, R.M. Bergman, O.N. Carlson H.A. Wolhelm, Molybdenum by Bomb Reduction of MoO_3. J. Metals 23, 33-44, (1971).

27. F.I. Panteleenko and L.G. Voroshin, Chromizing of Preliminarily Galvanized Carbon Steels, Izv. Vyssch. Uchben. Zoved. Chem. Metall. 18, 62-63 (1980).

28. L.S. Lyakhovich, L.G. Voroshin and G.V. Borisenok, Chromizing of Steels, Prog. Inetodykhim, 159-66, 176-32 (1979).

29. L.S. Lyakhovich, L.G. Voroshin and G.V. Borisenok, Thermochemical Treatment of Austentic Steel, Prog. Metody. Khim, 166-71, 76-32, (1979).

30. G.J. Yurasko, Metallothermic Powder, U.S. Patent 4, 202, 691.

31. C. Taguchi, Coating Composition for Molds, Jap. Patent 7951424.

CHAPTER - III

EXPERIMENTAL PROCEDURES, RESULTS, DISCUSSIONS AND CONCLUSIONS

ABSTRACT:

An entirely new method for the preparation of permanent magnetic alloys, using aluminothermic reduction is discussed. The methods of characterizing these alloys, using techniques of optimal metallography, chemical analysis, X-ray diffraction, micro-hardness measurement, magnetization and electrical resisvity measurements are also described. The results of the present investigation are also presented and discussed in this chapter.

3.1 EXPERIMENTAL PROCEDURE:

3.1.1 Preparation of Alloys:

The materials used in the preparation of alloys were Fe_3O_4 , obtained locally in the form of flakes with size ranging from (1 to 5 mm), Cr_2O_3 , NiO, CoO, CuO and Al powder (- 325 mesh), supplied by Sisco Research Laboratory, Bombay. Calcium oxide (CaO) was obtained in the form of lumps, supplied by Galxo Laboratory, Bombay.

TABLE 3.1

Experimental Charges (wt. in gms)

* Refers to Stochiometric.

Alloy composition (wt%)	Fe_3O_4	NiO	Al	Cr_2O_3	CoO	CuO	CaO	Total
(Fe-Ni-Al-Cr) system								
1. Fe-20% Ni-5% Al-5% Cr	530.44	152.70	288.00	43.86	-	-	272.16	1337.1
2. Fe-20% Ni-5% Al-6% Cr	555.54	168.00	235.96	52.62	-	-	270.23	1332.3
3. Fe-24% Ni-5% Al-7% Cr	530.70	183.24	285.00	61.40	-	-	269.32	1329.6
4. Fe-26% Ni-5% Al-8% Cr	505.30	198.54	284.04	70.14	-	-	268.42	1326.9
5. Fe-27% Ni-5% Al-9% Cr	489.24	206.16	283.92	78.96	-	-	268.14	1326.4
6. Fe-28% Ni-5% Al-10% Cr	472.68	213.78	283.27	87.72	-	-	267.70	1325.1
(Fe-Ni-Al-Co-Cu) system								
7. Fe-20% Ni-10% Al-5% Co-2% Cu	522.36	152.70	287.40	-	38.16	15.00	271.59	1237.2
8. Fe-18% Ni-10% Al-10% Co-3% Cu	489.24	137.46	287.01	-	76.32	22.56	271.22	1283.8
9. Fe-16% Ni-10% Al-12% Co-4% Cu	480.90	122.16	285.90	-	91.56	30.04	270.13	1280.7
10. Fe-15% Ni-10% Al-15% Co-5% Cu	458.34	106.92	285.35	-	114.42	37.56	269.66	1272.3
11. Fe-12% Ni-10% Al-20% Co-6% Cu	431.16	91.62	285.24	-	152.58	45.06	269.55	1275.

followed by addition of about 10 - 15 c.c. glycerin. The reaction starts spontaneously, the melt was cast in the mold.

Most of the characterizations involve regular shape samples of specibic dimension. For this, the specimens of suitable dimensions were cut from the cast ingots with the help of Silicon-carbide cutting wheel and microslicer cutting machine.

3.1.2 Heat Treatment

3.2.1 Annealing:

The specimens were annealed in H_2 gas with flow rate of 1 c.c./minute at 1000°C $\pm$ 4°C for 3 hours. The specimens were loaded on refractory trays, placed in the middle zone of the furnace. The temperature of the furnace was controlled within $\pm$ 5°C. The heating rate of the furnace was 3°C/minute and the holding time of the samples at 1000°C was 3 hours. The samples were cooled under hydrogen with rate of 8°C/minute.

3.2.2 Tempering:

The annealed specimens were further tempered at 650°C for $3\frac{1}{2}$ hours in H_2. The flow rate of H_2 is the same as in the case of annealing.

3.2.3 Magnetic Ageing:

The magnetic ageing was carried out in H_2 gas under constant magnetic field using polytronic Electro-magnet, Type HEM-75 S.R. No. - 12. For this a specially designed furnace with smaller diameter (in order to fit between the pole pieces of the magnet) was used. The specimens were aged at 650°C for 1/2 hr. at 1.2 K . Oe under hydrogen stream. At the end specimens were furnace cooled in the applied field in H_2 with flow rate of 1 c.c./minute. The heating rate was 3°C/min and cooling rate was 4°C/minute.

3.3 Chemical Analysis:

The large samples of each alloy were cut from the ingots and turned out to remove blow holes and pining defects, developed during casting. The alloy was homogenised at 1000°C for 3 hours in H_2 gas and chemically analysed and the analysed compositions of each alloy were reported in Table (3.2).

3.4 Optimal Metallography:

For the metallographic study, the flate surface of the specimens was first polished successively on 1/C through 4/O emery paper taking care that no deep scratches were produced during polishing. The specimens were thoroughly washed in flowing water and again

subjected to polishing on a rotary wheel covered with selvyt cloth using a water slurry of submicron size (0.05μ) alumina as a polishing abrasive. After polishing, the specimens were washed in running water and dried and etched with 10% Nital (a mixture of 10 c.c. of HNO_3 and 90 c.c. of methonal). The etching time varied from 2 swabs to 10 swabs depending upon the composition of specimens. The microstructures were examined using Zeiss Universal Metallograph and were recorded on a 35 mm Ilford photographic film (160 ISA).

3.5 X-ray Diffraction:

The specimens were mounted on perspex sheet of 3 cm square sized with araldite so that flate surface could be ground easily. The polished specimens with flat parallel surface, were studied using a Rich Seigfert 2002 D X-ray Generator and Isodebyeflux diffractometer. The Crkα (λ = 2.291002A°) was used as X-ray source using a graphite monochromater in the path of the diffracted beam. This offered partially background free, β-radiation free, high resolution diffraction patterns for phase(s) analysis, present in the synthesized products.

The diffraction pattern was obtained under following conditions:

Radiation - Crkα (λ = 2.291002A°)

Tube voltage = 40 K.V.

Tube current = 30 mA

Scanning rate = 3°/min in 2 θ

Chart speed = 3 cm/minute

Time constant = 10

Intensity range = 20 K Counts/minute

Angular Range of scanning = $25° \leq 2\theta < 152°$.

3.6 Microhardness Measurement:

Microhardness of polished samples as mentioned earlier, were measured using Leitz Miniload - 2 Microhardness Tester. The diamond pyramid indentor of the tester was forced onto the surface being tested with a load of 50 P force and the indent was made well within the grain boundary of each phase so that the hardness value obtained did not have any influence due to neighbouring grain. Measuring the length (d) of two diagonals of the indentation with the help of a microscope, the microhardness values were calculated in terms of Vickers Hardness Number using the expression

$$V.H.N. = 189 \times 10^3 \times \frac{F}{d^2}$$

where F is the applied load defined as F = 50 P = 490.3mN and d is the average length of diagonals (in unit of μm).

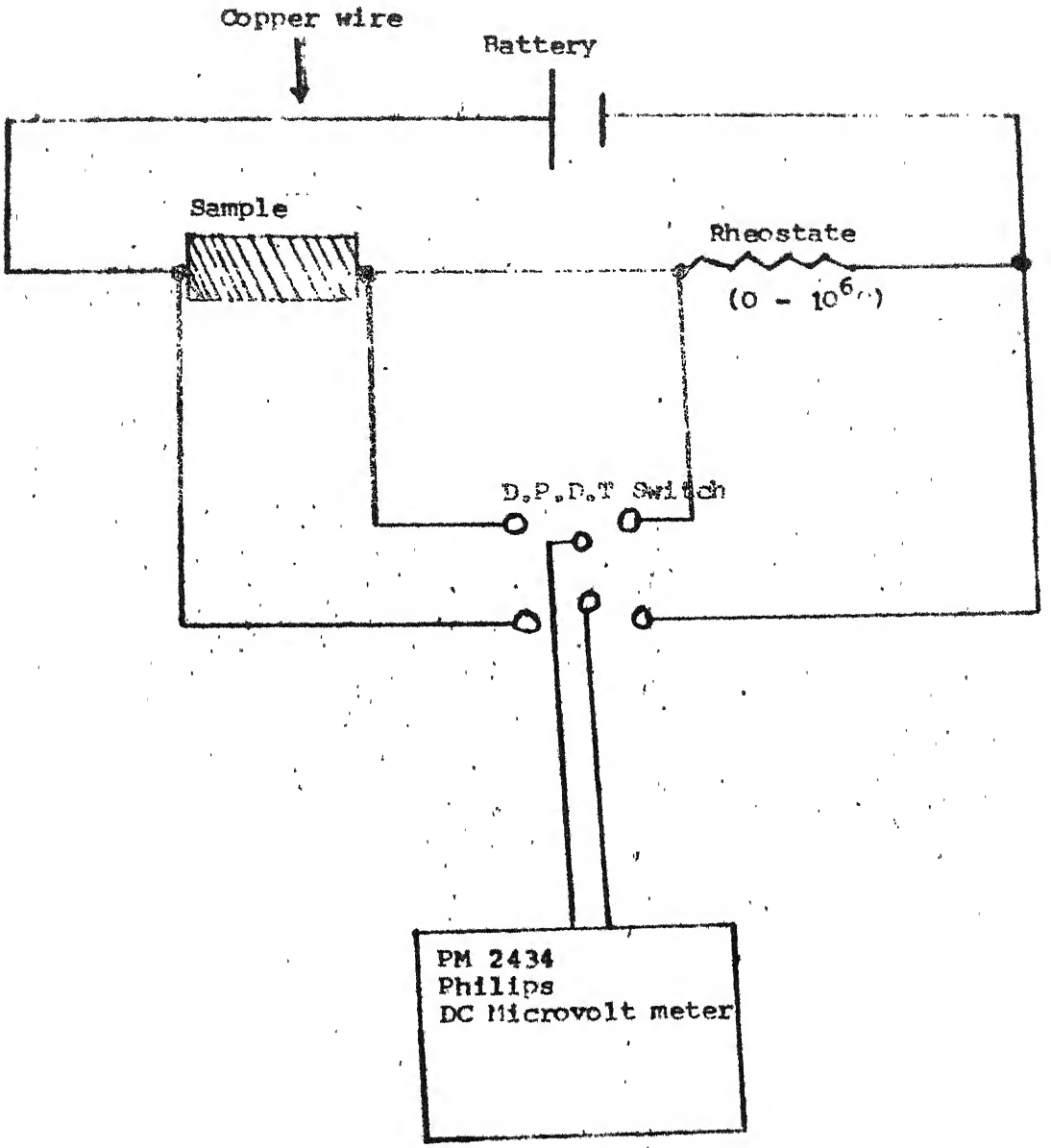

Fig. 3.1 : Circuit for measuring the Electrical Resistivity of magnetic materials.

The microhardness of each phase was measured on many grains and the average value was calculated. The microhardness of each alloy was measured in as cast and annealed conditions.

3.7 Resisvity Measurement:

The samples were polished. Two copper wire probes were fixed in the opposite faces of polished samples with the help of silver paint and araldite.

The circuit for measuring the resistance of sample is shown in Fig. (3.1). A rheostate was connected in series with the unknown resistance of the sample. The resistance of the sample was calculated by knowing the total voltage supplied and the voltage drop across the rheostate by PM 2434 Philips D. C. microvoltmeter. The resisvity of the sample was calculated by calculated resistance of the sample with the following relation

$$R = \rho \cdot \frac{l}{A} \text{ , where}$$

R is the resistance of sample in $\mu\Omega$,

ρ is the resisvity of sample in $\mu\Omega$ - cm ,

l is the length of specimen in cm. and A is the contact area of sample in cm^2.

3.8 Magnetic Characterization:

The properties of particular interest for present study of a permanent magnet are saturation magnetization (M_s), remanence magnetization (M_r) and intrinsic coercivity (^iHc) and dependence of these on various processing parameters.

Samples for magnetic studies were cut into suitable dimensions with the help of microslicer cutting machine provided their maximum dimensions did not exceed 3 cm x 3 cm x 3 cm. APAR 150A Vibrating Sample Magnetometer, supplied by Princeton Applied Research Corp., New Jersey, was used for measurement of M_s, M_r and ^iHc with the maximum attainable field of 10 K. Gauss. The as cast and annealed with tempered with and without magnetic field samples, were studied at room temperature. The principle of the magnetometer is described below in brief.

A sample of the material whose magnetic moment is to be measured is placed in a sample holder. The sample holder is mounted on the end of a rod and suspended and vibrated in the fixed of the electro-magnet. The sample is vibrated in an uniform magnetic field by means of a transformer at a amplitude. The induced field in the sample induces a e.m.f. in a pair of stationary pick up coils. The induced e.m.f. is amplified

by a suitable electromic circuit and converts it into magnetic moment in electro-magnet unit (e.m.u.).

The system is calibrated using the 3/32" dia x 3/32" long cylindrical sample of high purity Ni for which the saturation moment is 55 e.m.u/gm.

The sample is mounted between the electro-magnets in a perspex sample holder and is aligned and adjusted there by locating it symmetrically with respect to the detection coils. The main benefit of making this adjustment is that the different samples were adjusted to the same position, relative to the pick up coils, this minimizing the effect of geometry on the result of measurement. The sample is first taken to saturation by increasing the field strength (H) of the electro-magnet to its maximum value (10 K . Oe) where the magne-to panel meter reads the value of M_s in e.m.u. The field strength is then reversed to zero and the value of M_r is noted from panel meter. Field direction is then reversed and the field strength is increased slowly till the panel meter reads zero magnetic moment of the sample. Thus we know the value of intrinsic coercivity (^{i}Hc) at which the magnetic moment of the sample is zero.

3.2 RESULT:

3.2.1 Chemical Composition:

The results of the chemical analysis of various alloys (Analysed Composition) is reproduced in Table (3.2) in the last column. The first column represents the composition of starting materials (Nominal Composition) before the thermite ignition. The difference between these two is the result of evaporation of constituent elements or oxides due to high reaction temperature.

3.2.2 Optical Metallography:

The microstructures of Fe-Ni-Al-Cr system alloys reveal wide-spread precipitates of irregular spaced spherical particles of various shapes and sizes with some inclusions through out the matrix. The grain boundaries were found not to be clearly delineated. The optical micrographs revealed features of phases as one dark black and other grey. The dark areas are due to inhomogeneous distribution of alloying elements in Fe-matrix. Fig. (3.2) (a, b, c, d, e, f) show microstructures of alloys of this system both as cast and annealed conditions. The annealed microstructures as seen from Fig. (3.2) (d,e,f) show that precipitate particles and inclusions are elongated and highly dispersed to be distinctly resolved.

TABLE 3.2

Nominal and Analysed Composition of synthesized alloys

Sample No.	Nominal composition in wt.pct.						Analysed composition in wt. pct.					
(Fe-Ni-Al-Cr) System	Fe	Ni	Al	Cr	Co	Cu	Fe	* Ni	Al	Cr	Co	Cu
1.	70	20	5	5	-	-	82.34	11.62	2.54	3.50	-	-
2.	67	22	5	6	-	-	79.83	12.32	2.63	4.72	-	-
3.	64	24	5	7	-	-	76.60	14.92	2.52	5.96	-	-
4.	61	26	5	8	-	-	74.77	16.12	2.56	6.55	-	-
5.	59	27	5	9	-	-	72.32	17.66	2.59	7.43	-	-
6.	57	28	5	10	-	-	68.67	20.22	2.54	8.57	-	-
(Fe-Ni-Al-Co-Cu) System												
7.	63	20	10	-	5	2	77.25	14.02	4.56	-	3.01	1.16
8.	59	18	10	-	10	3	74.08	11.95	4.96	-	6.98	2.03
9.	58	16	10	-	12	4	73.17	10.94	4.89	-	8.04	2.98
10.	56	14	10	-	15	5	72.11	8.99	4.89	-	10.00	4.01
11.	52.	12	10	-	20	6	70.98	7.10	4.93	-	12.04	4.95

* Ni content is obtained by difference.

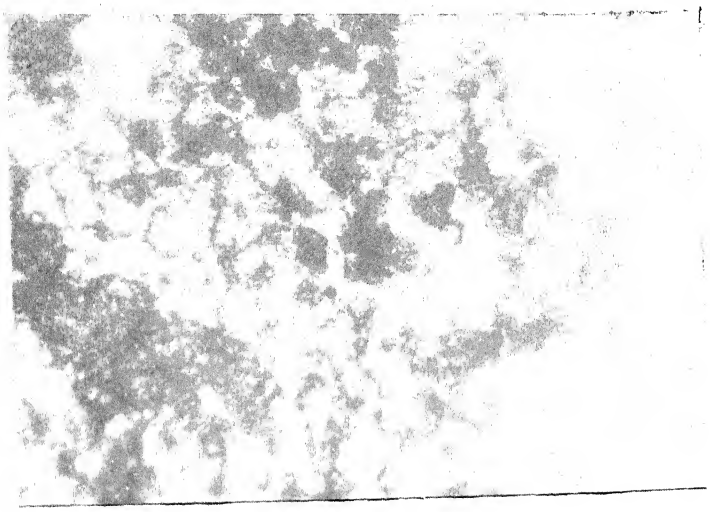

(a) : Microstructure of Fe-11.62% Ni, 2.54% Al, 3.50% Cr as cast (x 300)

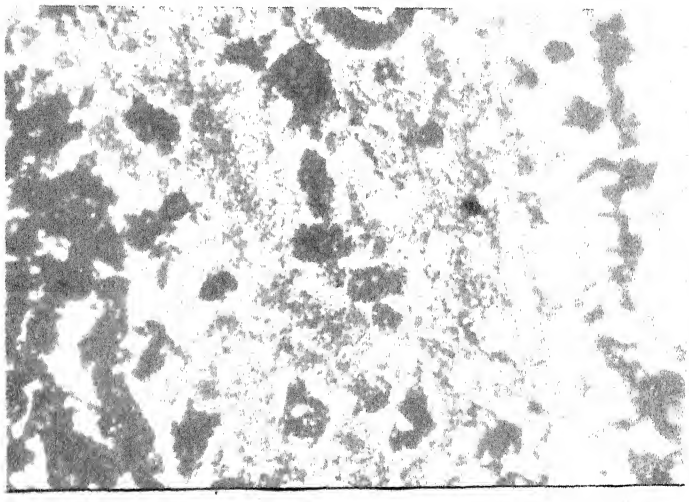

(b) : Microstructure of Fe-11.62% Ni, 2.54% Al, 3.50% Cr, annealed (1000°C, 3hrs) (x 300)

Fig. 3.2 : Optical Micrographs of Synthesized Alnico Alloys

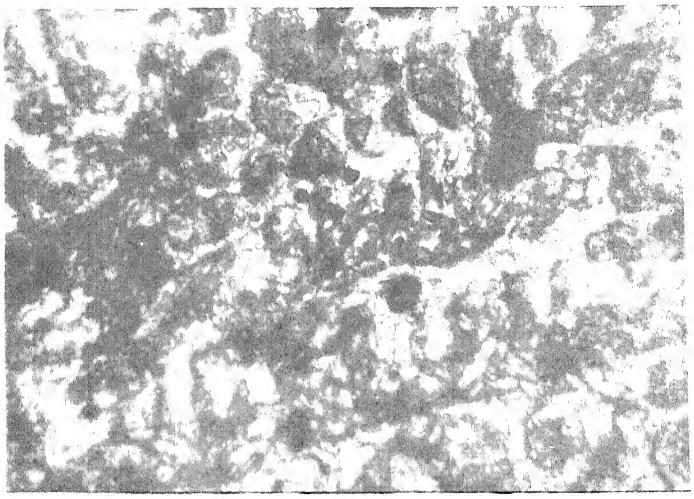

(c) : Microstructure of Fe-16.12% Ni, 2.56% Al, 6.55%Cr as cast (x 300)

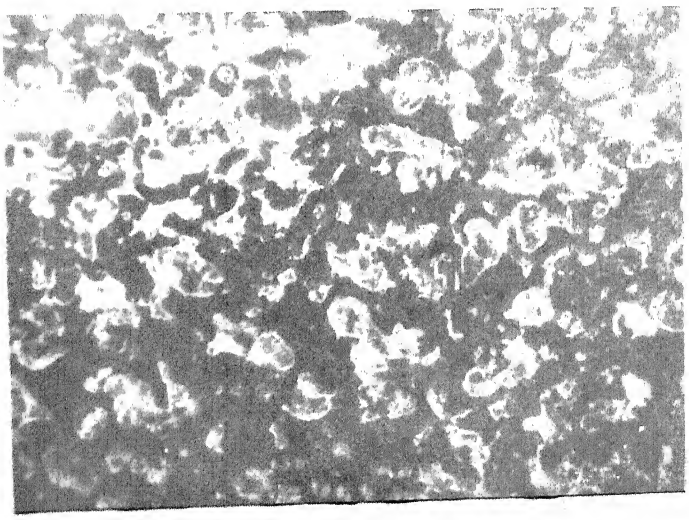

(d) : Microstructure of Fe-16.12% Ni, 2.56% Al, 6.55% Cr annealed (1000°C, 3 hrs) (x 300)

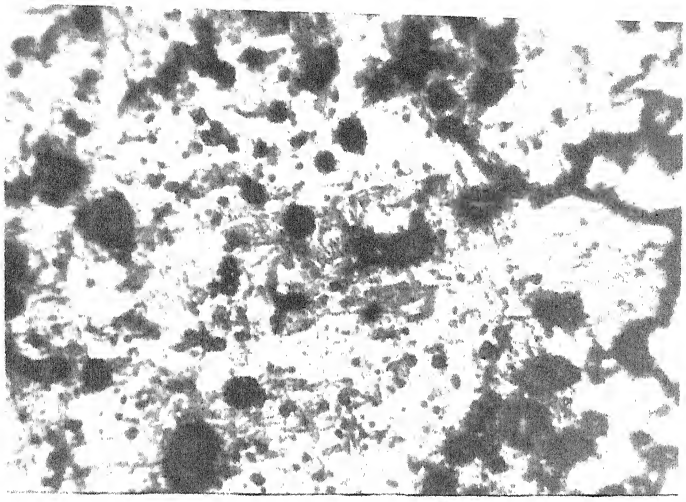

(e) : Microstructure of Fe-20.22% Ni, 2.54% Al, 8.57% Cr as cast (x 300)

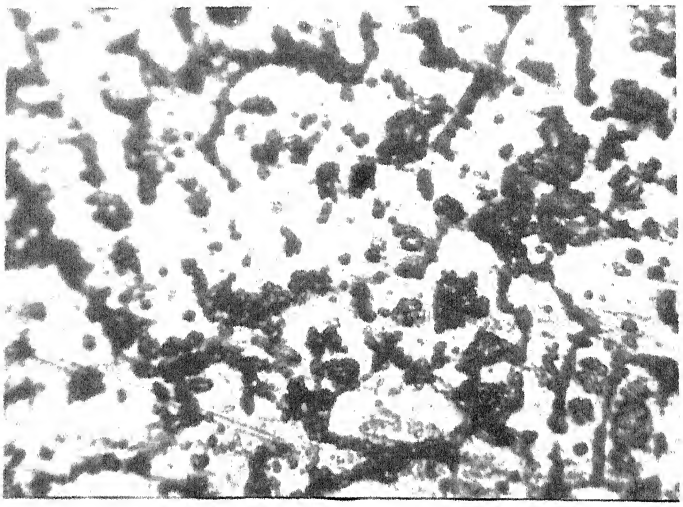

(f) : Microstructure of Fe-20.22% Ni, 2.54% Al, 8.57% Cr, annealed (1000°C, 3 hrs) (x 300)

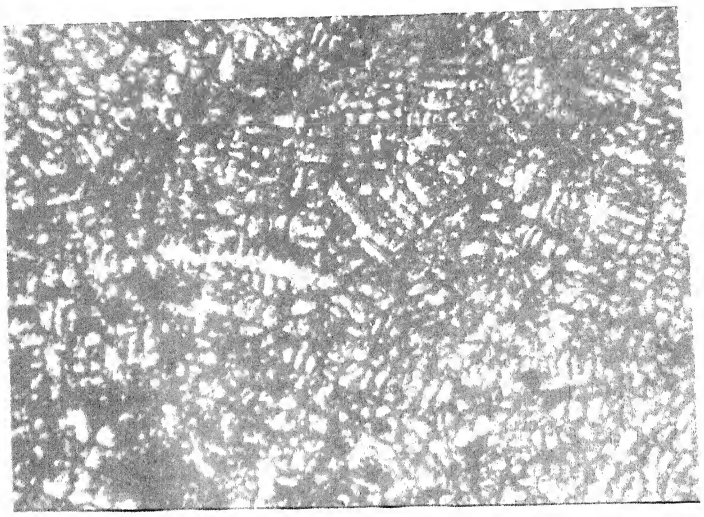

(g) : Microstructure of Fe-14.02% Ni, 4.56% Al, 3.01% Co, 1.16% Cu as cast (x 200)

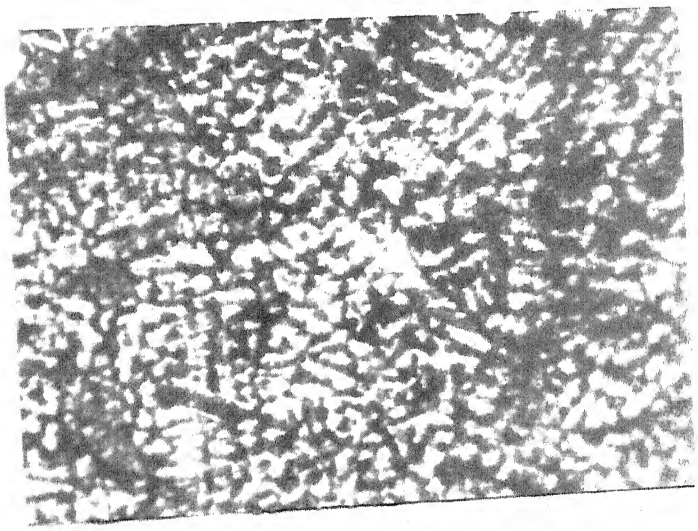

(h) : Microstructure of Fe-14.02% Ni, 4.56% Al, 3.01% Co, 1.16% Cu, annealed (1000°C, 3 hrs) (x 200)

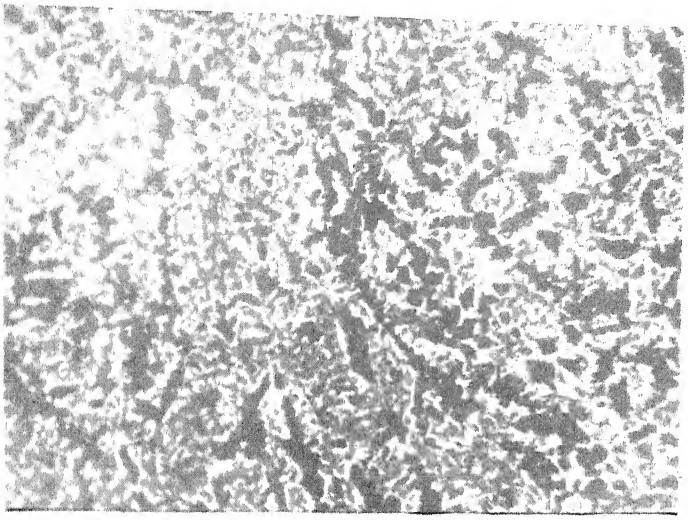

(k) : Microstructure of 10.94% Ni, 4.89% Al, 8.04% Co, 2.98% Cu, as cast (x 200)

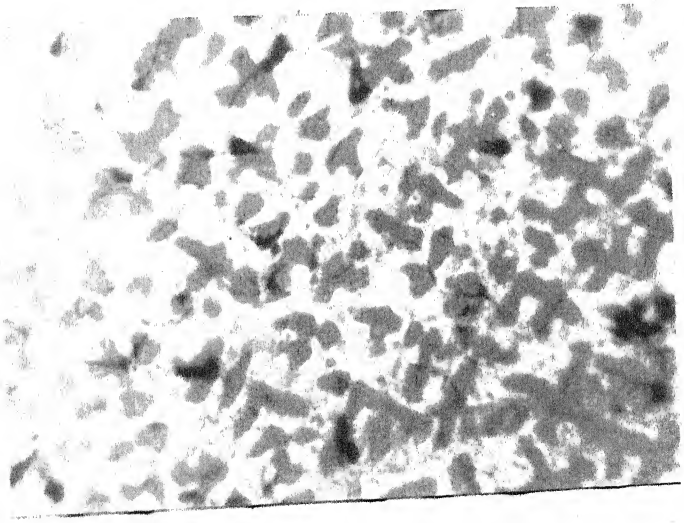

(l) : Microstructure of 10.94% Ni, 4.89% Al, 8.04% Co, 2.98% Cu, annealed (1000°C, 3 hrs) (x 200)

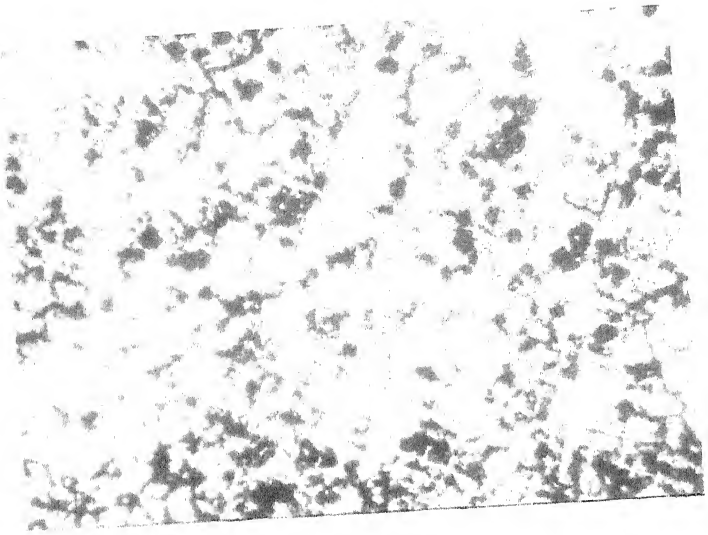

(m) : Microstructure of Fe-7.10% Ni, 4.93% Al, 12.04% Co, 4.95% Cu as cast (x 200)

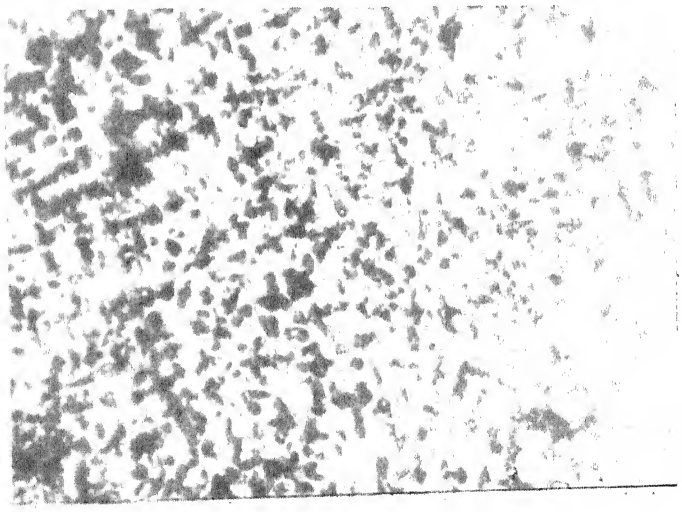

(n) : Microstructure of Fe-7.10% Ni, 4.93% Al, 12.04% Co, 4.95% Cu, annealed (1000°C, 3 hrs) (x 200)

The microstructures of Fe-Ni-Al-Co-Cu system alloys show a branch structure of dendrites with some inclusions of unequal size as in cast condition, shown in Fig. (3.2) (g,h,k). These are poorly resolved phase structures. The annealed microstructures of alloys of this system revealed the precipitates of irregularly spaced rod particles of various sizes, oriented with the long axis of the matrix as seen in Fig. (3.2) (l,m,n). The rods tend to group into plate like rows. After annealing, the size of precipitates is uniform, elongated and the precipitates are highly dispersed to be distinctly resolved.

3.2.3 X-ray Diffraction:

The results of X-ray diffraction analysis for each of the alloys is presented in Tables (3.3 to 3.13). These tables give the 2θ, d_{hkl}, relative intensity and the indices of the diffraction lines for the alloys of both systems respectively.

The X-ray diffraction patterns for (Fe-11.62% Ni, 2.54% Al, 3.50% Cr) and (Fe-11.95% Ni, 4.96% Al, 6.93% Co, 2.03% Cu) alloys are shown in Fig. (3.3) and in Fig. (3.4). The reflection pattern observed around the peak is broadened and the peak at 68.5° is indentified as the (220) peak of a b.c.c. phase (Fe_2Ni Al) with lattice parameter of 5.774A°.

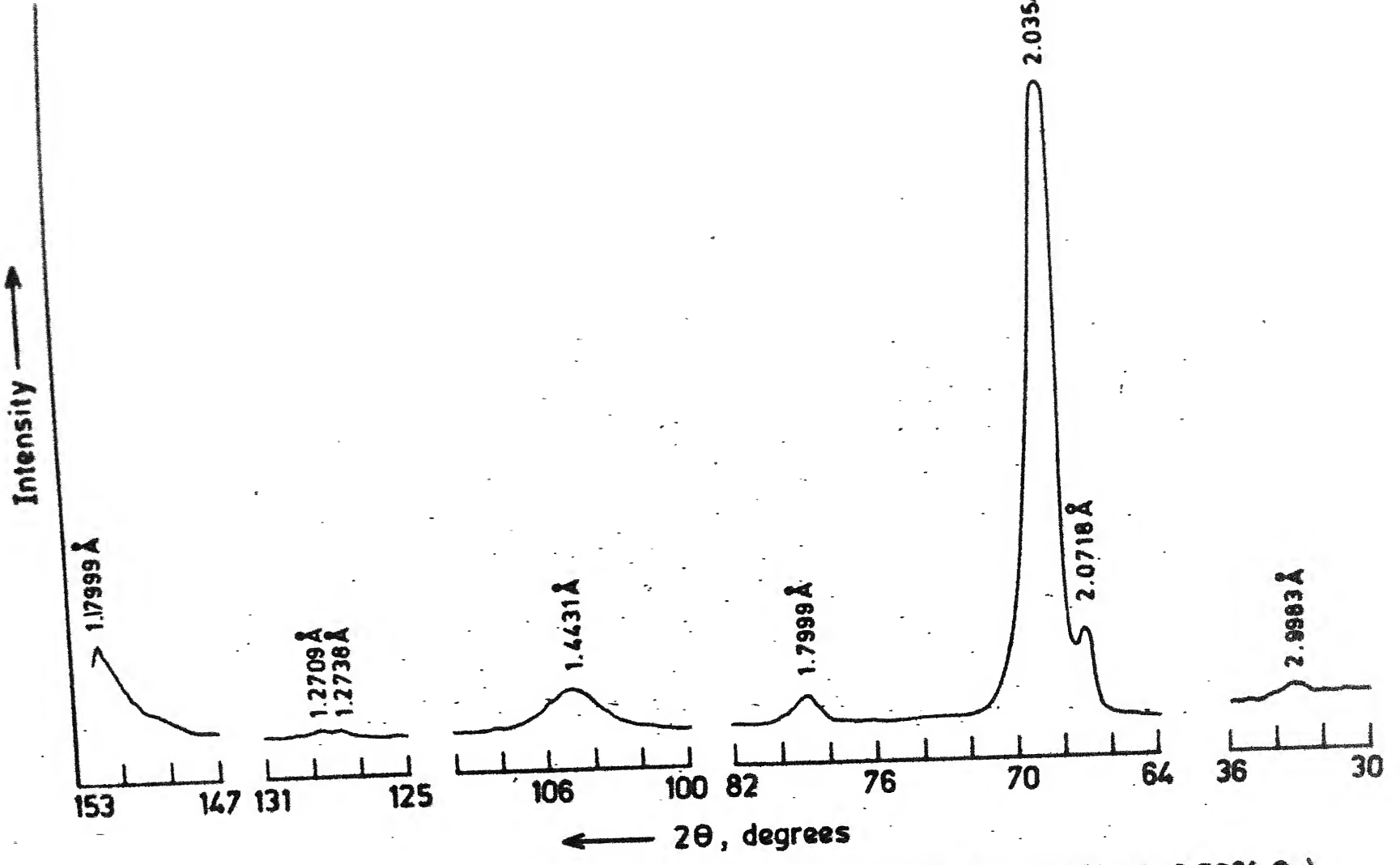

Fig. 3.3 X-ray diffraction pattern of the alloy (Fe - 11.62% Ni - 2.54% Al - 3.50% Cr) annealed at 1000°C for 3 hours.

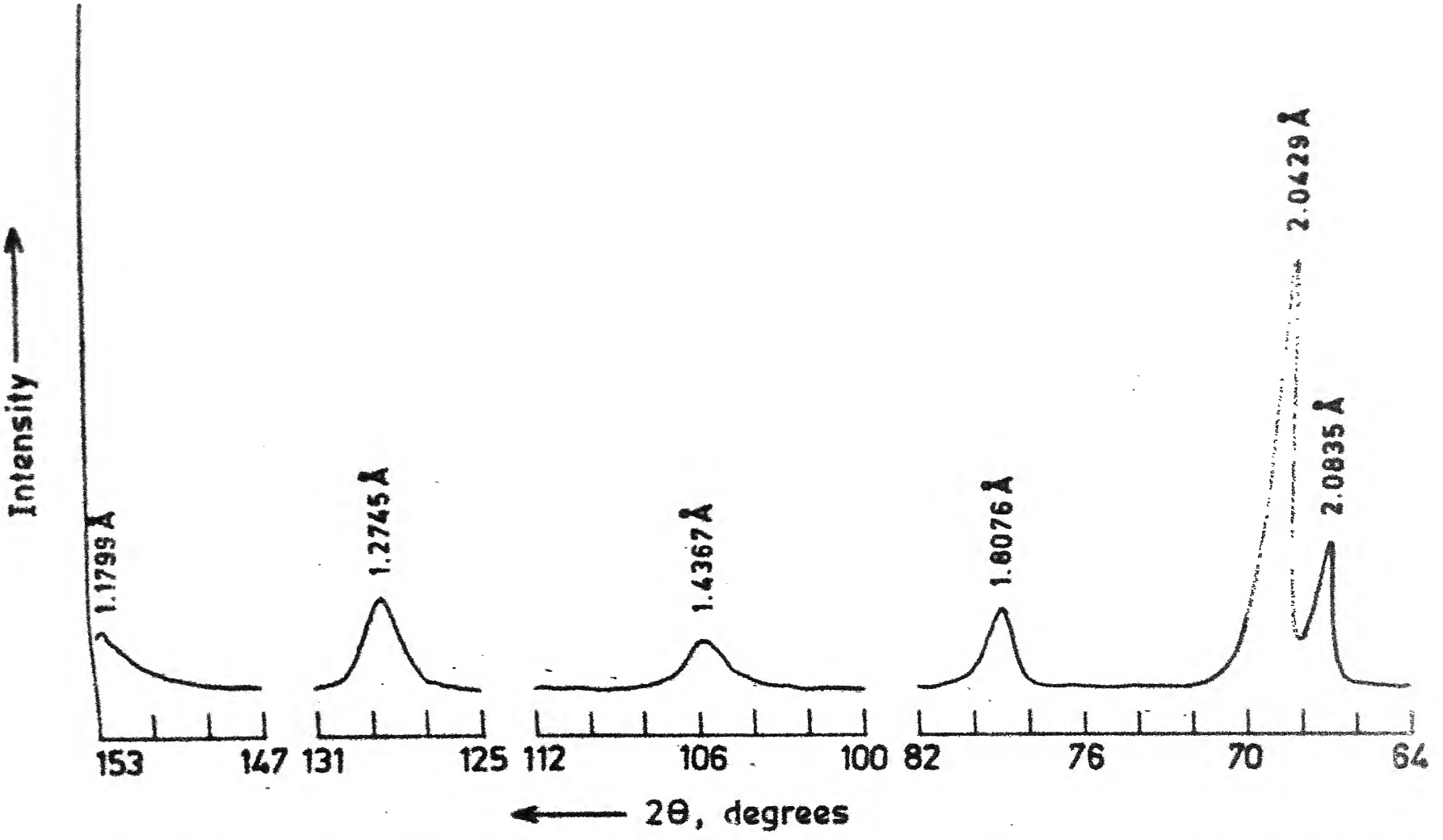

Fig. 3.4 X-ray diffraction pattern of the alloy (Fe - 11.95% Ni - 4.96% Al - 6.98% Co - 2.03% Cu) annealed at 1000°C for 3 hours.

TABLE 3.3

X-ray Diffraction Pattern of Fe-11.62% Ni, 2.54% Al, 3.50% Cr alloy, Annealed at 1000°C for 3 hrs in H_2

2 θ	d(Å°)	I/I_0	hkl
33.30	3.9979	5	200
66.20	2.0996	18	211
68.50	2.0353	100	220*
79.05	1.7999	5	310
105.08	1.4431	10	400*
123.13	1.2738	4	411, 330
123.65	1.2709	4	420
152.25	1.1799	18	332

CrKα Radiation λ = 2.291002 Å°,

Tc = 10 seconds, C.B.M. = 20 k,

scanning speed = 3°/minute,

chart speed = 3 cm/minute

* Reflections used for lattice parameter calculations.

TABLE 3.4

X-ray diffraction pattern of Fe-12.82% Ni, 2.63% Al, 4.72% Cr alloy, annealed at 1000°C for 3 hrs in H_2

2 θ	d(Å°)	I/I_0	hkl
32.65	4.0753	10	110
58.95	2.3281	20	200
62.35	2.2129	10	211
68.46	2.0364	100	220*
79.84	1.7851	20	310
87.08	1.6629	10	222
92.00	1.5925	15	321*
115.10	1.3552	5	400
148.50	1.1902	9	411,330

Cr K_α Radiation λ = 2.291002 Å°, Tc = 10 seconds, C.P.M. = 20 k, Scanning speed = 3°/minute in 2 θ, chart speed = 3 cm/minute

* Reflections used for lattice parameter calculations.

TABLE 3.5

X-ray diffraction pattern of Fe-14.92% Ni, 2.52% Al, 5.96% Cr alloy, annealed at 1000°C for 3 hrs in H_2

2 θ	d(A°)	I/I_0	hkl
35.50	3.7574	10	110
52.86	2.5736	25	200
58.28	2.3524	30	211*
63.44	2.0369	100	220*
78.95	1.8018	40	310
87.04	1.6635	10	222*
93.12	1.5164	5	321
105.36	1.4404	15	400
125.63	1.2875	20	411, 330
147.55	1.1930	20	420

CrKα Radiation λ = 2.291002 A°,

Tc = 10 Seconds, C.P.M. = 20 k,

Scanning speed = 3°/min, chart speed = 3 cm/min.

* Reflections used for lattice parameter calculations.

TABLE 3.6

X-ray diffraction pattern of Fe-16.12% Ni, 2.56% Al, 6.55% Cr alloy, annealed at 1000°C for 3 hours in H_2

2 θ	d(A°)	I/I_0	hkl
34.40	3.3733	10	110
46.36	2.3903	15	200*
56.5	2.4202	18	211
63.40	2.0373	100	220*
75.60	1.3690	25	310
77.04	1.6635	22	222
96.70	1.5330	30	321
105.30	1.4410	10	400*
123.40	1.2697	19	411, 330
150.30	1.1351	23	420

Crka Radiation λ = 2.291002 A°,

Tc = 10 seconds, C.P.M. = 20 k,

Scanning speed = 3°/min,

Chart speed = 3 cm/min.

* Reflections used for lattice parameter calculations.

TABLE 3.7

X-ray diffraction pattern of Fe-17.66% Ni, 2.59% Al, 7.43% Cr, alloy, annealed at 1000°C for 3 h rs in H_2

2 θ	d(A°)	I/I_0	hkl
33.8	3.9405	12	110
46.82	2.8832	15	200*
52.0	2.6131	20	211
68.38	2.0385	100	220*
74.7	1.8882	21	310
86.98	1.6644	27	222*
95.6	1.5463	32	321
105.23	1.4417	25	400
146.2	1.1972	19	411, 330

CrKα Radiation λ = 2.291002 A°

Tc = 10 seconds, C.P.M. = 20 k,

Scanning speed = 3°/min.

Chart speed = 3 cm/min.

* Reflections used for lattice parameter calculations.

TABLE 3.3

X-ray diffraction pattern of Fe-20.22% Ni, 2.54% Al, 3.57% Cr alloy, annealed at 1000°C for 3 hrs in H_2

2 θ	d (A°)	I/I_0	hkl
24.6	4.6377	14	110
16.79	2.3349	22	200
56.2	2.4320	8	211
63.32	2.0401	100	220*
75.73	1.8652	16	310
86.89	1.6631	19	222*
93	1.5792	20	321
105.11	1.4425	26	400
123.7	1.2412	15	411,330
117.4	1.1935	12	420

Cr-Kα Radiation λ = 2.291002 A°,

Fe = 10 seconds, C.P.M. = 20 k

Chart speed = 3 cm/min,

Scanning speed = 3°/min.

* Reflections used for lattice parameter calculations.

TABLE 3.9

X-ray diffraction pattern of Fe-14.02% Ni, 4.56% Al, 3.01 % Co, 1.16% Cu alloy, annealed at 1000°C for 3 hrs in H_2 .

2 θ	d(Å°)	I/I_0	hkl
62.8	2.1987	32	211
63.43	2.0372	100	220*
73.5	1.9145	16	310
37.05	1.6634	9	222*
135.	1.2309	17	321
146.3	1.1966	8	400

Crka Radiation λ = 2.291002 Å°,

Tc = 10 [illegible], C.P.M. = 20 k,

Scanning speed = 3°/min, Chart

Speed = 3 cm/min.

* Reflections used for lattice parameter calculations

TABLE 3.10

X-ray diffraction pattern of Fe-11.95% Ni, 4.96% Al, 6.93% Co, 2.03% Cu alloy, annealed at 1000°C for 3 hrs. in H_2

2 θ	d(Å°)	I/I_0	hkl
66.70	2.0835	34	211
68.2	2.0429	100	220*
78.65	1.8076	17	310
105.75	1.4367	9	222
128	1.2745	19	321*
152.25	1.1799	10	1100

CrKα Radiation λ = 2.291002 Å°,

Tc = 10 seconds, C.P.M. = 20 k,

Scanning speed = 3°/min, Chart speed = 3 cm/min.

* Reflections used for lattice parameter calculations.

TABLE 3.11

X-ray diffraction pattern of Fe-10.94% Ni, 4.87 % Al, 8.04% Co, 2.98% Cu, annealed alloy at 1000°C for 3 hrs in H_2

2 θ	d(A°)	I/I_0	hkl
63.5	2.1769	33	211
67.9	2.0506	100	220*
82.4	1.7391	20	310
86.3	1.6743	25	222*
97.2	1.5259	10	321
106.6	1.4287	15	400*

CrKα Radiation λ = 2.291002 A°,

Tc = 10 seconds, C.P.M. = 20 k,

Goniometer speed = 3°/min,

Chart speed = 3 cm/min

* Reflections used for lattice parameter calculations

TABLE 3.12

X-ray diffraction pattern of Fe-89% Ni, 4.89% Al, 10% Co, 1.01% Cu annealed alloy at 1000°C for 3 hrs. in H_2.

2 θ	d(Å°)	I/I_0	hkl
36.5	3.6571	27	110
46.7	2.8890	32	200
59.0	2.3264	27	211
68.2	2.0428	100	220*
77.6	1.8281	21	310
84.3	1.7069	18	222
95.8	1.5442	15	321*
107.2	1.4232	9	400
114.5	1.3619	16	411, 330*
126.8	1.2811	9	420

Cr$K\alpha$ radiation λ = 2.291002 Å°,

Tc = 10 seconds, C.P.M. = 20 k,

Scanning speed = 3°/min,

Chart speed = 3 cm/min.

* Reflections used for lattice parameter calculations.

TABLE 3.13

X-ray diffraction pattern of Fe-7.1% Ni, 4.93% Al, 12.04% Co, 4.95% Cu annealed alloy at 1000°C for 3 hrs in H_2.

2 θ	d(A°)	I/I_0	hkl
30.1	3.6976	28	110
46.3	2.9140	31	200
58.7	2.3368	29	211
68.1	2.0452	100	220*
77.1	1.8319	23	310
81.2	1.7087	25	222*
95.7	1.5451	30	321*
107.00	1.4249	35	400*
115.24	1.3564	14	411, 330

CrKα Radiation - = 2.291002 A°,

Tc = 10 · ·.l., C.P.M. = 20 k

Scanning speed = 3°/min,

Chart speed = 3 cm/min.

* Refl. ·· ·· used for lattice parameter calculations.

3.2.4 Microhardness Measurement:

The microhardness measurement was carried out to determine the hardness number of the as cast and annealed alloys. The representative microhardness value of each alloy was obtained as an average of several measurements on each specimen in terms of Vickers Hardness Number.

The result of hardness measurement for all the alloys are shown in Table (3.14). The variation of microhardness with a specific transition metals (Cr, Co, Cu) content or total content of precipitating elements is shown in Figs. (3.5 to 3.9). The microhardness of alloys is found to increase linearly with the addition of precipitating elements (single or in combination) in all the cases. Amongst Cu, Co and Cr, the variation in microhardness with the addition of Cu is steepest in comparison to those with Co or Cr. In each case, the annealed alloys have lower V.H.N. than that of the cast alloys.

3.2.5 Electrical Resisvity Measurement:

The measured electrical resisvity of various alloys is presented in Table (3.15). The corresponding resisvity verses alloying element weight percentage is shown in Fig. (3.10) for Fe-Ni-Al-Cr system and in -

TABLE 3.14

Microhardness values of Alnico magnet alloys of varying composition as cast and as annealed (at 1000°C for 3 hrs. in H_2) conditions.

Sample No.	Composition (in wt. pct) balance Fe.	Microhardness* (V.H.N.)	
		As cast	Annealed at 1000°C for 3 hours in H_2.
(Fe-Ni-Al-Cr) system			
1.	11.62% Ni, 2.54% Al, 3.5% Cr	495	435
2.	12.82% Ni, 2.63% Al, 4.72% Cr	540	475
3.	14.92% Ni, 2.52% Al, 5.96% Cr	605	545
4.	16.12%, Ni, 2.56% Al, 6.55% Cr	625	565
5.	17.66% Ni, 2.59% Al, 7.43% Cr	675	620
6.	20.22% Ni, 2.54% Al, 8.57% Cr.	725	665
(Fe-Ni-Al-Co-Cu) System			
7.	14.02% Ni, 4.56% Al, 3.01% Co, 1.16% Cu	513	446
8.	11.95% Ni, 4.96% Al, 6.98% Co, 2.03% Cu	625	561
9.	10.94% Ni, 4.87% Al, 9.04% Co, 2.98% Cu	660	585
10.	8.99% Ni, 4.89% Al, 10% Co, 4.01% Cu	720	645
11.	7.10% Ni, 4.93% Al, 12.04% Co, 4.95% Cu	780	701

* Microhardness values indicated above are the average values of [illegible] measured on several alloys.

TABLE 3.15

Electrical resisvity values of Alnico magnet alloys of varying composition as cast and annealed (at 1000°C for 3 hrs. in H_2) conditions.

Sample No.	Composition (wt. %) balance Fe	Resisvity at Room Temperature (30°C) ($\mu\Omega$-cm)	
		As cast	Annealed at 1000°C for 3 hrs. in H_2
(Fe-Ni-Al-Cr) System			
1	11.62% Ni, 2.54% Al, 3.50% Cr.	88	65
2.	11.82% Ni, 2.63% Al, 4.72% Cr.	91	71
3.	14.92% Ni, 2.52% Al, 5.96% Cr.	98	75
4.	16.12% Ni, 2.56% Al, 6.55% Cr	103	79
5.	17.66% Ni, 2.59% Al, 7.43% Cr.	107	84
6.	20.22% Ni, 2.54% Al, 8.57% Cr.	110	87
(Fe-Ni-Al-Co-Cu) System			
7.	14.02% Ni, 4.56% Al, 3.01% Co, 1.16% Cu	95	69
8.	11.95% Ni, 4.96% Al, 6.98% Co, 2.03% Cu	100	74
9.	10.94% Ni, 4.87% Al, 8.04% Co, 2.98% Cu	103	77
10.	8.99% Ni, 4.89% Al, 10% Co, 4.01% Cu	104	79
11.	7.10% Ni, 4.93% Al, 12.04% Co, 4.95% Cu	106	81

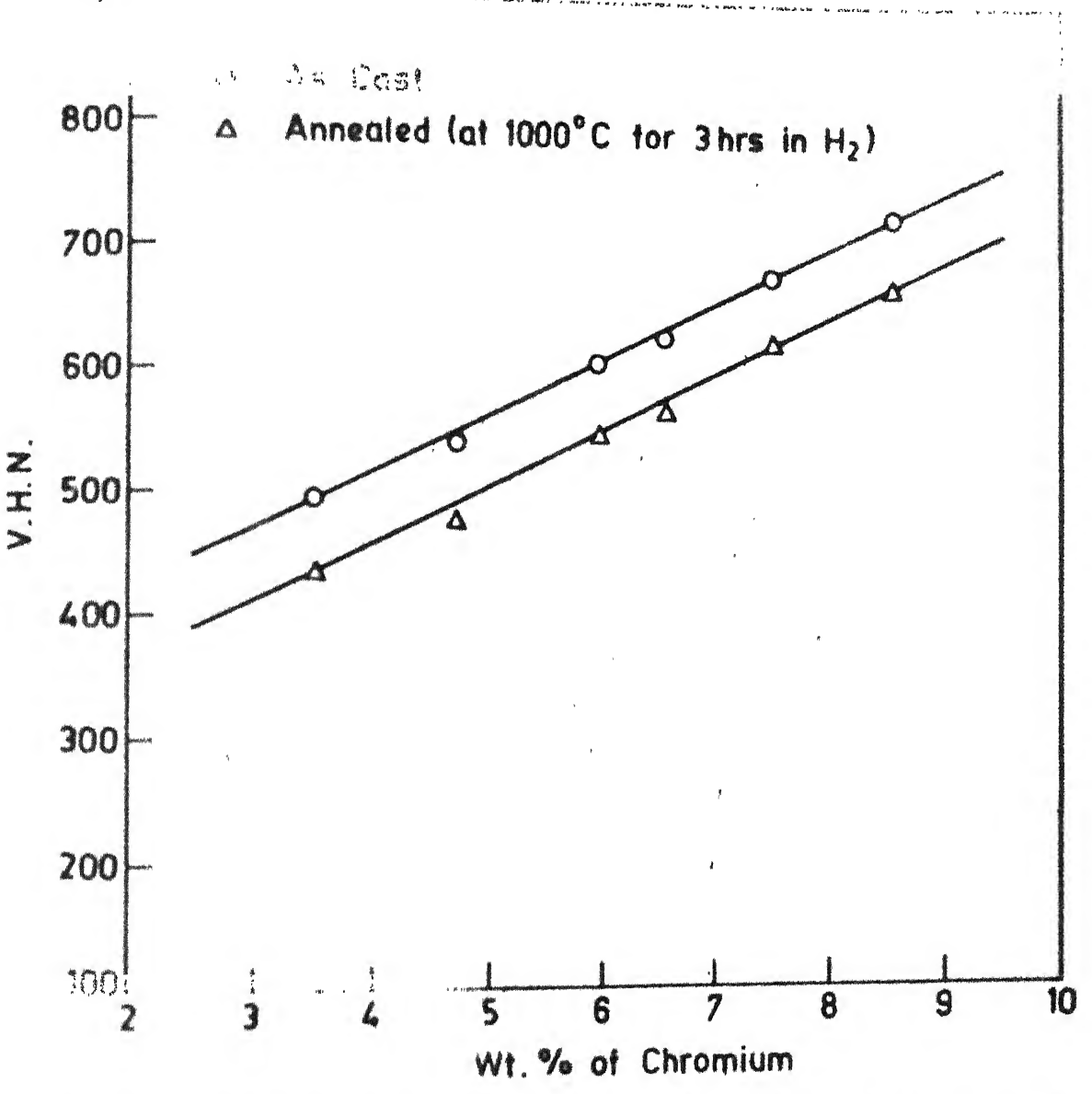

Fig. 3.5 Variation of V.H.N. with wt.% of Cr in Fe-Ni-Al-Cr alloys.

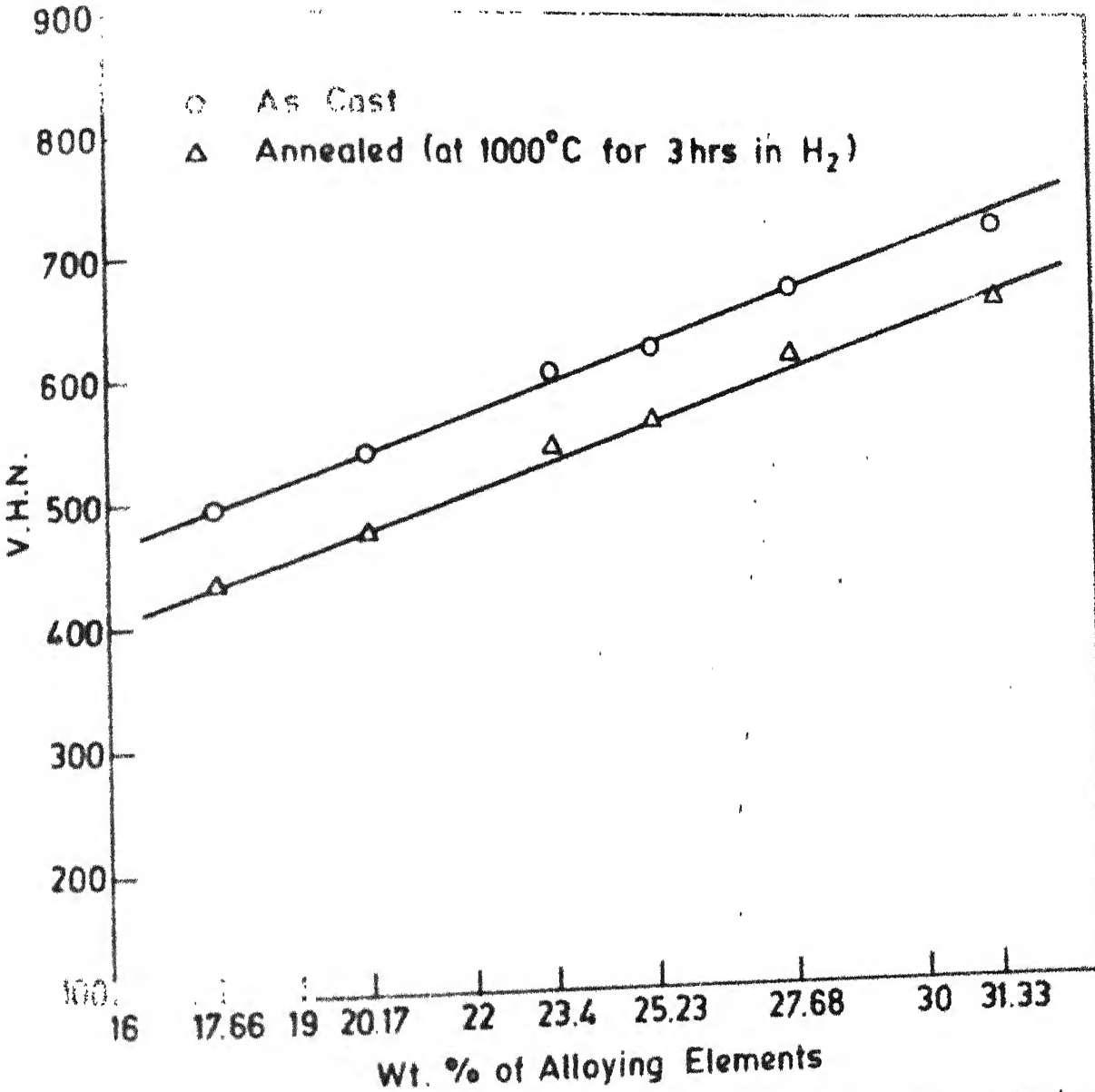

Fig. 3.6 Variation of V.H.N. with wt. % of alloying elements in Fe-Ni-Al-Cr alloys.

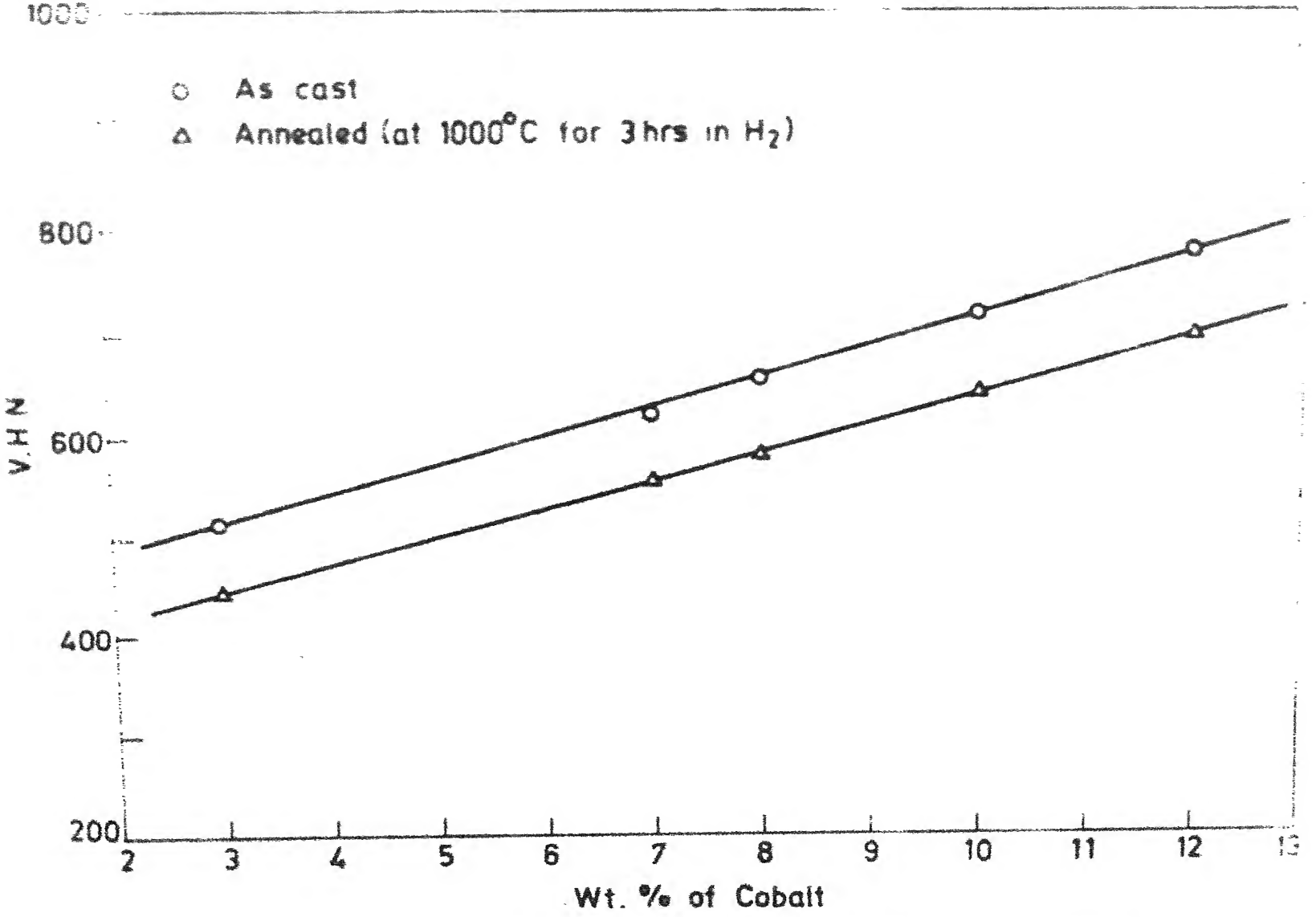

Fig. 3.7 Variation of V.H.N. with wt. % Co in Fe-Ni-Al-Co-Cu alloys.

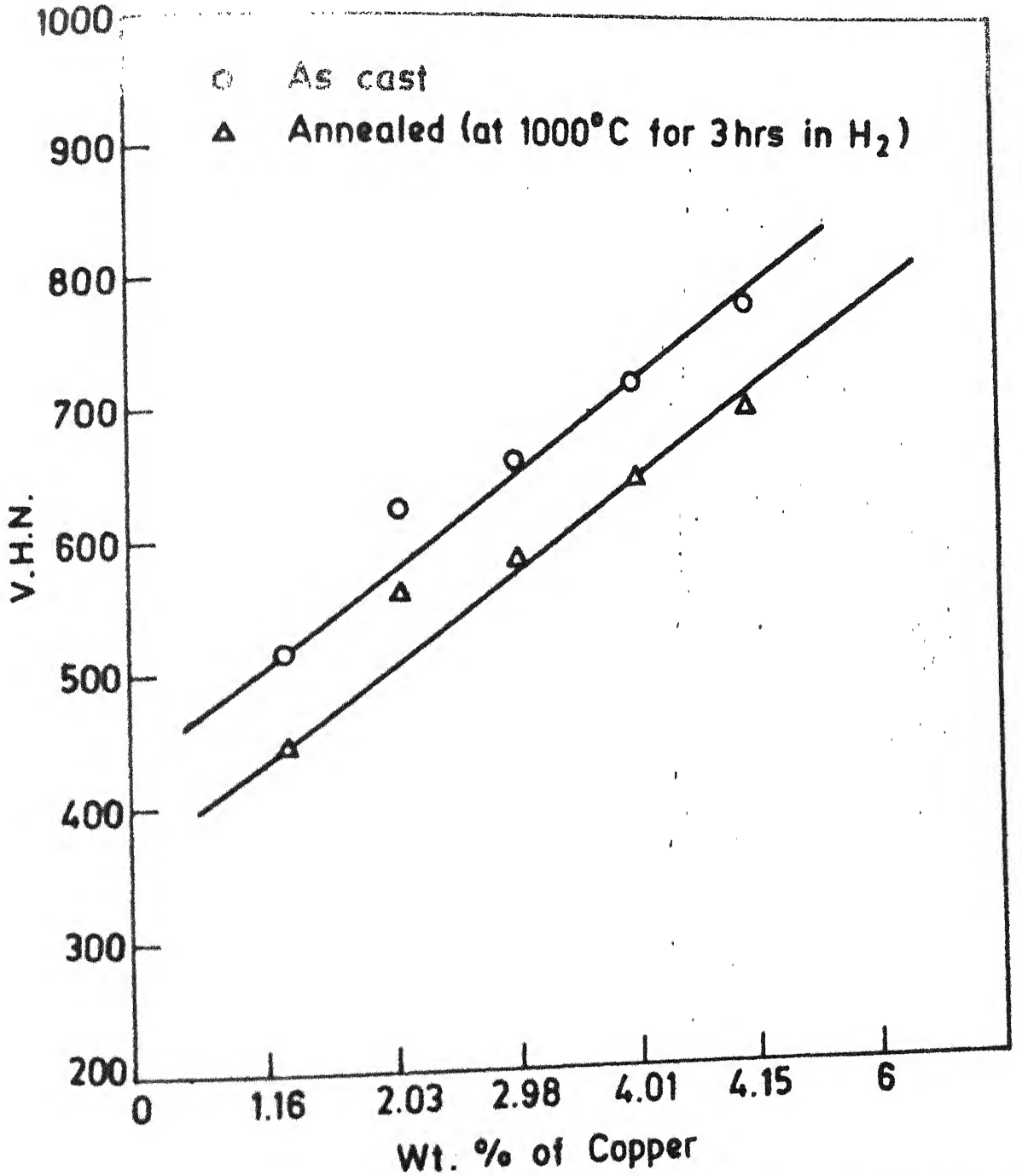

Fig. 3.8 Variation of V.H.N. with wt.% of copper in Fe-Ni-Al-Co-Cu alloys.

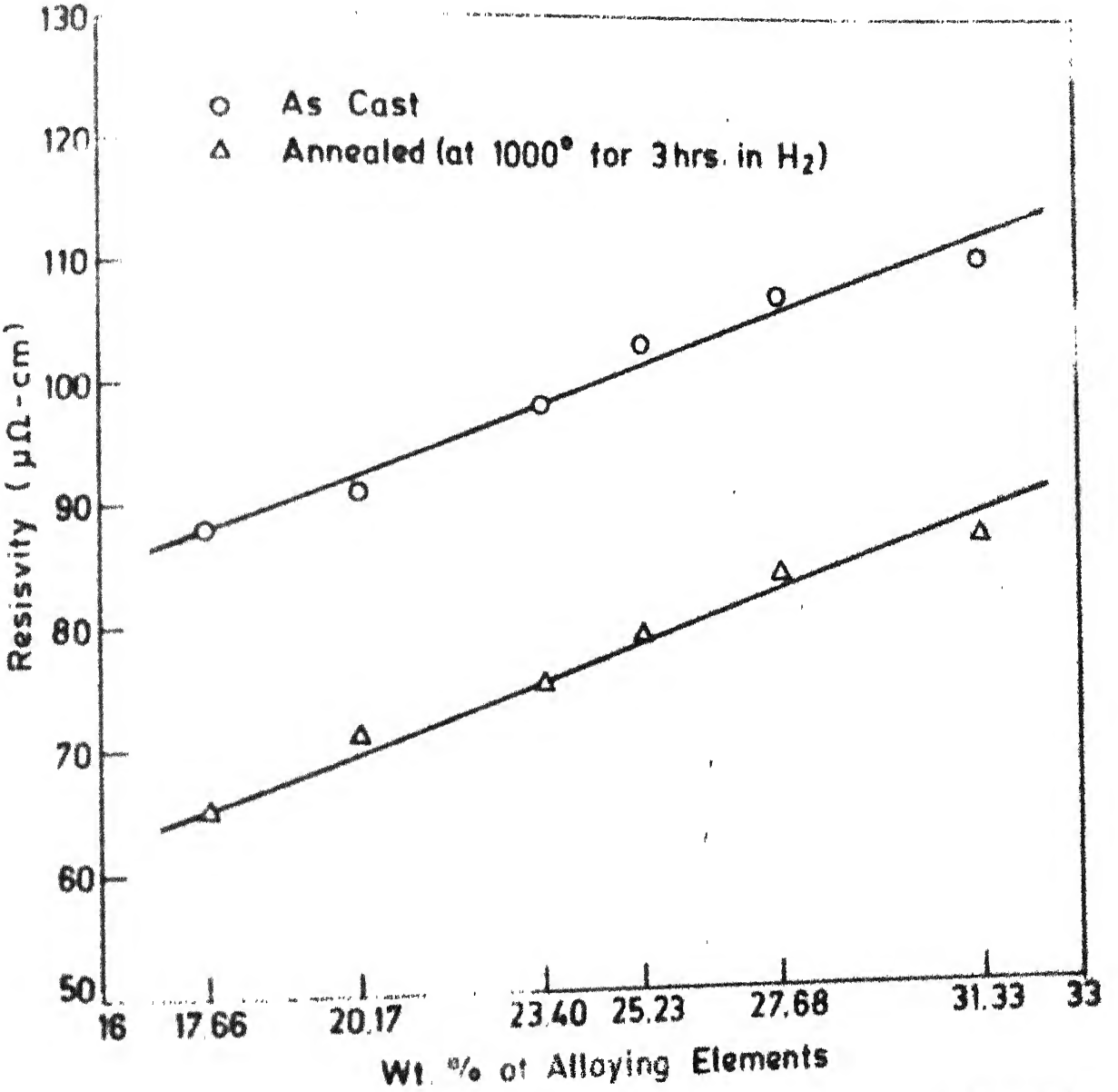

Fig 3.10 Variation of resisvity with wt. % of alloying elements in Fe-Ni-Al-Cr alloys.

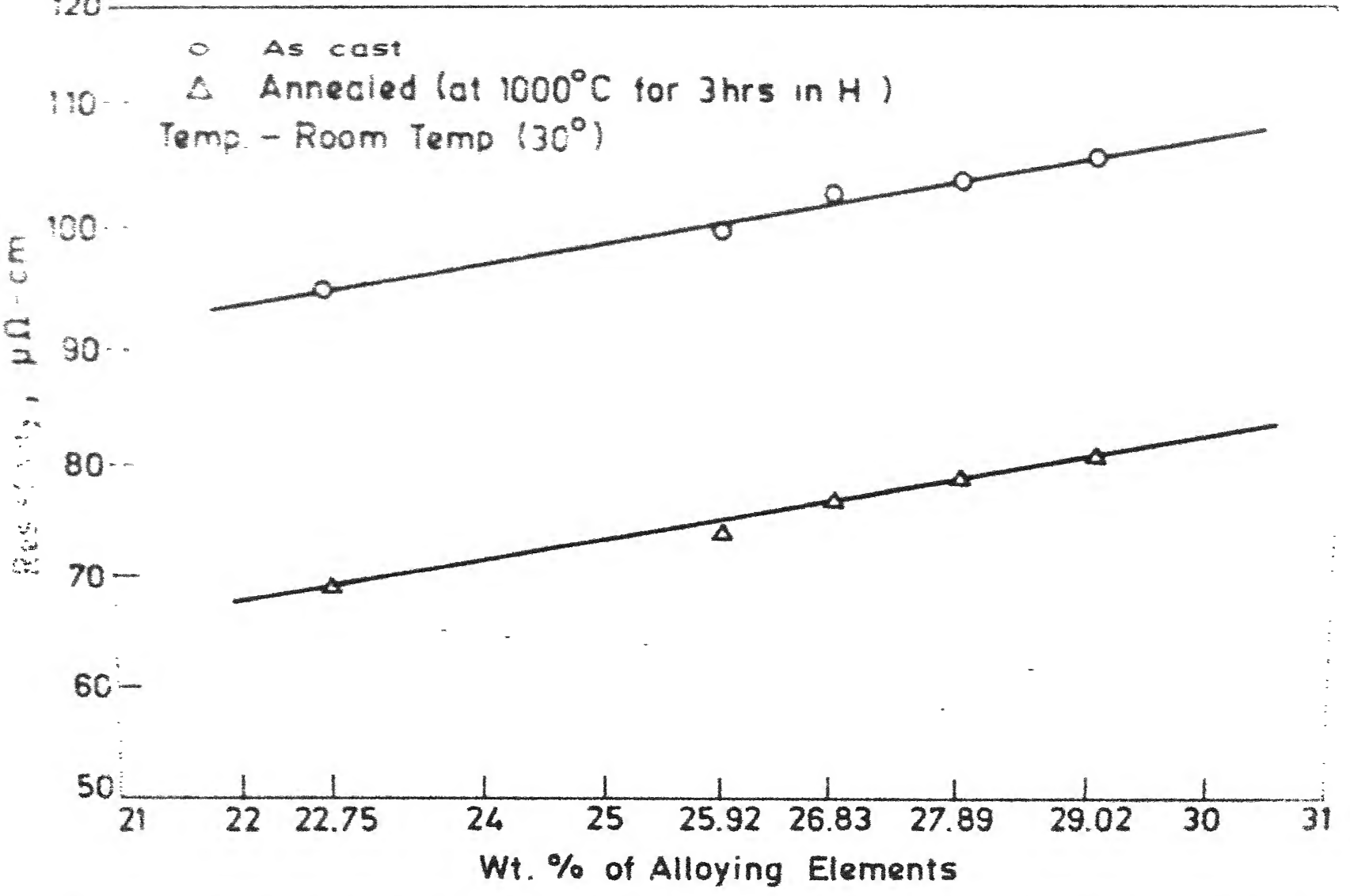

Fig. 3.11 Variation of resistivity with wt. % of alloying elements in Fe-Ni-Al-Co-Cu alloys.

Fig. (3.11) for Fe-Ni-Al-Co-Cu system respectively. It is clear that alloying elements inhance the resisvity with increasing addition. In each case, the annealed alloys have lower value of resisvity than that of the cast alloys.

3.3.5 Magnetic Measurements:

The summary of magnetic measurement for saturation magnetization (M_s), Remanence Magnetization (M_r) and Coercivity ($_iH_c$) is presented in Table (3.16). This is based on experimental study on alloys of (Fe-Ni-Al-Cr) and (Fe-Ni-Al-Co-Cu) systems after giving the following heat treatments : (1) Annealed at 1000°C for 3 hrs. and tempered at 650°C for $3\frac{1}{2}$ hrs. in H_2 and (2) Magnetically aged at 650°C at 1200 Oe for 1/2 hour in order to determine the degree to which the magnetic properties can be developed. The magnetization results are also presented in Figs. (3.12 to 3.13) as plot of M vs H in the first quadrant. The coercive force and remanence magnetization were determined by extrapolation of the demagnetization curve obtained in the second quadrant. Figs. (3.12 to 3.13) show that all the alloys are essentially magnetically saturated in magnetic field ranging from 5.9 to 7.9 KG. For all alloys of both systems, these curves indicate gradual improvement in the changing trend towards loop squareness and increase in saturation magnetization (M_s), remanence magnetization (M_r) and intrinsic coercivity ($_iH_c$) values from the cast state to the magnetically ageing state. However, there

TABLE 3.16

:tic properties of alloys of (Fe-Ni-Al-Cr) and (Fe-Ni-Al-Co-Cu) system measured by magnetometer

le No.	Composition (in wt. pct.) balance Fe.	As cast			Annealed at 1000°C for 3 hrs. and tempered at 650°C for $3\frac{1}{2}$ hrs in H_2			Magnetically annealed at 650°C at 1200 Orsted for 1/2 hr.		
		M_s e.m.u/c.c	M_r e.m.u/c.c	i_{Hc} (orsted)	M_s e.m.u/c.c	M_r e.m.u/c.c	i_{Hc} (Orsted)	M_s e.m. u/c.c	M_r e.m. u/c.c	i_{Hc} (Orsted).
i-Al-Cr em										
1.	11.62% Ni, 2.54% Al, 3.50% Cr.	940	15.84	52	917	19.45	59	965	21.81	62
2.	12.82% Ni, 2.63% Al, 4.72% Cr	775	13.87	58	855	16.94	64	895	18.93	66
3.	14.92% Ni, 2.52% Al, 5.96% Cr	720	11.92	63	790	14.63	69	835	17.54	72
4.	16.12% Ni, 2.56% Al, 6.55% Cr	690	11.07	66	760	13.56	71	795	16.84	73
5.	17.66% Ni, 2.59% Al, 7.43% Cr	640	9.15	69	700	11.66	76	742	14.48	79
6.	20.22% Ni, 2.54% Al, 8.57% Cr.	575	7.70	75	630	10.34	81	665	13.09	84

Contd.....

Contd... Table 3.16

tic properties of alloys of (Fe-Ni-Al-Cr) and (Fe-Ni-Al-Co-Cu) system measured by magnetometer

e No.	Composition(in wt.pct.) balance Fe	As cast			Annealed at 1000°C for 3 hrs. and tempered at 650°C for $3\frac{1}{2}$ hrs in H_2			Magnetically annealed at 650°C orsted for 1/2 hr.		
		M_s e.m. u/c.c	M_r e.m. u/c.c.	i_{Hc} (orsted)	M_s e.m. u/c.c	M_r e.m u/c.c	i_{Hc} (orsted)	M_s e.m. u/c.c	M_r e.m. u/c.c	i_{Hc} (orsted
l-Al-Co-Cu ystem										
7.	14.02% Ni, 4.56% Al, 3.01% Co, 1.16% Cu	775	18.85	68	880	27.29	78	940	32.90	84
8.	11.95% Ni, 4.96% Al, 6.98% Co, 2.03% Cu.	915	29.05	91	1015	38.57	98	1070	46.02	104
9.	10.94% Ni, 4.87% Al, 3.04% Co, 2.98% Cu	945	31.96	94	1050	44.12	102	1100	53.04	108
10.	8.99% Ni, 4.89% Al, 10% Co, 4.01% Cu	985	36.51	101	1095	48.18	110	1150	56.35	114
11.	7.10% Ni, 4.93% Al, 12.04% Co, 4.95% Cu.	1020	39.72	105	1125	52.88	113	1180	61.36	118

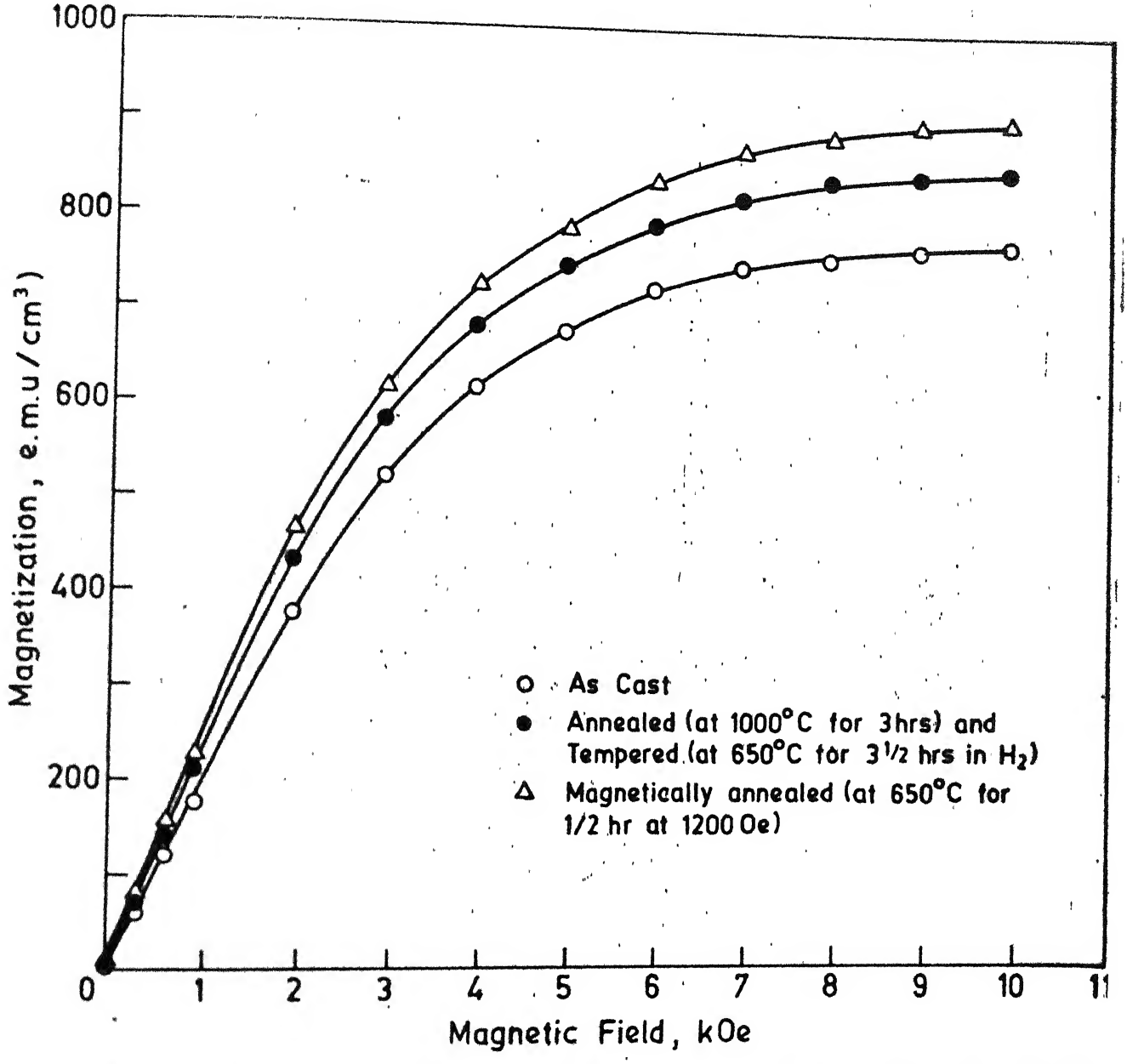

Fig. 3.12 Magnetization curves (First Quadrant) for Fe-14.92% Ni, 2.52% 5.9% Cr

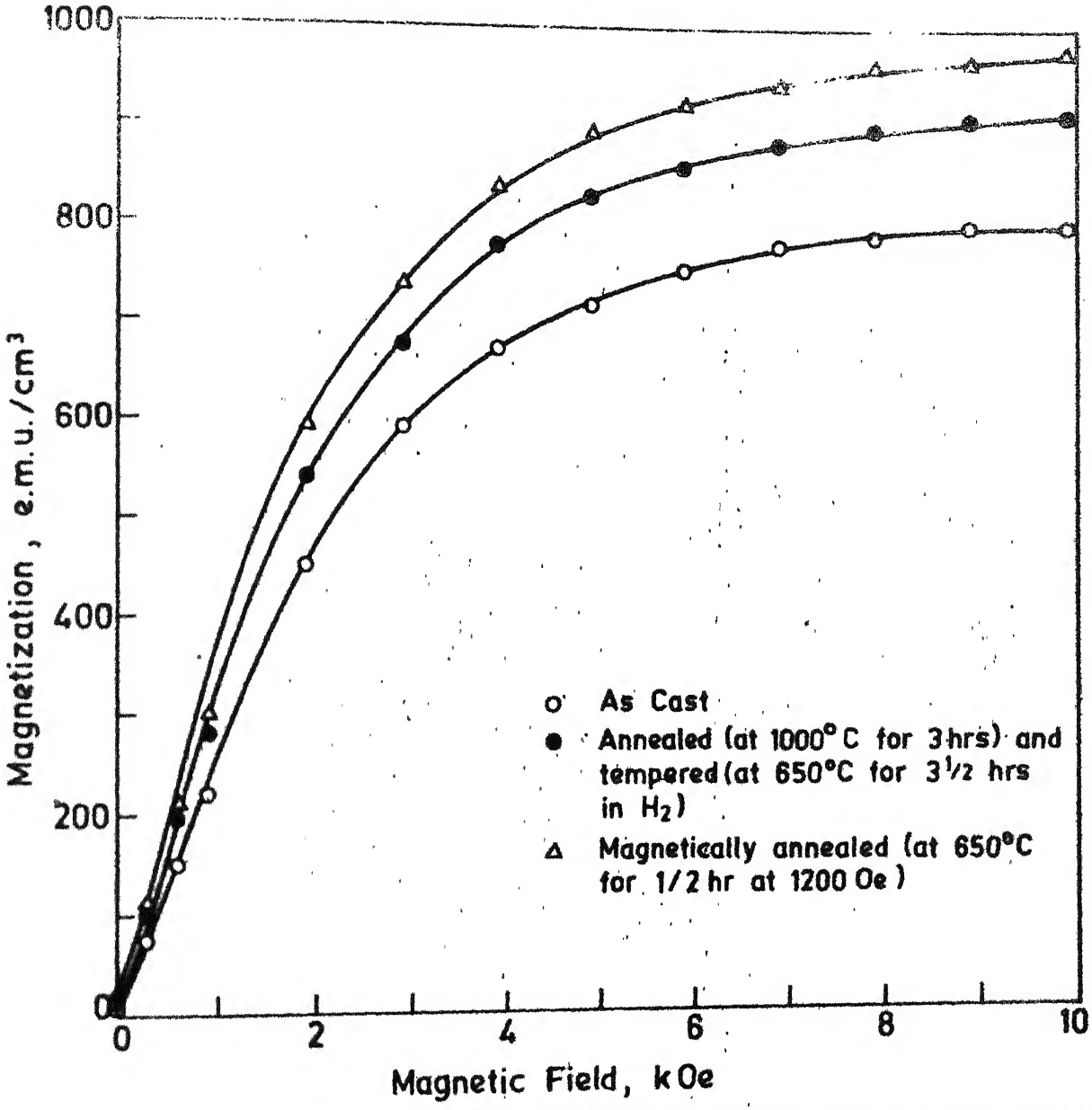

Fig. 3.13 Magnetization curves (First Quadrant) for Fe-14.02% Ni, 4.56% Al, 3.01% Co, 1.16 % Cu .

is not much difference in the initial magnetization parts drawn for different heat treatment conditions. The gap between magnetization and demagnetization curves for Fe-Ni-Al-Co-Cu system alloys is larger than that of Fe-Ni-Al-Cr system alloys. Thus the alloys of Fe-Ni-Al-Co-Cu system show better approach for loop squareness.

3.3 DISCUSSIONS:

The result obtained in the present investigation are being discussed below under following headings:

1. Chemical Composition
2. Metallographic Features
3. X-ray Diffraction Studies
4. Microhardness Measurement
5. Resisvity Measurement
6. Magnetic Behaviour.

3.3.1 Chemical Composition:

The results of chemical analysis have been presented in Table (3.2). The nominal and analysed composition of all alloys are different. This is atributed to the vaporization of the elemental components, because of very high temperature involved in the process of fabrication. In fact the control of composition of alloys is a serious problem in the present process.

3.3.2 Metallographic Features:

The microstructures of alloys of (Fe-Ni-Al-Cr) and (Fe-Ni-Al-Co-Cu) systems differ from each-other. Also the structural inhomogenety seen in micrographs of the same type of alloys results due to inhomogenety in temperature distribution between mold wall and the bulk of the melt.

The Fe-Ni-Al-Cr type alloys reveal wide precipitates of irregular shape and size with some inclusions through out the matrix both as in cast and annealed conditions, as shown in Fig. (3.2) (a,b,c,d,e,f,).

During soldification, the sold particles are continuously forming which pass through such zones where the shear forces are weak and the soldified particles may remain in contact with each-other for a some duration without disruption by the fluid forces. This contact duration may be sufficient enough for the formation of much larger particles in size as result of particle coalescence phenomena. The increased content of Cr in the alloy is responsible for increased proportion of inclusions which may be due to insoluble phases such as oxides and other intermetallics. Also the high thermal gradient and fast cooling leads to formation of irregular precipitates in size and shape. The microstructures of

Fe-Ni-Al-Co-Cu system alloys show the precipitates in the form of dendritic structure and as irregularly spaced rod particles of various sizes both as in cast and as annealed conditions respectively as shown in Fig. (3.2) (g,h,k,l,m,n). The presence of such particles may be atributed to the effect of copper content on the growth kinetics of α' phase. Chien and Kattamis (4) have shown that the growth rate of α' phase in the alloys increases with increase in copper content. The effect of processing conditions on particle size and its distribution has been found to be different for different alloy composition in this system also.

The quality control of alloys of both the systems by the control of microstructures is very complex due to inherent difficulties involved with the thermite process.

3.3.3 X-Ray Diffraction Studies:

X-ray diffraction results of the phases present in the alloys of (Fe-Ni-Al-Cr) and (Fe-Ni-Al-Co-Cu) systems are difficult to analysis due to non-equilibrium precipitation of phases during rapid soldification. There is co-existence of several phases in each system. Usually for similar system, annealing around 1000°C for several days is recommended in order to obtain a single phase. The X-ray diffraction showed the presence of

very strong line corresponding to a B.C.C. α′ (Fe_2 Ni Al) phase with the lattice parameter (a) = 5.774A°. The most intense peak is broad and is observed in the 2 θ range of 68° - 69° (Cr radiation) corresponding to (220) reflection. The intensity of this peak did not change visibly with the change in composition of alloys of both systems. Also no systematic change in intensity of other lines with change in composition of the alloys was noticed. Though several second phase precipitates are expected to occur, the X-ray diffraction has revealed only one α′ phase (Fe_2 Ni Al). This α′ phase is dispersed in the weakly magnetic matrix.

3.3.4 Microhardness Measurement:

The result of the microhardness measurement of Fe-Ni-Al-Cr and Fe-Ni-Al-Co-Cu systems for as cast and as annealed conditions is presented in Table (3.14). The data indicates that the addition of Ni, Al, Cr, Co and Cu to Fe - matrix increases the Vickers Hardness Number as shown in Figs. (3.5 to 3.9). These indicate linear dependence of V.H.N. on the concentration of alloying elements in both systems. This can be atributed to distortion introduced in the Fe (B.C.C.) lattice as result of the difference in atomic radii of matrix and the alloying elements. The atomic radii of the elements are r_{Fe} = 1.24A°, r_{Al} = 1.43A°, r_{Ni} = 1.24A°, r_{Cr} = 1.25A°,

r_{Co} = 1.25A° and r_{Cu} = 1.28A°. The strain field associated with the lattice distortion may offer significant resistance to movement of mobile dislocations during hardness measurement. This may result from the solute atoms. Also the presence of fine precipitates will significant obstacle to dislocation motion. As the matrix distortion and amount of fine precipitates are directly proportional to the concentration of alloying elements, the Vickers Hardness varies accordingly.

3.3.5 Resisvity Measurement:

The result of the resisvity measurement for as cast and as annealed alloys of both the system is presented in Table (3.15). The corresponding variation is shown in Figs.(3.10 to 3.11). These again indicate the linear increase irresisvity with increase in addition of alloying elements. This behaviour can be atributed due to increased electron scattering due to local stress field as a result of solute atoms and second phase particles and dislocations in the Fe-matrix. All samples of alloys, annealed at 1000°C for 3 hrs. in H_2 exhibit lower values of resisvity than those of cast samples due to relief of residual stress, developed during casting.

3.3.6 Magnetic Behaviour:

The magnetization behaviour of those alloys is shown in Figs. (3.12 to 3.13) for samples with different preparation history as indicated in the inset. As is expected, the magnetic properties such as M_s , M_r and ^iHc are higher in the case of magnetically aged (at 650°C for 1/2 hr at 1200 Oe) alloy in comparison to other conditions. The magnetic ageing in a constant magnetic field through close to curie point is supposed to help the alignment of magnetic domains parallel to the applied field direction and inducing loop squareness and high values of M_s , M_r and ^iHc.

All the results presented in Table (3.16) show that the saturation condition for all alloy samples occurs at a reasonably large field (5.9 to 7.9 K . Oe). This may arise due to high demagnetizing factors for small specimens. Moreover, the effect of impurities like carbon on magnetic properties is obscure in the present case. The values of intrinsic coercivity (^iHc) are found to vary with composition and history of alloy preparation.

3.3.6.1 Effect of Cr on Magnetic Properties:

The effect of Cr addition on magnetic properties of Fe-Ni-Al system has been shown in Figs. (3.14 to 3.16). Both the saturation magnetization (M_s) and

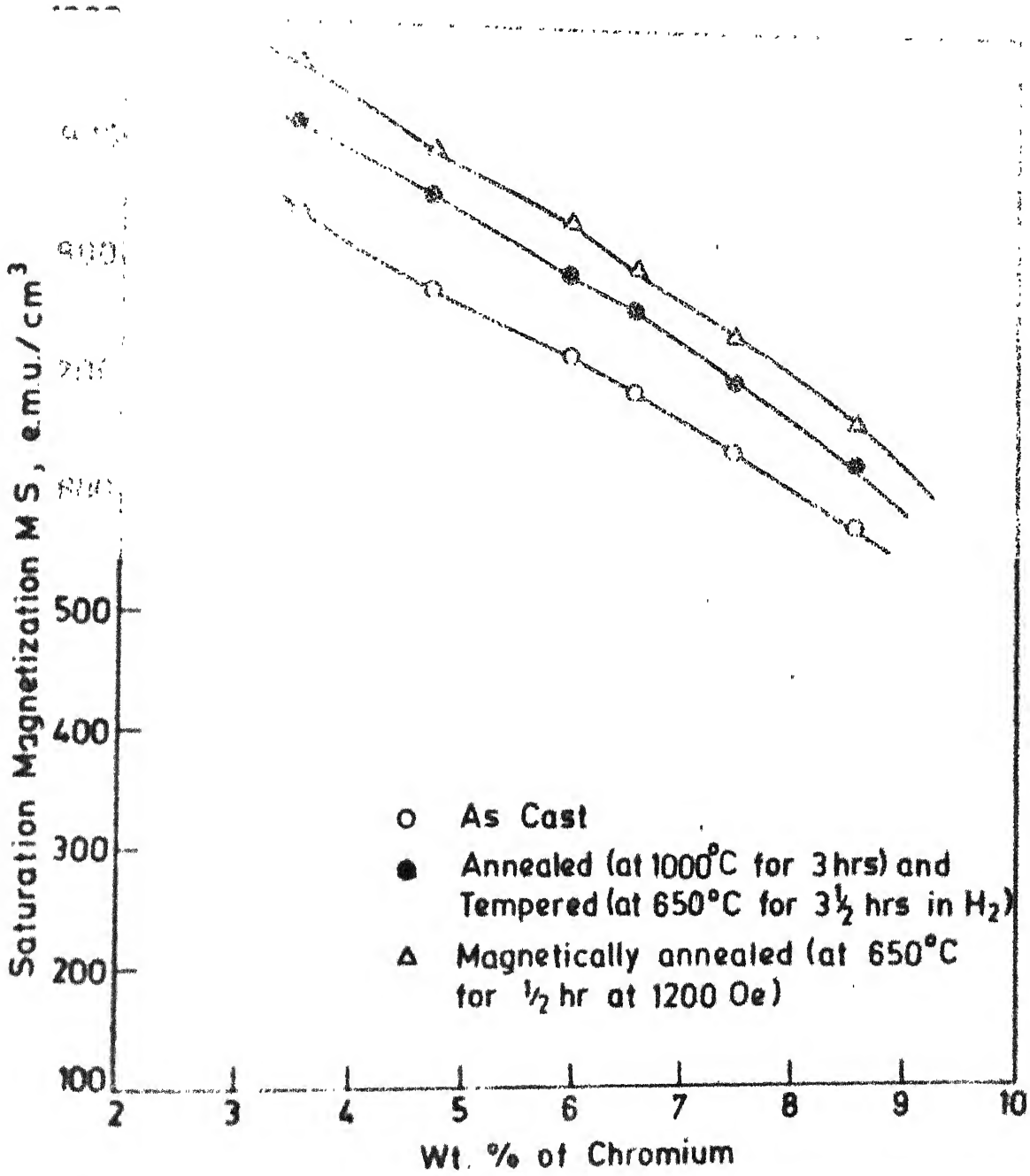

Fig. 3.14 Variation of saturation magnetization MS with weight % of Cr in Fe-Ni-Al-Cr alloys.

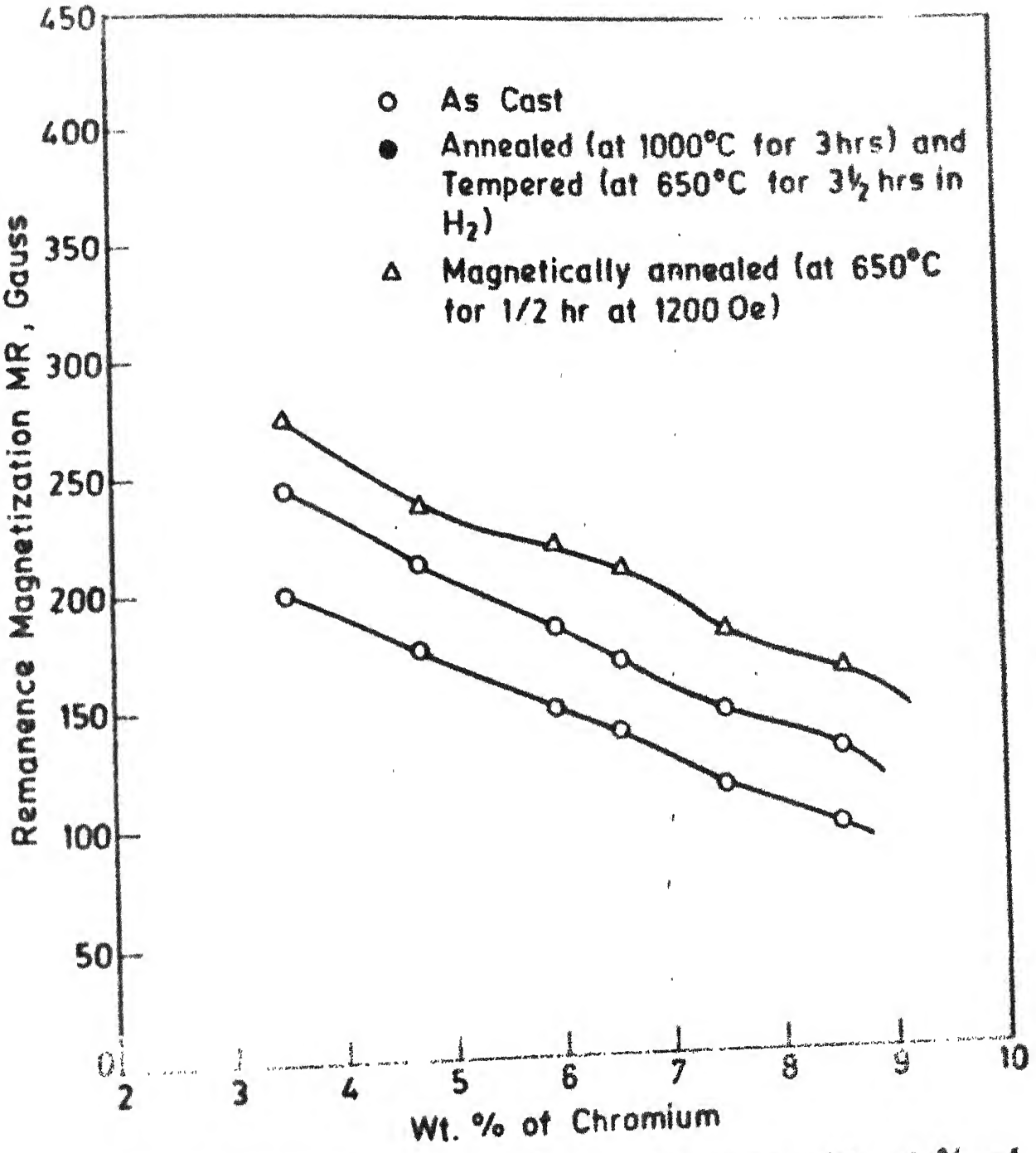

Fig. 3.15 Variation of remanence magnetization with wt. % of Cr in Fe-Ni-Al-Cr alloys.

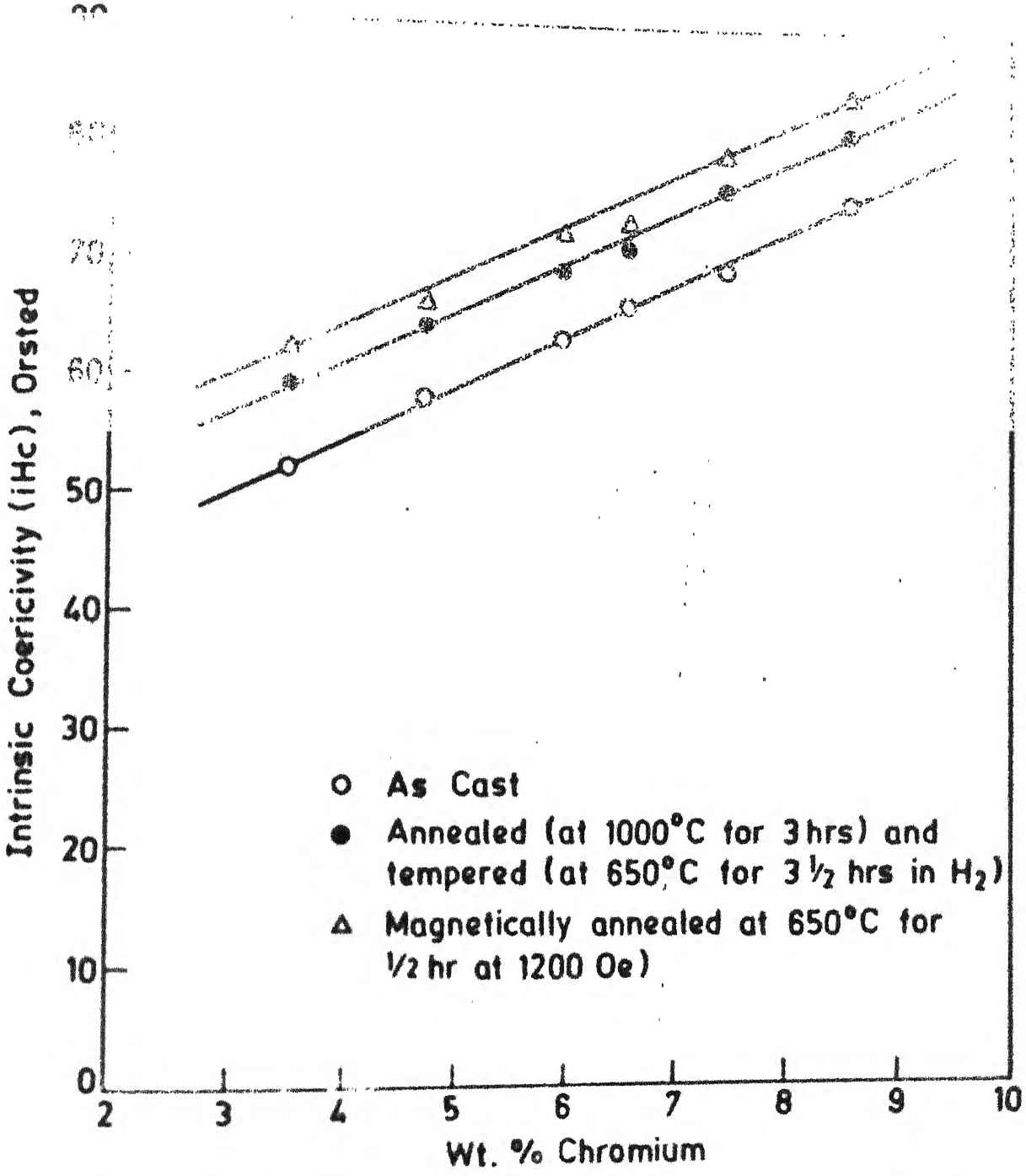

Fig. 3.16 Variation of intrinsic coericivity (iHc) with wt. % of Cr in Fe-Ni-Al-Cr alloys

remanence magnetization (M_r) are found to decrease with increasing Cr. However, the coercivity is seen to increase with increased Cr content.

A decrease in the values of M_s and M_r are explained as following way. A addition of Cr to Fe-Ni-Al system induces the formation of inhomogeneous inclusions with non-unifor distribution with respect to their shape and size. The inclusions causes either the formation of magnetic poles or a stressed domain structure. This reduces the values of M_s and M_r. This also increase coercive force by introducing hindrance to magnetization and demagnetization processes due to interaction between domain walls and inclusions (5,6).

The principle of the modern 'inclusion' theory was enunciated by Neel (7) and some modification in the above theory have been taken up later on in order to account for the effect of non-magnetic inclusions such as Fe_3C in the ferro-magnetic matrix. Goodengh (3) has discussed the effect of inclusions or precipitates (causing reversal magnetization) on the coercive force in polycrystalline ferro-magnetic materials. His predictions indicate that ^{i}Hc should increase with 2/3 power of volume of granular inclusions and for lamilar precipitates, ^{i}Hc should increase linearly with the precipitate volume. The effect of shape and size of

inclusions on ^{i}Hc has also been considered.

3.3.6.2 Effect of Cobalt on Magnetic Properties:

The dependence of magnetic properties of Fe-Ni-Al system on cobalt content is presented through Figs. (3.17 to 3.19). It is evident from Figs. (3.17 to 3.19) that the addition of Co increases M_s, M_r and ^{i}Hc. The increase in M_s and M_r values may be atributed to the formation of a ferro-magnetic (Fe-Co) phase in the in the alloys along with α' phase. Though X-ray analysis has not shown definitely the presence of such phase, it is felt that a small amount of ferro-magnetic (Fe-Co) phase is formed which inhances M_s and M_r values. The increased intrinsic coercivity may be atributed to the increased shape anisotropy, associated with precipitate particles. Thus the addition of Co has beneficial effect in inhancing magnetic properties of a permanent magnet.

3.3.6.3 Effect of Nickel on Magnetic Properties:

The effect of Nickel content on the magnetic properties of Fe-Ni-Al system is shown in Figs. (3.20 to 3.21). The addition of Ni to this system is found to decrease the values of M_s and M_r as shown in Figs. (3.20 to 3.21). This may be atributed to fact that the addition of Ni reduces the average atomic magnetic moment of the alloy, because magnetic moment of Ni (^{m}Ni = 0.60 μB)

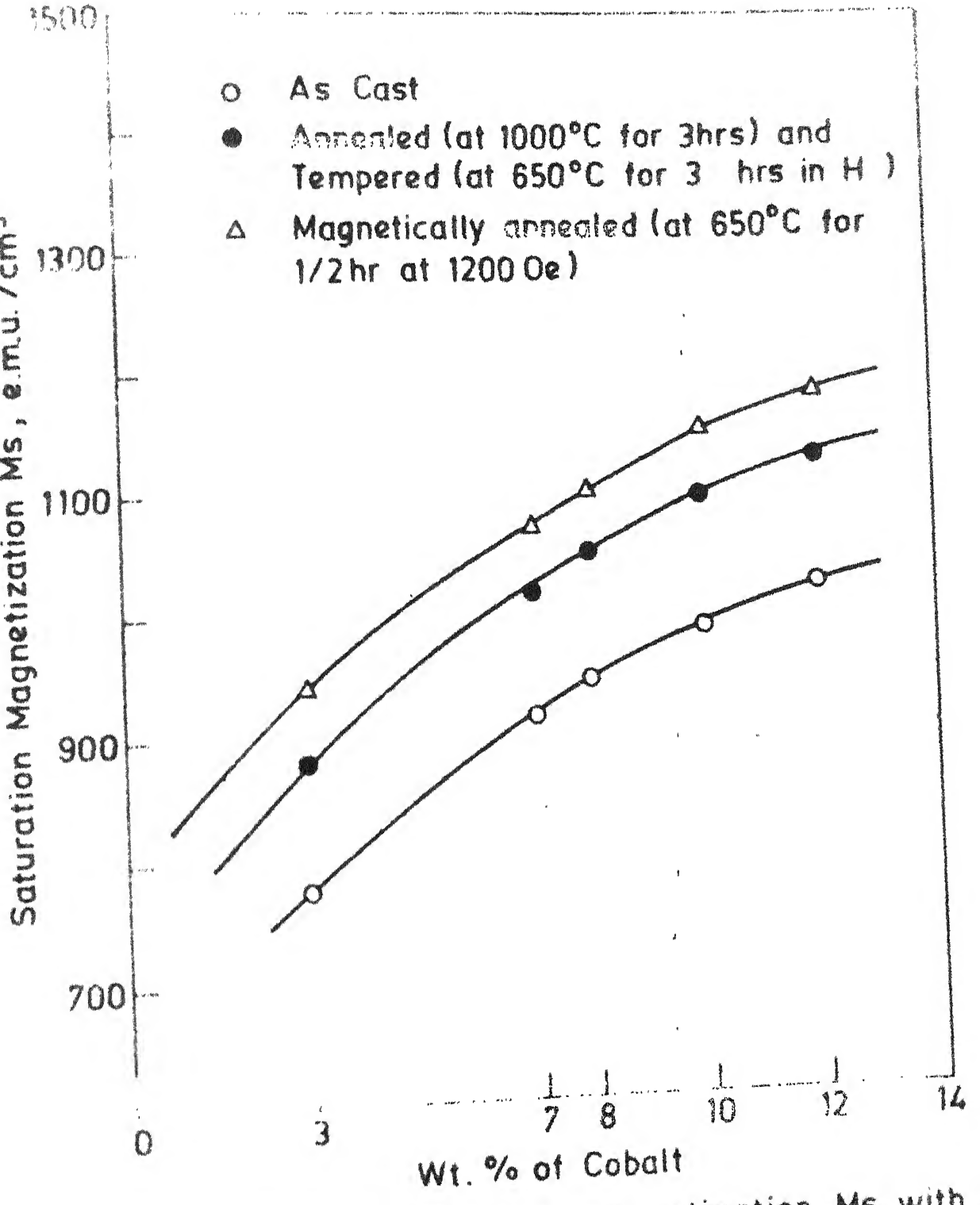

Fig. 3.17 Variation of saturation magnetization Ms with wt.% of Co in Fe-Ni-Al-Co-Cu alloys.

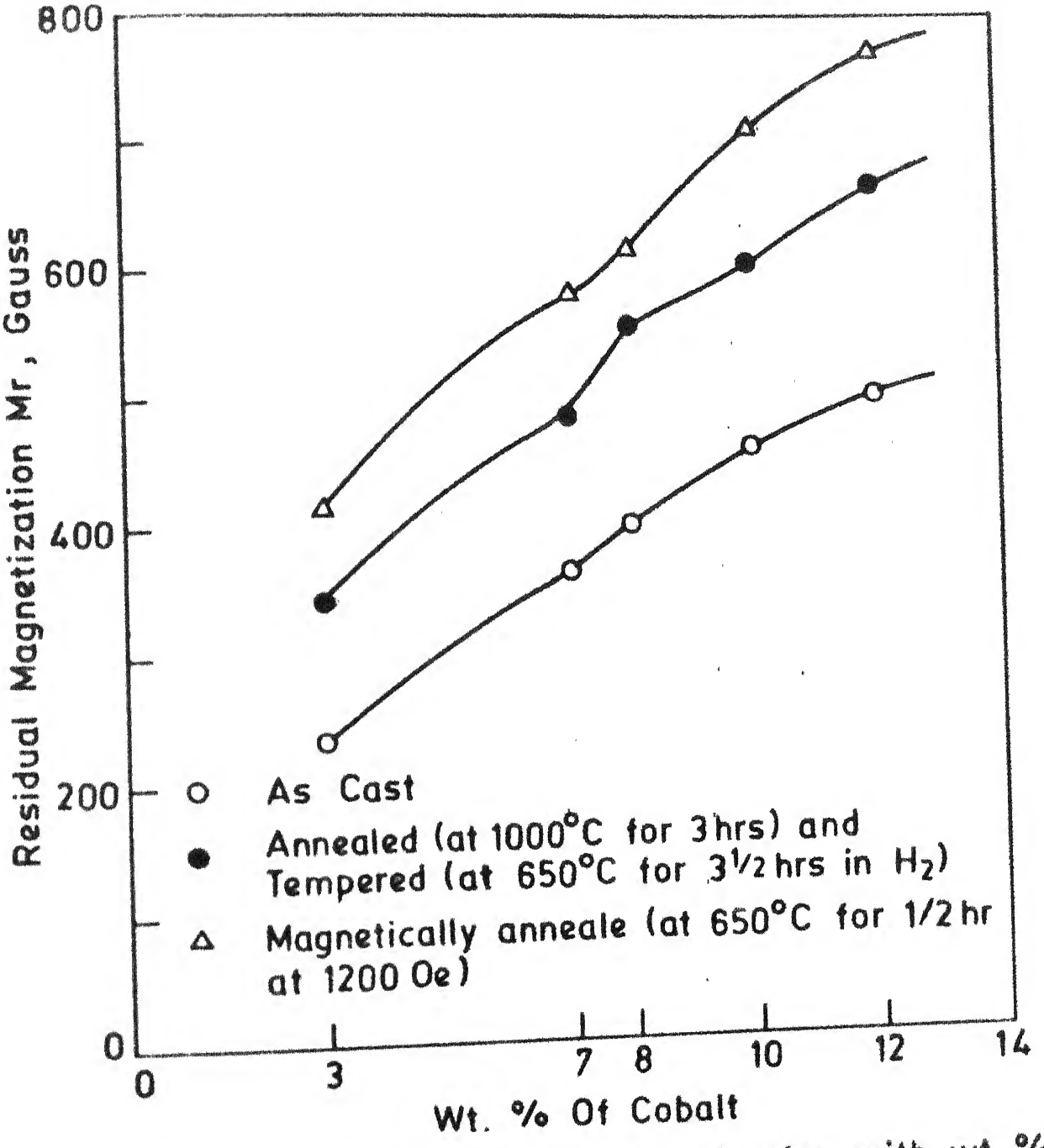

Fig. 3.18 Variation of residual magnetization with wt. % of cobalt in Fe-Ni-Al-Co-Cu alloys.

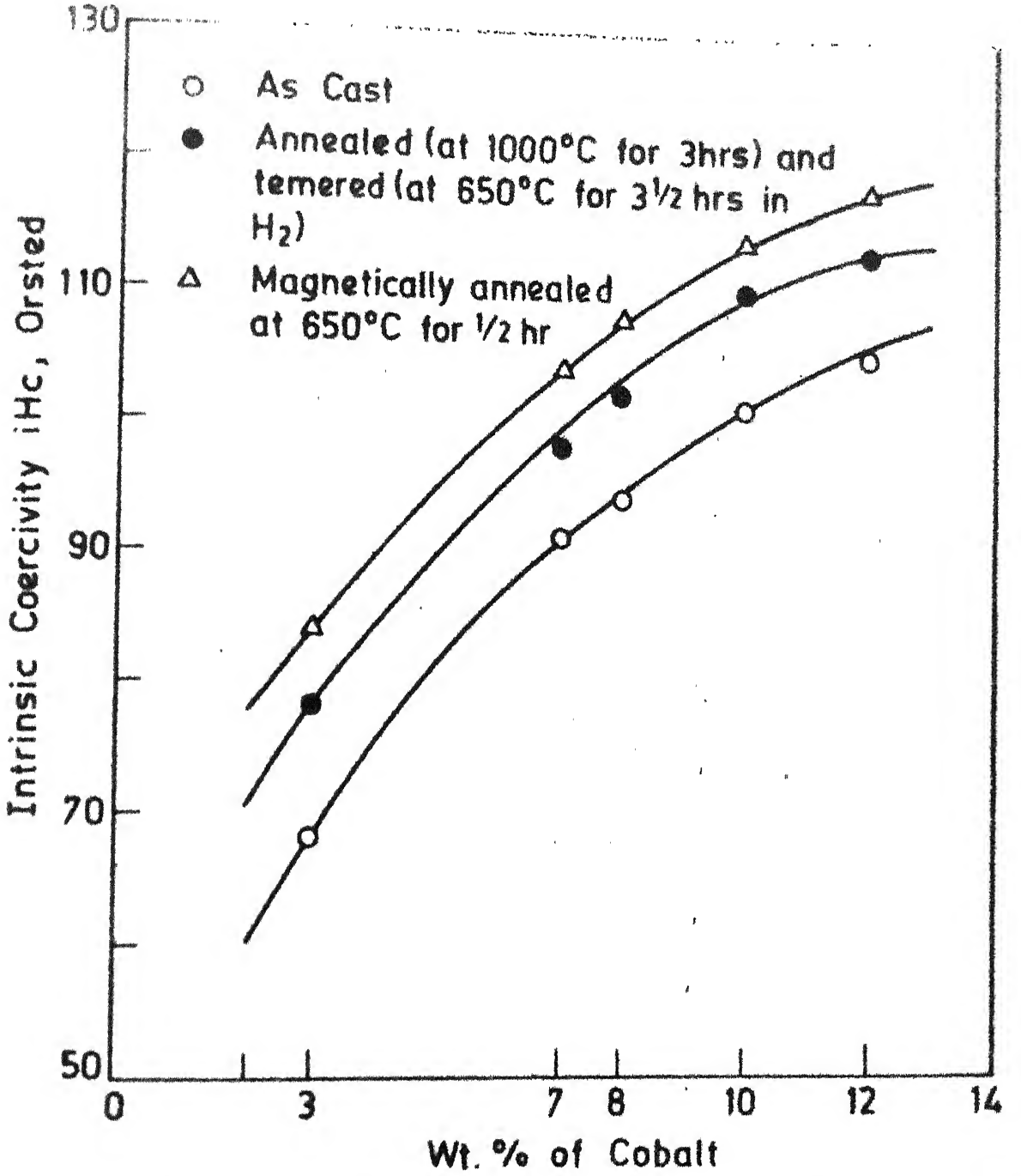

Fig. 3.19 Variation of intrinsic coercivity iHc with wt. % of cobalt in Fe-Ni-Al-Co-Cu alloys.

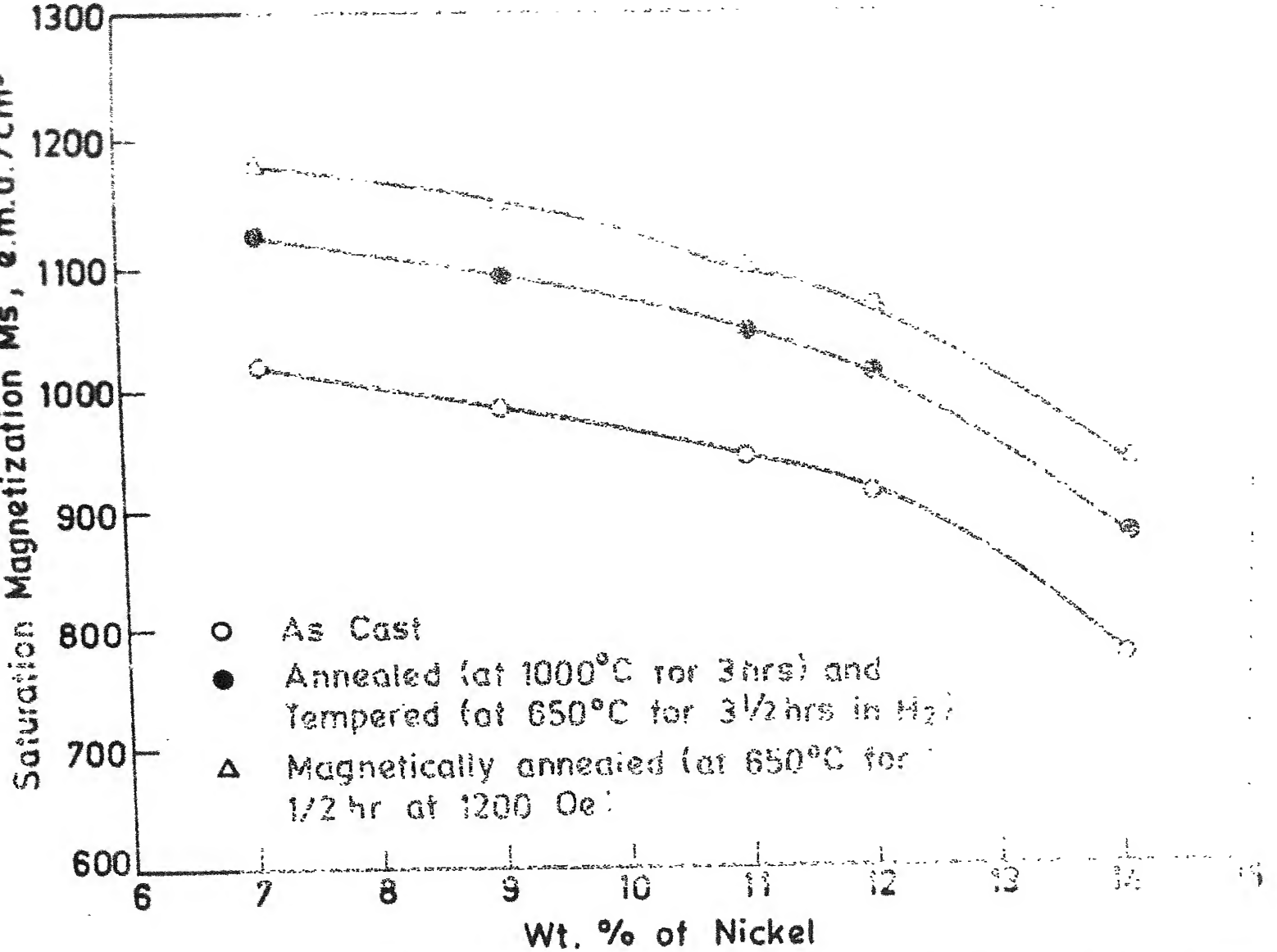

Fig. 3.20 Variation of saturation magnetization with Ni content in Fe-Ni-Al-Co-Cu alloys.

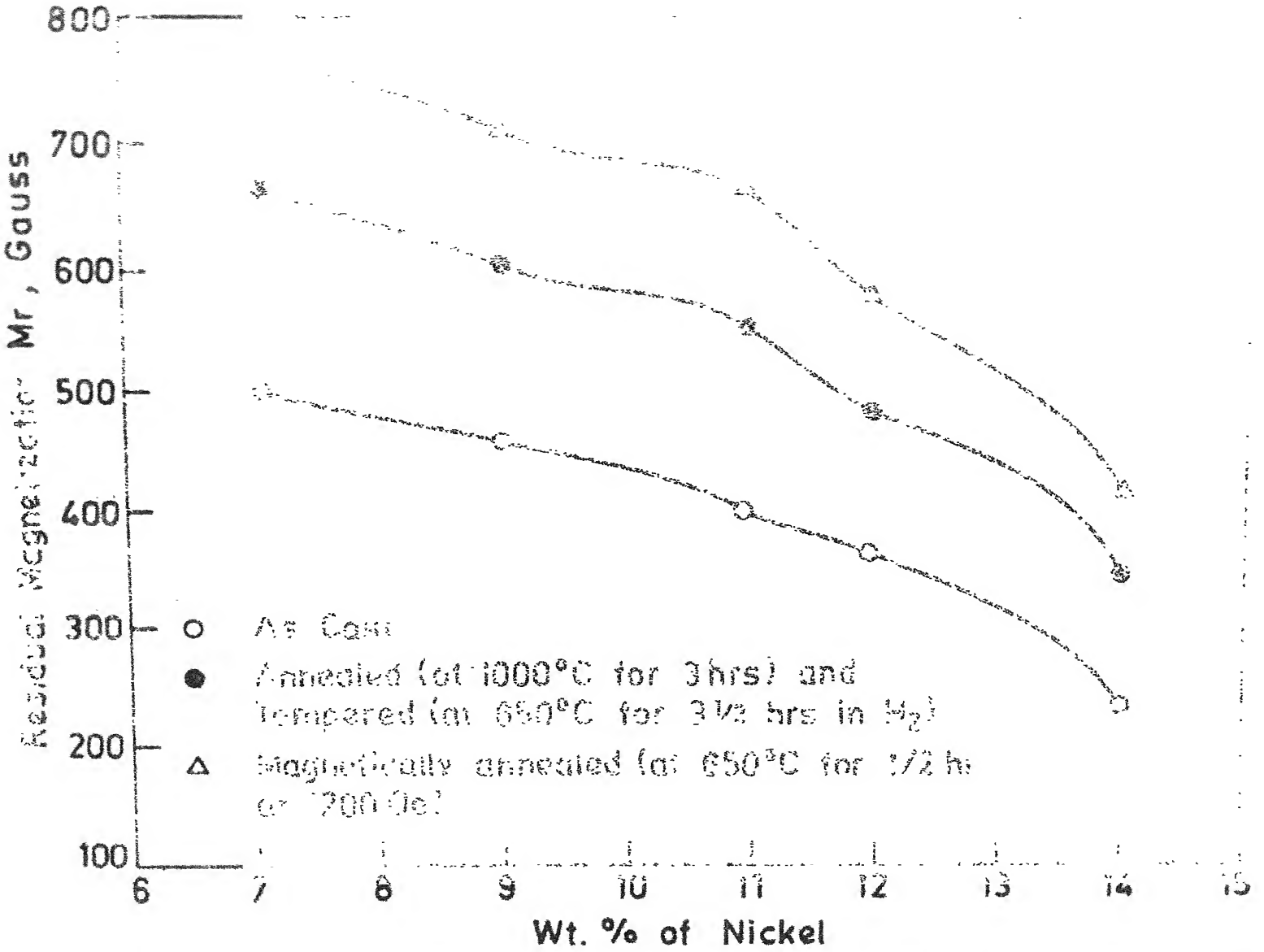

Fig. 3.21 Variation of residual magnetization Mr with Ni content in Fe-Ni-Al-Co-Cu alloys.

is less than that of iron (^{m}Fe = 2.22 μB).

3.3.6.4 Effect of Copper on Magnetic Properties:

The effect of Cu content on magnetic properties of Fe-Ni-Al system has been presented in Figs. (3.22 to 3.24). From the above, we find that the addition of Cu increases M_s , M_r and ^{i}Hc values. The addition of Cu was found to increase the precipitation rate of ferro-magnetic α' phase in the weak magnetic matrix and induces significant shape anisotropy, giving rise to increased values of M_s, M_r and ^{i}Hc. The improvement in the values of M_s and M_r due to Cu addition can also be explained using Stoner and Wohlfarth model (9) in which magnetization is assumed to reverse by coherent rotation.

3.3.6.5 Effect of Tempering:

The annealed samples of all the alloys were tempered at 650°C for $3\frac{1}{2}$ hrs. in H_2 atmosphere. The results reported in Table (3.16) show that tempering improves M_s , M_r and ^{i}Hc values in all the cases. Tempering causes greater difference between the spontaneous magnetization of α' phase and weak magnetic phase due to transfer of Fe atoms from the weak magnetic phase to α' phase by diffusion process. This results in more effective shape anisotropy of the precipitate particles.

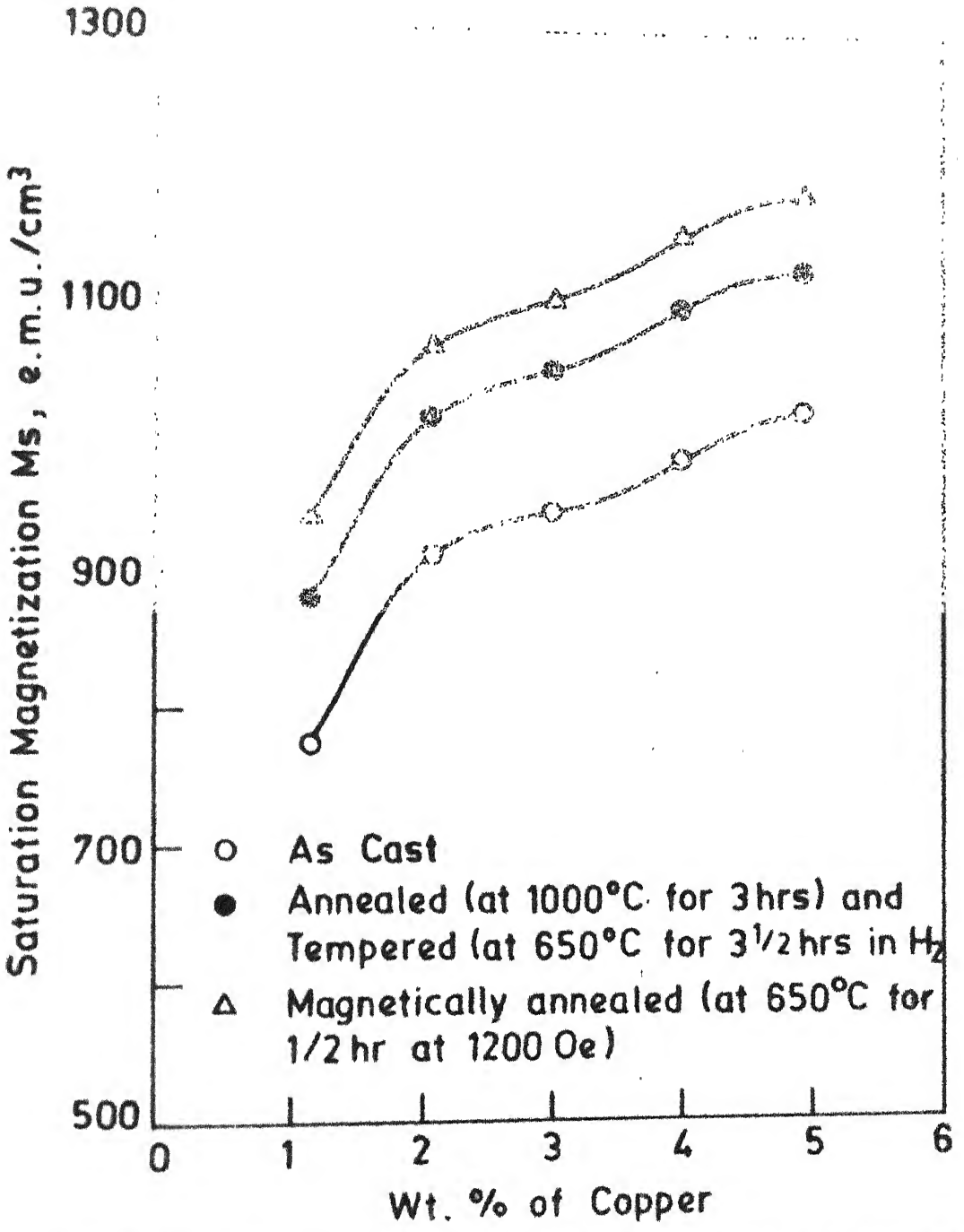

Fig. 3.22 Variation of saturation magnetization with wt. % of Cu in Fe-Ni-Al-Co-Cu alloys.

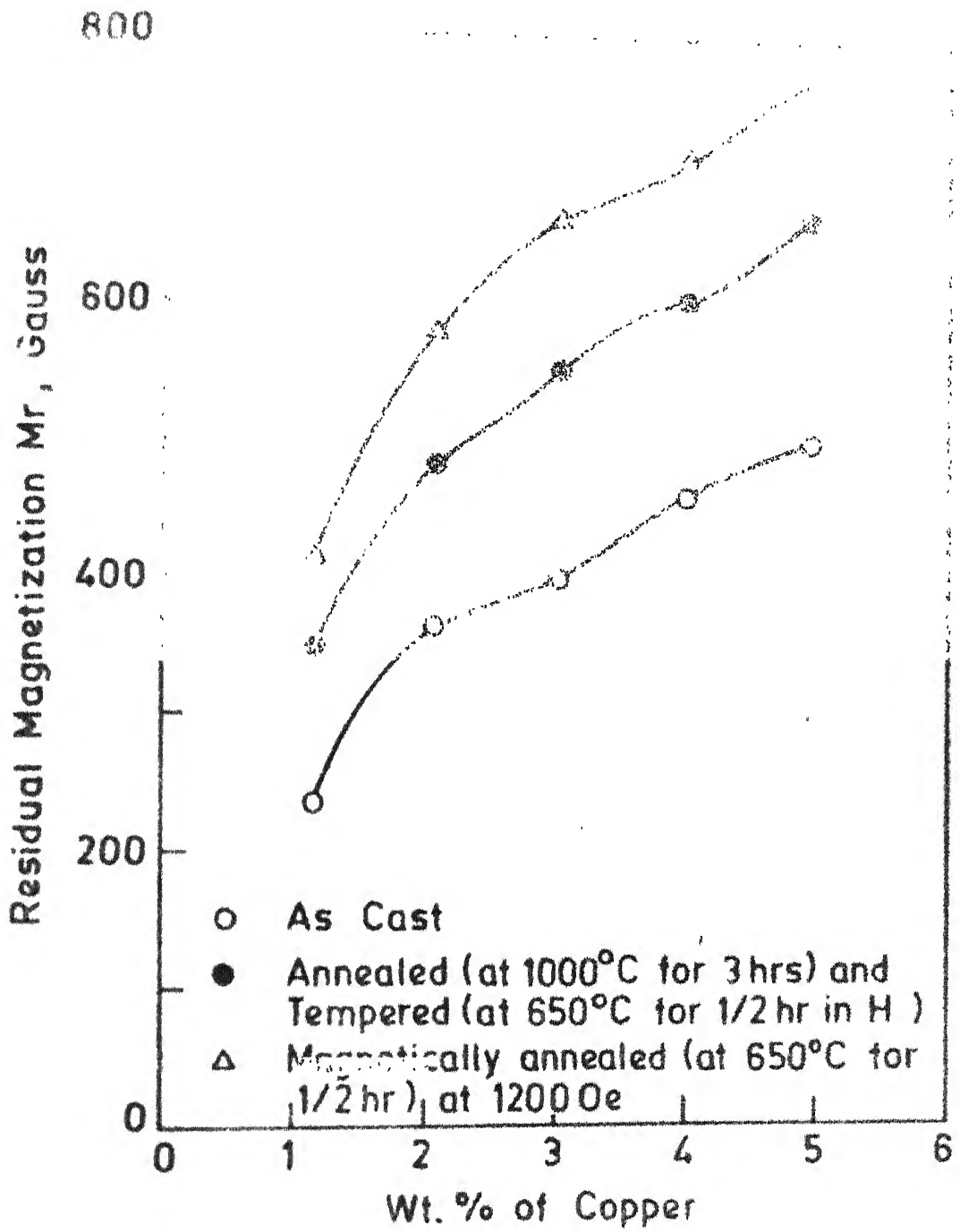

Fig. 3.23 Variation of residual magnetization Mr, with wt. % copper in Fe-Ni-Al-Co-Cu alloys.

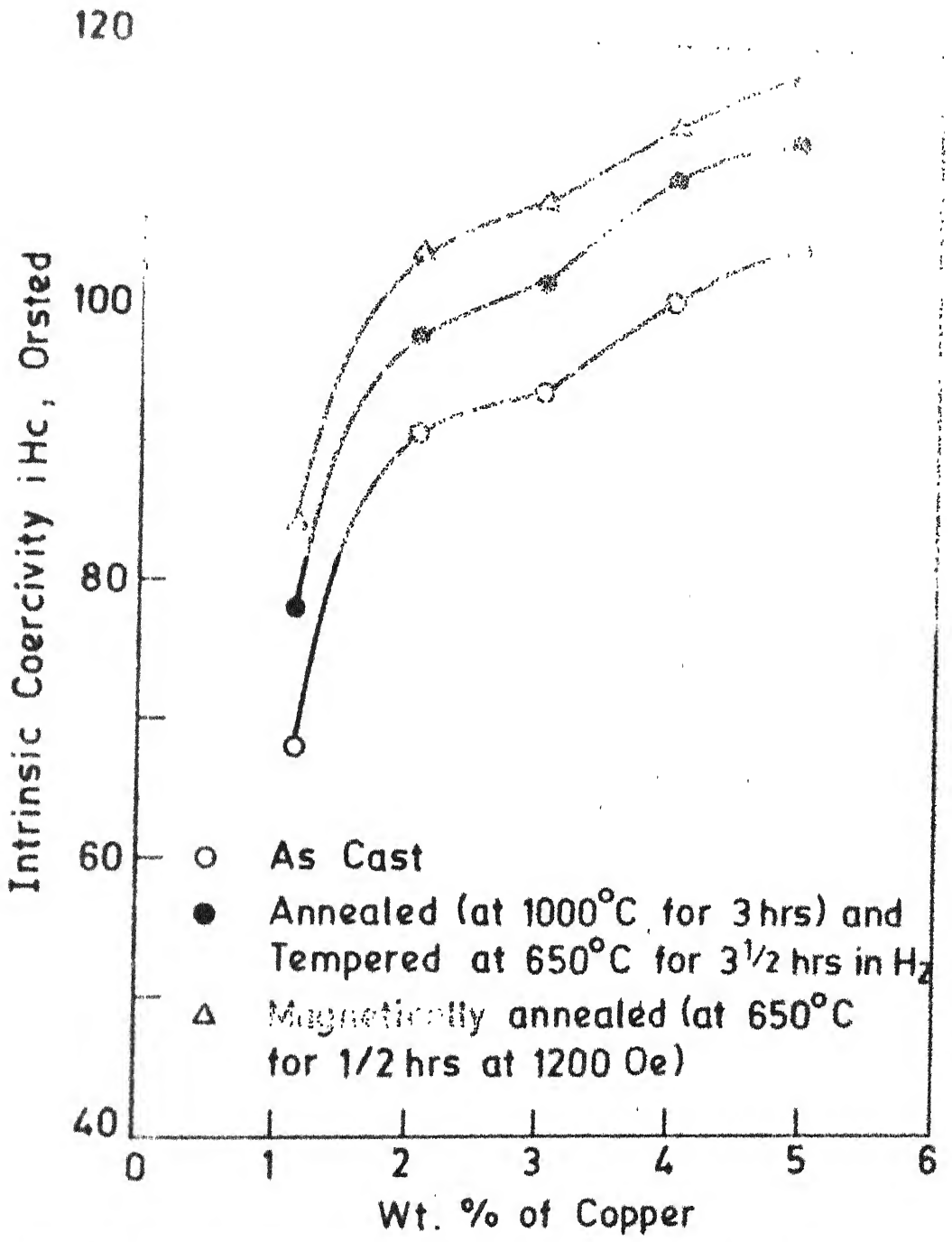

Fig. 3.24 Variation of intrinsic coercivity with wt. % of Cu in Fe-Ni-Al-Co-Cu alloys.

Tempering also causes the clear cut phase separation of α' precipitates (strong magnetic) and the elongation of α' particles on the expense of matrix (weak magnetic). This inhances M_s , M_r and ^iH_c values.

3.3.6.6 Effect of Magnetic Ageing:

The magnetic ageing causes preferential alignment of the spinodally decomposed particles along the field direction or as near as possible, depending on the orientation of [100] of the precipitate particles (10). The elongation of α' particles inhances shape anisotropy leading to higher value of intrinsic coercivity in the field direction. Thus magnetic ageing results in improved magnetic properties.

3.4 CONCLUSIONS:

The present investigation was undertaken to test the conviction of employing metallothermic process for producing hard ferro-magnets using metal oxides in stead of metals. The results of studies on the alloys of both systems led as to the following conclusions:

1. It is possibility to produce hard magnets using the thermite process.

2. The major difficulty occurs in controlling the composition and microstructure of the alloys.

3. The effect of copper addition in Fe-Ni-Al-Co-Cu system is to produce abnormally large rod like precipitates both in the cast and annealed samples.

4. The second phase precipitate is a b.c.c. type α' phase with a = 5.774Å°. Smaller constituents could not be determined due to their minute amounts.

5. Vickers Hardness and electrical resisvity were found to increase linearly with addition of alloying element concentration.

6. The addition of Cr increases the intrinsic coercivity (^{i}Hc), but lowers M_s and M_r values.

7. The addition of Co and Cu improves the values of M_s , M_r and ^{i}Hc.

8. The annealing (1000°C for 3 hrs.) togather with tempering (650°C for $3\frac{1}{2}$ hrs in H_2) results in higher values of M_s , M_r and ^{i}Hc.

9. The magnetic ageing (650°C for 1/2 hr at 1200 Gauss) reveals promising improvement in the values of M_s , M_r and ^{i}Hc.

REFERENCES

1. R. Rawlings, Practical Physical Metallurgy, edited Butterworths, 1961.

2. B.D. Cullity, Elements of X-ray Diffraction, Addison-Wesley Publishing Company, INC, New-York.

3. M. Uma Devi, Phase Equilibria and Magnetic Characterization of RE - Co - Fe - Cu - Zr Alloys, in the Composition Range of R.E. Transistion Metal = 1:7 - M. Tech. thesis, July 1935.

4. K.H. Chien and T.Z. Kattamis, Z. Metallkunde, Vol. 61, P-475, 1970.

5. B.D. Cullity, Introduction to Mag. Materials, Addison-Wesely Publ. Co., 1972, Page 322-325.

6. E.P. Wohlforth, J. Appl. Phys., 35, 783-790 (1964).

7. L. Neel, Analysis of Grenoble University 22, P. 299, (1948).

8. John B. Goodenough, Phy. Rew, 95, 917, 1954.

9. E.C. Stoner and E.P. Wohlfarth, Phil. Trans. Roy. Soc. (Lond), A 240, 599, 1948.

10. Y. Iwama, Trans. Japan Inst. Metals, 17, 481, 1976.

Thesis
669.95
P886d

A98010

98010

ME - 1986 M - PRA - DEV